Fracture Critical Analysis Procedures and Design and Retrofit Approaches for Pony Truss Bridges in Ohio

Prepared by:
James A. Swanson, Ph.D.
Gian Andrea Rassati, Ph.D.
Eric F. Dues, P.E., S.E.

Prepared for:
Ohio's Research Initiative for Locals
The Ohio Department of Transportation,
Office of Statewide Planning & Research

State Job Number 135031 (2015-ORIL6)

October 1, 2016

Final Report

U.S. Department of Transportation
Federal Highway Administration

Technical Report Documentation Page

1. Report No.	2. Government Accession No.	3. Recipient's Catalog No.
FHWA/OH-2016/13		

4. Title and Subtitle	5. Report Date
Fracture Critical Analysis Procedures and Design and Retrofit Approaches for Pony Truss Bridges in Ohio	**Oct 1, 2016**
	6. Performing Organization Code

7. Author(s)	8. Performing Organization Report No.
James A. Swanson, Gian Andrea Rassati, Eric F. Dues	

9. Performing Organization Name and Address	10. Work Unit No. (TRAIS)
University of Cincinnati **765 Baldwin Hall** **Cincinnati, OH 45221-0071**	
	11. Contract or Grant No.
	SJN 135031 (2015-ORIL6)

12. Sponsoring Agency Name and Address	13. Type of Report and Period Covered
Ohio Department of Transportation **1980 West Broad Street** **Columbus, Ohio 43223**	
	14. Sponsoring Agency Code

15. Supplementary Notes

16. Abstract
The study outlined in this report aimed to quantify the available redundancy in pony truss bridge systems constructed using standard designs and practices in the state of Ohio. A method of conducting refined three-dimensional nonlinear finite element analyses that can be used to assess the level of redundancy in bridge pony systems was developed and used to study the performance of pony truss bridges. It was found that when they are properly detailed and constructed, deck systems in pony-truss bridge can be inherently redundant. To a lesser extent, it was also found that truss members in properly designed and constructed bridges can also be redundant.

17. Keywords	18. Distribution Statement
bridge, fracture critical, fracture, truss, pony-truss, redundancy, nonlinear analysis, refined analysis, load path	**No restrictions. This document is available to the public through the National Technical Information Service, Springfield, Virginia 22161**

19. Security Classification (of this report)	20. Security Classification (of this page)	21. No. of Pages	22. Price
Unclassified	**Unclassified**		

Form DOT F 1700.7 (8-72) **Reproduction of completed pages authorized**

Fracture Critical Analysis Procedures and Design and Retrofit Approaches for Pony Truss Bridges in Ohio

Prepared by:
James A Swanson, Ph.D.
University of Cincinnati

Gian Andrea Rassati, Ph.D.
University of Cincinnati

Eric F. Dues, P.E., S.E.
Gannett Fleming, Inc.

October 1, 2016

Prepared in cooperation with the Ohio Department of Transportation,
Ohio's Research Initiative for Locals, and the U.S. Department of Transportation,
Federal Highway Administration

Acknowledgments

The research team would like to acknowledge the contribution and support provided by the Ohio Department of Transportation (ODOT), Ohio's Research Initiative for Locals (ORIL), and the Federal Highway Administration (FHWA). Specifically, the research team would like to acknowledge the support of the ORIL technical advisory committee including Michael Brokaw, Scott Coleman, David Morgan, Eric Steinberg, Matthew Shamis, Brett Boothe, Dennis Gonano, and Bill Lozier. The research team would also like to acknowledge US Bridge for their assistance in providing bridge plans used in the study. Finally, the research team acknowledges Martin Butler's significant contributions to the completion of the project.

Table of Contents

Chapter 1 - Introduction

1.1: Introduction:

Non-redundant bridges are those bridges that do not contain alternate load paths should a member in the structure fail. Redundancy can be achieved in several ways including internal member redundancy, load path redundancy, or structural redundancy. Specifically, pony truss bridges, which are the target of the proposed study, represent a system type that is often considered to be (a) non-redundant based on load-path because the trusses are almost always simply supported, and (b) non-redundant structurally because the bridges typically utilize only two trusses and the failure of either truss is generally considered to lead to the complete collapse of the bridge. A member whose failure would lead to the collapse of the entire structure is categorized as a fracture critical member and is subject to increased scrutiny during fabrication and construction, and more in-depth inspections at shorter intervals. Because non-redundant bridges are often associated with increased inspection and maintenance costs, they represent a particular challenge to bridge owners.

While pony truss systems are often considered to be non-redundant based on prevailing assumptions made during analysis, design, and load rating, they have been shown to contain considerable inherent redundancy owing to actual design and construction methods. While trusses are generally considered to have frictionless pinned joints, actual truss construction universally includes gusset-plated connections that have dozens of rivets or bolts that render the joints far from frictionless. Further, floor systems in pony truss bridges are often considered to be secondary in that they are assumed to support traffic or live loads and carry those loads to truss joints, but are assumed to not participate in carrying those loads to the abutments or piers. In actuality, however, floor systems – especially when stringers are continuous over floor beams - can act in parallel with bottom chord truss members to help carry loads to the supports in the event of a failure of a truss member.

1.2: Goals and Objectives:

The overall goal of the investigation is to reduce inspection and maintenance costs associated with pony truss bridges (PTBs) in the state of Ohio by developing procedures that can be used to quantify the level of redundancy in pony truss bridge systems so that fracture critical members may be reclassified as non-fracture critical. Additional goals include This goal will be achieved through systematical analyses based on a suite of (a) micro-scale finite element models that will be used to identify failure modes, reserve strength, and inherent redundancy of connections and members, and (b) macro-scale finite element models that will be used to examine system performance including (i) three-dimensional behavior of systems and (ii) the behavior of systems when secondary members are considered to act in concert with the primary structural system. Further, analytical tools and protocols will be proposed that can be used to mitigate the inspection burden for bridge owners with respect to pony-truss bridges, and to guidance will be

provided for the repair and retrofit of existing non-redundant bridges and design recommendations for new bridges such that redundancy can be provided.

1.3: Organization of Report

This report is organized into seven chapters including this one. In Chapter 2, a review of the pertinent literature and background materials including nonlinear analysis procedures, assessment of redundancy, and treatment of fracture critical members is presented. Chapter 3 starts off with a general description of pony truss details, continues with a summary of assumptions made and common practice in the analysis and design of PTBs, and closes with a discussion of secondary load paths that may exist in PTBs. A detailed description of reports and design guides that will be used as a basis for the methods recommended in this report is presented in Chapter 4. Chapter 5 begins with a summary of the method proposed for a fracture critical analysis (FCA) of pony truss bridges and concludes with detailed background and commentary about each of the steps in the proposed FCA procedure. Chapter 6 consists of a series of high resolution finite element (FE) analyses that were performed as a means of validating the lower-resolution FE analyses that are part of the FCA procedure. Finally, strategies that can be used in the repair and retrofit of existing PTBs or the design of new PTBs to minimize or eliminate fracture critical members is presented in Chapter 7. Background calculations and examples can be found in the appendices to this report.

Chapter 2 - Background and Literature Review

2.1: Background:

Following the collapse of the Silver Bridge, federal legislation was enacted in 1968 requiring the biennial inspection of all bridges 20 feet or longer in the United States. In 1973, the Ohio Revised Code required the annual inspections of bridges 10 feet or longer (ORC 5501.47, 2010), thus requiring an inspection frequency that is more stringent than that mandated by federal legislation, National Bridge Inspection Standards (NBIS) (NBIS, 2004), and the Bridge Inspection Reference Manual (BIRM) (FHWA-NHI 12-049, 2012). This reaction to a catastrophic bridge failure and resulting loss of life was warranted and understandable, and was certainly a step forward in the area of bridge safety, but is the inspection interval of two years – or the Ohio Department of Transportation's (ODOT's) interval of one year - entirely rational? Reliability approaches develop links between the probability of failure and time interval between inspections with the underlying principle that the inspection interval should be sufficiently small so that any potential problems that develop between inspections can be identified during the next inspection before they develop into failures. The risk based approaches outlined in the National Cooperative Highway Research Program (NCHRP) document 12-82 (NCHRP, 1982) develop relationships between inspection intervals, the probability of occurrence of a problem, and the consequence of that problem on the integrity of the structure. This relationship is quantified in reliability matrices like those shown in Figure 1 of that report that can be used to rationally determine inspection intervals for bridges. Using rubrics, engineers determine factors quantifying the probability of occurrence (O) and consequences of occurrence (C) of an event, and compute an Inspection Priority Number (IPN) as the product of O and C, which is then used for the prioritization of potential failure modes in the assessment of inspection interval for a bridge (Applebury, 2011). Larger values of O and C correspond to increased probabilities of failure, P_f, and more severe consequences of occurrence, respectively.

In 2005 the Federal Highway Administration opened the door to increasing the interval between inspections to as long as four years in some cases (CFR23, 2011). While this "48 Month Policy" represents a step forward in applying reliability based theory to the inspection of our nation's bridges, bridges without load-path redundancy and bridges with fracture critical members are exempted and still require biennial inspections.

2.2: Consideration of Redundancy:

Members whose tensile failure is likely to lead to the collapse of the entire bridge are categorized as fracture critical members (FCMs). Thus structural redundancy plays a key part in the identification of FCMs. Given that FCMs require a higher level of scrutiny and shorter inspection intervals, the presence of FCMs on a bridge increases inspection and maintenance costs for bridge owners. Hence eliminating FCMs – or even reducing the number of FCMs – by reclassification in a bridge system can significantly reduce costs.

This reclassification is often accomplished by identifying alternative load paths in the event of a member failure, or quantifying redundancy in the member or structure.

Modern analytical techniques can include previously overlooked truss details to provide additional structural system redundancy. First, trusses that are evaluated based on pinned-joint analyses are actually constructed using gusset plates that often have performance characteristics closer to moment resisting connections than idealized frictionless pins. Secondly, trusses are often evaluated as two-dimensional planar systems when in fact they are constructed as three dimensional bridges. Even in the absence of top chord truss-to-truss connections, the three-dimensional behavior of a pony truss bridge can differ significantly from its two-dimensional behavior. Finally, elements of the bridge system that are not considered to be part of the main load-carrying superstructure can, during extreme events, participate along with trusses to keep a member failure from resulting in a complete bridge collapse.

Several slightly different definitions for a "fracture critical member" are provided in the FHWA and AASHTO documents. The current National Bridge Inspection Standards (NBIS) definition for a FCM is *"a steel member in tension, or with a tension element, whose failure would probably cause a portion of or the entire bridge to collapse."* (NBIS, 2004)

The AASHTO Manual for Bridge Evaluation (MBE), 2nd Edition, defines FCMs as *"steel tension members or steel tension components of members whose failure would be expected to result in a partial or full collapse of the bridge."* (AASHTO-MBE, 2016)

The AASHTO LRFD Bridge Design Specifications (LRFD), 7th Edition, defines a FCM as a *"component in tension whose failure is expected to result in the collapse of the bridge or the inability of the bridge to perform its function."* (AASHTO-LRFD, 2015)

2.2.1: 2012 FHWA Memorandum on Redundancy:

Identifying redundancy in a bridge can help avoid FCMs in design. In June of 2012 the FHWA released a memorandum in an effort to clarify requirements and classification of fracture critical members (FHWA 2012a). This memo points out that redundancy can be achieved in a number of ways. It should be noted, however, that simply identifying redundancy is not sufficient; the redundant load path must also have sufficient strength in the event of a failure or fracture.

2.2.1.1: Structural Redundancy:

Structural redundancy refers to systems that are indeterminate based on features such as continuity in beams, multiple stays in a cable-stayed bridge, or other features inherent to a bridge. Pony-trusses are typically designed as determinate planar structures, even when the restraint provided by the gusset-plate connections is considered. As a result, one might dismiss the notion of structural redundancy within the context of pony-truss bridges. The members in the floor systems of PTBs may be structurally redundant.

Floor beams that span between the two trusses are typically detailed with moment connections at each end. If those end connections have enough restraint and strength, then the floor beams will be fixed-fixed beams and be two degrees indeterminate, or two degrees redundant. While stringers are generally designed and detailed as simply-

supported beams that run parallel to the trusses spanning one bay from floor beam to floor beam (or from floor beam to abutment), they could span continuously across multiple bays providing several degrees of redundancy depending on the number of spans.

2.2.1.2: Internal Member Redundancy:

Internal member redundancy refers to the idea that a single member may itself be redundant because it is fabricated in such a way that fracture of one component of the cross section will not necessarily result in the loss of the entire cross section. In such members, a fracture in one element of the cross section is prevented from propagating throughout the entire cross section. Thus the possibility of a single fracture event resulting in the inability of the member to carry load is eliminated. Riveted or bolted built-up members, stay cables, and post tensioning cables in concrete girders are examples of internally redundant structural members because the fracture of a single element – a plate in the case of a built-up member, or a strand in the case of a stay cable – doesn't render the member completely useless.

2.2.1.3: Load-Path Redundancy:

Load path redundancy refers to the presence of multiple primary elements that are able to redistribute loads and maintain structural stability in the event of a member failure and is addressed in a number of design documents. The American Society of Civil Engineers (ASCE) addresses redundancy by stating that structures in which the removal of one load path results in no more than a 33% reduction in strength are considered redundant (ASCE/SEI 7-10). The Ohio Department of Transportation (ODOT) Bridge Design Manual states that bridges with five or more girders are considered redundant, that bridges with 3 or fewer girders are considered non-redundant, and that bridges with 4 girders may or may not be considered redundant based on lateral spacing of the girders. The FHWA provides tables for determining the redundancy factor based on the number of girder lines present and the spacing of the girders (FHWA-IF-12-052). These definitions are all similar in concept, but are best applied to girder bridges. Extrapolating these ideas to a pony truss bridge would indicate that all pony truss bridges are inherently non-redundant despite the fact that their behavior in the event of a primary-member loss would differ significantly from that of a girder bridge.

2.2.1.4: System Redundancy:

System redundancy refers to the ability of the three-dimensional behavior of the system to remain stable in the event of a member failure even though the system was designed based on assumptions that the load path is non-redundant. Engagement of secondary structural elements, or engagement of structural elements in a way different from how they were assumed to behave during design, is referred to as system redundancy. In most cases, this system redundancy is established using a refined analysis of the structure.

The 2012 FHWA memo states, *"If refined analysis demonstrates that a structure has adequate strength and stability sufficient to avoid partial or total collapse and carry traffic in the presence of a totally fractured member (by structural redundancy), the member does not need to be considered fracture critical for in-service inspection protocol. The assumptions and analyses conducted to support this determination need to become part*

of the permanent inspection records or bridge file so that it can be revisited and adjusted as necessary to reflect changes in bridge conditions or loadings."

Details, guidelines, and/or requirements for these types of analyses are not provided in the memo or elsewhere. Development of guidelines for performing this type of refined analysis is one of the objectives of the research work described in this report. It is expected, and a continued review of the literature will demonstrate, that these refined analyses are typically 3D analyses that often incorporate nonlinear geometrical and/or nonlinear material behaviors.

2.2.1.5: Fracture Control Plan:

The 2012 FHWA memorandum also indicates that members that are to be reclassified from fracture critical to non-fracture critical should have been fabricated under a modern fracture control plan consistent with those introduced in 1978. This would essentially render moot a refined analysis for any bridges fabricated prior to 1978.

AASHTO developed "Guide Specifications for Fracture Critical Non-Redundant Steel Bridge Members" in 1978 (AASHTO, 1978) that defined the requirements of a fracture control plan. In 1995 these requirements were incorporated as Section 12 of AWS D1.5 (2010). A fracture control plan begins with FCMs being identified in the design plans. The ASSHTO "Standard Specifications for Transportation Materials and Methods of Sampling and Testing" requires steels used to FCMs to meet higher Charpy V-notch toughness requirement and contain fine-grained material. Additional fabrication procedures and inspection, and more strict shop certification are required to meet the AWS D1.5 Bridge Welding Code requirements for fracture critical fabrication.

2.3: Literature Review:

A review of the pertinent literature on the topic of fracture critical members is presented within this section.

2.3.1: Furuta, Shinozuka, and Yao 1985:

Furuta, Shinozuka, and Yao established a means of determining the probability of loading exceeding capacity in structural systems with fuzziness introduced by linguistic variables given in visual inspections. They also examined and defined a number of means of measuring structural redundancy based on this work based on deterministic, probabilistic, and fuzzy set theories.

Previous work defined redundancy in a number of different ways, including the following.

Degree of Indeterminacy: It is widely agreed that indeterminacy is useful for redundancy and when the concept of redundancy was first discussed degree of indeterminacy was one of the first suggested means of measuring it. Unfortunately it is quite possible for a member to be highly indeterminate and yet still fail as soon as any one member fails as shown in Frangopol and Curley (1987).

Redundant Factor:

$$RF = \frac{\text{Intact Strength}}{\text{Intact Strength - Damaged Strength}} \tag{2-1}$$

Reserve Resistance Factor:

$$REF = \frac{\text{Environmental Load at Collapse}}{\text{Design Environmental Load}} \tag{2-2}$$

Residual Resistance Factor

$$RIF = \frac{\text{Environmental Load at Collapse (Damaged)}}{\text{Design Environmental Load (Undamaged)}} \tag{2-3}$$

Multiplying the reserve resistance factor by the residual resistance factor gives a deterministic answer as to whether a damage state will survive a given loading. This is a better measure than merely the degree of indeterminacy but still disallows a continuous level of damage such as would be likely to appear in aging infrastructure. A more realistic means of describing damage states is from linguistic variables, which will define the capacity not as deterministic, but as a fuzzy set.

Definitions:

- λ - amplification factor to induce collapse load by multiplying Load F and considering Plastic Capacity M_{pi}
- $\bar{\lambda}$ - amplification factor to induce collapse load considering the fuzzy set of Plastic Moment Capacity $\bar{M}^*_{pi}$, which is the result of some damage.

The redundant factor is now fuzzy and is defined as

$$\bar{r} = \frac{\lambda}{\lambda - \bar{\lambda}} \tag{2-4}$$

However, the collapse load and design load are not in truth deterministic either, so they should be defined probabilistically as S_C and S_D. This allows the resistance residual factor defined above to be defined probabilistically as,

$$REF = \frac{S_C}{S_D} \tag{2-5}$$

and the probability of reserve strength is defined based on the resistance factor as,

$$p = P\left[\frac{S_C}{S_D} < v\right] \tag{2-6}$$

with v being some number greater than 1.

The residual strength is defined as a fuzzy reduction factor $\bar{\phi}$ based on verbal descriptions of damage,

$$RIF = \frac{\overline{S}_C^*}{S_C} = \overline{\phi} \tag{2-7}$$

with $\overline{S}_C^*$ representing the collapse load for the damaged structure, which allows the probability of residual strength to be written as

$$\overline{p}^* = \mathrm{P}\left[\frac{\overline{S}_C^*}{S_D} < v\right] = \mathrm{P}\left[\frac{\overline{S}_C^*}{S_D} < \frac{v}{\overline{\phi}}\right] \tag{2-8}$$

Then another fuzzy redundancy factor can be defined as

$$\overline{r} = \frac{\text{Probability of Reserve Strength}}{\text{Probability of Residual Strength}} \tag{2-9}$$

This will vary from 1 to 0 with 1 being indicative of an entirely redundant structure and 0 indicating an entirely nonredundant structure. The fuzzy redundancy factor does give more information regarding the redundancy of a structure than the non-fuzzy version, but it is a bit more difficult to obtain.

2.3.2: Frangopol and Curley 1987:

The authors investigated load path redundancy based on case histories by Csagoly and Jaeger (1979). They showed that indeterminacy is a necessary, but not a sufficient condition, to establish redundancy, and used the redundant factors from Furuta et. al. (1985) with the difference that the fuzziness introduced by verbal descriptions of damage states in Furuta et. al. was removed for a crisp number describing levels of damage. They compare statically determinate and indeterminate trusses assuming brittle, ductile and hardening behavior showing the difference in redundancy from those behaviors.

The definitions of redundancy examined by Frangopol and Curley include:

Degree of Redundancy:

$$R_I = F - E \tag{2-10}$$

where:

F - number of unknown reactions

E - number of equilibrium equations

This is not an entirely exhaustive way of measuring redundancy, however, since it does not account for the strength of the components in the structure. This is shown by a simple six member truss which reaches ultimate capacity at the same load as first member failure. This simple example of a cascading failure establishes how little use the degree of redundancy is as a measure of redundancy.

Reserve Redundant Factor:

$$R_2 = \frac{L_{Intact}}{L_{Design}} \tag{2-11}$$

where:

L_{Intact} - collapse load of intact structure

L_{Design} - design load

Residual Redundant Factor:

$$R_3 = \frac{L_{Damaged}}{L_{Design}} \tag{2-12}$$

where:

$L_{Damaged}$ - collapse load of damaged structure

Strength Redundant Factor:

$$R_4 = \frac{L_{Intact}}{L_{Intact} - L_{Damaged}} \tag{2-13}$$

If load factors are used as in Furuta et. al. (1985) so that λ is the amplifying load factor to induce collapse of the intact structure and $\bar{\lambda}$ is the amplification load factor to induce collapse of the damaged structure, the strength redundant factor may be rewritten as:

$$R_4 = \frac{\lambda}{\lambda - \bar{\lambda}} \tag{2-14}$$

The strength redundant factor presented by Frangopol and Curley is the same as from Furuta et. al. with the fuzziness of the sets removed. The damage is instead represented by a damage factor (D.F.) which is a discreet value indicating the reduction of capacity. The linguistic variables considered were “Intact,” “Slight,” “Moderate,” “Severe,” and “Complete,” which indicate reductions in capacity of 0%, 25%, 50%, 75%, and 100%, respectively.

The probabilities were replaced with deterministic definitions of capacity and loads, with the benefit that the product of the reserve redundant factor and the residual redundant factor gave a definitive answer as to the sufficiency of the structure in a damaged state. Additional probabilistic components are introduced later in the paper.

Several examples are provided in the paper, illustrating the redundant factors of structures with different behavioral assumptions at member failure, considering behaviors such as brittle failure, ductile failure, and strain hardening reserve capacity. The authors also provide several examples that include plots of the strength redundancy factor vs. collapse load factor with points determined by applying damage to members. Since the strength redundant factor is a function of only the collapse load factor, $\bar{\lambda}$, the shape of the curves of course remained the same. However, the value of these plots is in specifying where damage states fall on the plot, which can indicate how critical a member’s individual performance is to the structure as a whole.

Probabilistic components are introduced including:

The reliability index is defined as,

$$\beta_i = \frac{M_i}{\sigma(M)_i} \tag{2-15}$$

where M_i is the mean of the performance function of the i^{th} element and $\sigma(M_i)$ is the standard deviation of the performance function of the i^{th} element. The loads and capacity are assumed to be normally distributed.

The performance function is defined as,

$$M_i = S_i - Q_i \tag{2-16}$$

where S_i is the random strength of the i^{th} member and Q_i is the random load on the i^{th} member.

The Probabilistic Damage Factor is defined as,

$$DF = \frac{S_{Intact} - S_{Damaged}}{S_{Intact}}, \tag{2-17}$$

where S_{Intact} and $S_{Damaged}$ are the mean values of the intact and damaged strengths

For considering entire structures, individual members were assumed to fail at the point the probability of member failure reached 50%, that is, when the performance function reached 0. The probabilistic means of determining redundancy in systems is similar to the second fuzzy redundancy factor presented in Furuta et. al. (1985), represented by the probabilistic redundant index, β_R,

$$\beta_R = \frac{\beta_{Intact}}{\beta_{Intact} - \beta_{Damaged}}. \tag{2-18}$$

In this equation β_{Intact} is the reliability index of the intact system and $\beta_{Damaged}$ is the reliability index of the damaged system. This value will range from 0 to infinity with 0 representing a structure with no chance of carrying its load and an infinite value given for an intact structure.

2.3.3: Ghosn and Moses 1998 (NCHRP Report 406):

A much more deterministic method for quantifying redundancy is presented in NCHRP Report 406 (1998). The report represents a comprehensive work outlining methods for quantifying redundancy of structures based on a reliability approach. In the report, “system reserve ratios” are computed for critical members as the ratio of the capacity of a system in its damaged state to the capacity of the system in its undamaged state. The procedure is implemented by applying dead load plus an incrementally larger live load to the bridge in nonlinear finite element software until failure occurs, first to a model representing the undamaged structure and then to models representing the structure during each of the damaged states that are being considered.

A detailed synopsis of NCHRP 406 is presented in Chapter 4, before it is used as a basis for the fracture critical analysis procedure.

2.3.4: Ghosn, Moses, Frangopol 2008:

"Redundancy and Robustness of Highway Bridge Superstructures and Substructures"

This report suggest and calibrates a system factor, ϕ_s, to obtain a targeted reliability index for bridge systems based on member failure, collapse, or the ability to remain functional following damage. A simplified means of obtaining the reliability index for the limit states - ultimate, functional, and damaged - was proposed. A redundancy ratio is defined as the ratio of the number of live loads needed to reach a limit state to the number of live loads needed to cause first member failure. Advisable redundancy ratios are included in the report.

The system factors suggested fulfill the same function as ηR in the AASHTO standards. Though the current specification rather arbitrarily places the factor on the load and this work places the system factor on the capacity the behavior they attempt to capture is the same.

System safety is a function of the configuration of the members, the ductility of the members, and the correlation of the member's strengths. Each of these is addressed in turn. To examine the effects of correlated strength a simple structure of parallel bars was considered and a system safety factor, SSF, and resistance-sharing factor, RSF_i were defined as

$$SSF = \frac{\Sigma R_i}{P} \tag{2-19}$$

$$RSF_i = \frac{K_i}{\Sigma K_i} \tag{2-20}$$

where R_i is the mean resistance of member i,P is the mean of the load, and K_i is each members stiffness. Considering the variability of the loads and capacities to be the same and examining varying levels of correlation between the strengths of members it was shown that for ductile systems the systems reliability index is reduced by having more correlated member strengths. Brittle systems did not have the same problem, though this was because of cascading failure as soon as any one member failed.

To examine the effects of member configuration different resistance-sharing factors were applied to the simple two-bar structure and the reliability index and system safety factors plotted. Cascading failure potential resulted in the brittle assumption giving a lower system reliability index for evenly distributed loading than if all load were carried by only one member, however the impact of this was small. The ductile assumption was found to result in a significantly higher system reliability index for a well distributed load than load carried by only one member.

The proposed system factor is based on maintaining a targeted system reliability index under the assumption of lognormal behavior of loads and capacities. The targeted system reliability index would be given as

$$\beta = \frac{\ln\left(\frac{\overline{R}}{\overline{P}}\right)}{\sqrt{V_R^2 + V_P^2}} = \frac{\ln\left(\frac{LF\ \text{HS-20}}{LL\ \text{HS-20}}\right)}{\sqrt{V_{LF}^2 + V_{LL}^2}} = \frac{\ln\left(\frac{LF}{LL}\right)}{\sqrt{V_{LF}^2 + V_{LL}^2}} \tag{2-21}$$

where LF is defined as the load multiplier to induce failure and LL as the load multiplier to obtain the expected maximum live load. These load multipliers are applied to an HS-20 truck load which may then be factored out. This equation also combines all of the variables which affect capacity into the load multiplier LF, which is somewhat conservative on the strength correlation front. Four different load multipliers are considered, they are LF_u, LF_f, LF_d, and LF_1 for the failure states of ultimate collapse, functional inadequacy, collapse of damaged structure, and first yield, respectively. From these, deterministic measures of redundancy can be determined in the form of reserve ratios for each state, given as:

$$R_u = \frac{LF_u}{LF_1} \tag{2-22}$$

$$R_f = \frac{LF_f}{LF_1} \tag{2-23}$$

$$R_d = \frac{LF_d}{LF_1} \tag{2-24}$$

The minimum values Ghosn et. al. suggest should be obtained for these values are 1.30, 1.10, and 0.50 for R_u, R_f, and R_d respectively. This value for damaged state correlated to a probability of survival under regular truck loading of 80%.

Probabilistic measures are also given in the form of relative reliability indices, which are given as:

$$\Delta\beta_u = \beta_{Ultimate} - \beta_{Member} \tag{2-25}$$

$$\Delta\beta_f = \beta_{Functionality} - \beta_{Member} \tag{2-26}$$

$$\Delta\beta_d = \beta_{Damaged} - \beta_{Member} \tag{2-27}$$

Ghosn et. al. note that for the damaged state the expected maximum live load should be taken from a 2 year maximum load to account for the inspection period rather than the 75 year lifetime maximum load considered for the other failure states.

2.3.5: Schenck, Laman, and Boothby 1999:

“Comparison of Experimental and Analytical Load-Rating Methodologies for a Pony Truss Bridge”

To determine a means of rating the safety of existing pony truss bridges a pony truss bridge in Pennsylvania was modeled using STAAD III and this model compared to the bridge itself with considerations for corrosion of steel members, spalling of the deck, and load dynamics as well as the ease of obtaining sufficiently detailed information. The bridge was loaded with trucks both at a crawl and at the posted speed limit to provide

experimental data. The experimental data was then compared to numerical models produced in STAAD III with different end fixity for the connections between the stringer and floor beam, and the floor beam to the truss. The most accurate numerical model was found to be the one which most closely resembled the assumptions the bridge had almost certainly been designed with, floor beams fixed to the truss, stringers pinned to the floor beam, and the slab fully composite with the stringers.

The experimental rating factor was given as,

$$RF_{Exp} = \left(\frac{\sigma_{All} - \sigma_{DL}}{\sigma_{LL}} \right) \left(\frac{M_{Calib}}{M_{Rating}} \right) \tag{2-28}$$

where σ_{All} is the allowable stress $0.55F_y$ for inventory rating and $0.75F_y$ for operating rating, σ_{DL} is the dead load stress, σ_{LL} is the live load stress, M_{Calib} is the maximum moment test vehicle, and M_{Rating} is the maximum moment from a rating vehicle.

The experimental rating factor was calculated based on M_{RATING} from an HS-20 and ML-80 truck load considering the experimental data from the bridge as well as the numerical models. The different rating factors were compared to show the amount of refinement adding detail applies to the rating factors and what members are likely to become insufficient first.

2.3.6: Barth, Michaelson, and Stains 2012:

"Towards the Development of Redundancy Assessment Protocols for Steel Truss Bridges"

Barth, Michaelson, and Stains (2012) considered the literature available on the topic of bridge redundancies and selected the methodology presented in NCHRP Report 406 (Ghosn and Moses, 1997) as the means of determining redundancy. This required a linear model to determine what members met the fracture critical definition defined by AASHTO (2010) as "components in tension whose failure is expected to result in the collapse of the bridge or the inability of the bridge to perform its function," as well as to determine the load for first member failure. A nonlinear model is also required to analyze the damaged structure. Towards that end a model was developed in ABAQUS of a bridge over Little Mill Creek in Jackson County West Virginia. The intact highly detailed model was validated to the intact bridge using strain indicators and a loaded truck.

Members identified as fracture critical were removed in the highly detailed model and redundancy calculations performed for each fracture critical member. The bridge was found to be nonredundant based on the prescribed minimums in NCHRP Report 406 which is to have the damaged redundancy factor, R_d, be at least 0.5

2.3.7: FHWA-NHI-12-049 2012:

The FHWA NHI 12-049 Bridge Inspection Reference Manual is a comprehensive guide for bridge inspectors and owners to completely understand the intricacies of bridge inspection. The Manual provides detailed instructions for the application of the National Bridge Inspection Standards, which regulates inspection procedures, frequency of inspections, qualifications of inspection personnel, contents of inspection reports, and

maintenance of bridge inventory. The manual covers safety fundamentals, inspection procedures for various bridge typologies and materials, including inspection guidelines for specific details such as bearings, substructures, waterways, etc. Steel trusses are covered in Section 10.4 and material on fracture critical is on page 10.4.24 of the manual. Finally, the Manual contains specific guidelines for the preparation of inspection reports.

2.3.8: Diggelman, Connor, and Sherman, 2013 (FHWA-HRT-13-104):

Prior to the demolition of the US-421 Bridge over the Ohio River between Madison, Indiana and Milton, KY, members identified as fracture critical by simple load path redundancies were removed. The structure was a 149' long Pratt truss with seven panels built in 1930's from built up members riveted together. The original deck had been replaced by a prefabricated Exodermic deck system. The results indicate a significantly more redundant structure than is obtained from generally held design assumptions.

A review of past destructively tested of bridges and historic collapses, including case studies of fractures which did not result in a collapse, was conducted. The destructive tests examined included tests only of two-girder bridges. Among the case studies mentioned, only girder bridges exhibited unexpected redundancy.

2.3.8.1: Experimental Study:

Strain gauges were placed throughout the truss. Five points on the main chords were monitored, with two strain gauges on the top and two on the bottom of each member to measure bending. Diagonals, verticals, and bracing received similar treatment, although W-shaped members only required two strain gauges to record the member's behavior. Eight locations on diagonal, vertical and bracing members were monitored. Stringers and floor beams were all W-shaped and thus only required two strain gauges to monitor, five locations among the stringers and floor beams were monitored.

Stress data for fatigue analysis was collected while the bridge was still in service over the course of 71.9 days using the rain flow counting algorithm and ignoring cycles of less than 1.5^{ksi}. AASHTO's constant-amplitude fatigue limit was compared to the resulting stress range histograms to determine members probable remaining fatigue life, all members were estimated to have fatigue lives of over 100 years, beyond which predictions are questionable.

Time history data was also collected through the strain gauges, triggered by high stresses. This provided many time histories of particularly large loads going over the bridge. As these triggered events merely recount the bridges stress experiences the exact nature of the loads was unknown, however, many common load types such as tractor-trailers will give distinct stress time histories, particularly in the stringers. These time histories give peak stresses for common traffic, including the perhaps less than revelatory fact that loads greater than the posted limit likely crossed that bridge.

The final loadings of the intact bridge were controlled load testing, where trucks of known weight and dimensions were driven at a crawl as well as parked to obtain the bending and axial response of the members to a known load. The parked loading was used to confirm the accuracy of the numerical model.

A controlled demolition was the final portion of FHWA-HRT-13-104. Sand weighing 145,000 pounds was spread along the center three panels of the bridge, this amount being significantly greater than the live loads recorded for fatigue analysis. Comparison between the finite element and sand loaded bridge showed the finite element model to be somewhat conservative throughout, especially with respect to the stringers and floor beams which exhibited significantly less load than predicted by the model.

2.3.8.2: Finite Element Modeling:

A numerical model of the bridge was built using SAP2000. Shell elements were used for the deck and frame elements were used for the truss members, stringers, and floor beams. The yield stress used was 36^{ksi} and ultimate tensile strength of 58^{ksi} as the material specification on the plans was “carbon steel”. After demolition, material testing was able to be performed to confirm these assumptions.

Although the usual design method of truss design assumes pinned connections for connections between truss members and stringers with floor beams, this model used fixed connections for both. The long term data was used to confirm that, within the normal load range, these assumptions are reasonable.

The finite element model was also used to predict the effect of the removal of fracture critical members, both diagonal and along the bottom chord would have. The predicted effect of removing a bottom chord member was a stable structure, while removing the diagonal was predicted to induce collapse.

2.3.9: ASCE 41 2013:

ASCE41-13 is a standard that applies to the seismic evaluation and retrofit of existing buildings; in particular, it provides information on how to investigate and evaluate potential performance deficiencies of a building with respect to a series of preset performance objectives. While the focus of this standard is exclusively on the seismic behavior of buildings, the underlying concepts can be rationally generalized to other cases in a performance-based design framework, including the case of existing bridges. Using a more general terminology, the evaluation process begins with the establishment and selection of a performance objective and of a set of structural and nonstructural performance levels, which represent goals of design. The evaluation procedure then calls for the establishment of a demand level, and for the collection of as-built information. At this point, depending on the type and configuration of the structure, an appropriate evaluation procedure, including applicable analysis approaches and acceptance criteria, is followed, resulting in an evaluation report. The standard also presents a multi-tiered retrofit process. This process follows similar steps to those in the evaluation process with the exception that in place of evaluation procedures a multi-tiered set of retrofit procedures and strategies are presented, aimed at meeting the targeted performance objective. The concepts outlined as part of the ASC41-13 standard have been largely borrowed for the study presented herein, using rational adaptations to the case of pony truss bridges whenever necessary. A more detailed synopsis of ASCE 41-13 is presented in Chapter 4.

2.3.10: Barth and Michaelson 2014:

To develop a method to assess the reliability of truss bridges Barth and Michaelson begin with a finite element model capable of both linear and nonlinear analysis built in ABAQUS version 6.10 using shell elements to model the deck and beam elements to model floor beams and the truss elements. The connections between truss elements as well as the connections between stringers and floor beams were modeled as pinned connections. The deck was made fully composite with the stringers using the rigid beam multi point constraints. The vehicle load used throughout was the AASHTO HL-93 design truck (AASHTO, 2010) with the rear axle spacing maintained at the minimum distance of 14 ft as only simple-span structures were considered.

The statistical data used by Barth and Michaelson is as follows:

1. Dead loads are assumed to be normally distributed, with a bias factor of 1.05 and a coefficient of variation of 0.10 based on representative values for factory made components from Nowak and Collins (2000). However, these are the values for cast-in-place concrete in the second edition, proper values for factory made component dead loads are λ_D =1.03 and COV=0.08 (Nowak & Collins, 2013)
2. Live loads were presumed to follow a type I Extreme values distribution with a bias factor of 1.25 and a coefficient of variation of 0.12 based on Nowak and Collins (2000, 2013) which was based on the average daily truck traffic and an assumed lifetime of 75 years
3. The dynamic load allowance was considered a constant 1.854
4. The load combination used was the Extreme Event IV as defined in the PennDOT Design Manual, Part 4 (2012), a load combination exactly suited for the loss of one element. The dead load factor is 1.05 and the live load and impact factor is 1.15
5. Capacity of steel tension elements were assumed to follow a lognormal distribution with a bias factor of 1.05 and a coefficient of variation of 0.11 based on (Nowak and Collins 2000). The tension resistance factor was taken as 0.95 throughout.
6. The capacity of the members in compression was also taken as following a lognormal distribution, though the statistical data changes with the slenderness of the member. The statistical data was taken from the Ziemian (2010) data used to develop the original SSRS curves. The resistance factor was taken as a constant 0.90 throughout.

The procedure, as laid out by Barth and Michaelson, is as follows:

1. Member capacities are determined.
2. A finite element model capable of both linear and nonlinear analysis is built, including all main load carrying elements.
3. Dead and live loads are applied, with trucks moving side by side and positioned side by side both longitudinally and transversely to establish maximum load effects.
4. Determine the fracture critical members as well as especially critical members, it is important to recall that the definition AASHTO gives for fracture critical members

specifies that they are members in tension, so flexure and compressive members which could induce collapse by failing should also be considered when examining a bridge's redundancy.

5. Simulate damage conditions by severing one of the members identified in step 5 such that it provides no resistance for the system.
6. Perform the analysis with the live load at each panel point following the application of the dead load. Do this analysis for each of the members found to be especially consequential in Step 4.
7. Combine the load effects according to the load combination and multiply the member resistances by their resistance factors.
8. For each cut chord case and each panel point live load location perform a Monte Carlo simulation. The results of the Monte Carlo will give the probability of the bridge surviving the load condition, as well as the statistical data.

2.4: Literature Summary:

The means of establishing the reliability of a bridge vary widely, from simple deterministic methods such as simply counting degrees of indeterminacy to calculation-heavy Monte-Carlo simulations and fuzzy logic based redundancy factors. Many focus on targeting reliability indices which can fit easily within the LRFD design paradigm of targeting a reliability index for individual member performance.

Furuta et al. established a means of determining the probability of a loading exciding capacity of a whole structure under a continuum of damage, unfortunately fuzzy logic is an important component of considering the damage states is unwieldy in most conditions. Targeting a probability of reserve strength is appealing and if knowledge of damage can be increased to the point it may be rounded up to absolute, or the fuzziness may be accounted for more simply this approach could easily become a simple means of quantifying reliability.

Frangopol and Curley attempted just that in 1987, replacing the fuzziness of the damage to members with discreet values reducing some of the mathematical complexity. From this approach the reliability index of a damaged stated may be obtained with relative ease. With the caveat that when a member reached a 50% probability of failure it was removed from the analysis, this allows for only one analysis, rather than the branching fault tree that would result from attempting a rigorous probabilistic solution.

Ghosn et al. continue the study of reliability by establishing a means of finding a system factor. This is a more rigorous means of establishing the ηR factor found in the AASHTO standards. Though they apply it to the capacity side of the equation rather than the loading side, the effects it accounts for are the same and the position is arbitrary. The system factor allows for directly targeting a reliability index for the system as a whole. Better yet, the probabilistic behavior may be predicted using deterministic analysis in this case as long as the variances of the capacity are known, making this a particularly simple analysis to perform. This method bears a close resemblance to NCHRP 406 which shares the benefit of using the probabilistic way individual members are designed and the variances

there to obtain the behavior of the entire structure. This shows great promise for simply calculating redundancy of structures. The relative reliability indexes serve as measures of reliability as well as allowing easy comparison to designs known and accepted as reliable.

Schenck et al (1999) and Stains (2012) give insight into how to model pony truss bridges for the sake of reliability analysis. Stains focuses on highly detailed models, featuring the inclusion of gussets, modeling members with shells, and comparing the model to an existing bridge. All this fulfilling the process described in NCHRP 406. Schenck examines sparser models, regarding the end releases of stringers and releases in the truss members, also in relation to an actual bridge. In this case finding the effects of model detail has on the rating factors and which member fails first.

Diggelman et al. also considered an existing bridge. In their case the bridge was being demolished and so not only could analytical models be checked against it, but in this case damage could be done to the bridge while member stress and deflection was monitored. The demolition showed that normal analysis of truss structures is excessively conservative and found significant sources of redundancy. They also found that truss members and stringers should be modeled as fixed rather than pinned.

Finally, Barth and Michaelson established a means of establishing redundancy through a Monte-Carlo simulation. A brute force method that nonetheless gives significant information regarding the probability of redundancy. This method is computationally demanding though this may prevent it from being widely used. In favor of more deterministic approaches such as those of NCHRP report 406 or Ghosn et al. eventually perhaps the system factor will be implemented or something like it for all structures.

Chapter 3 - Pony-Truss Bridges

3.1: Pony-Truss Bridge Description and Typical Details:

A pony-truss bridge (PTB) is a bridge system comprised of two parallel trusses simply supported at their ends that in turn support a floor system. Each truss is comprised of a top chord in compression, a bottom chord in tension, and diagonal members framing between the top and bottom chords at panel points that can be either in tension, compression, or subject to load reversals between tension and compression. Vertical members are often included at the panel point of the trusses, which are typically zero-force members and are included as lateral bracing for the top chord of the truss. Floor beams span from the panel points of one truss to the panel points of the other, either perpendicular to the trusses or parallel to the skew. Stringers run parallel to the trusses and are supported by the floor beams. Decking, supported by the stringers, can be constructed of wood, asphalt on metal decking, open or concrete-filled steel grids, or concrete. Nominal lateral framing, often consisting of rods or light angles, is generally included in the floor system to carry lateral loads to the abutments. A typical PTB is shown in Figure 3-1.

Figure 3-1: A Typical Pony-Truss Bridge in Ohio

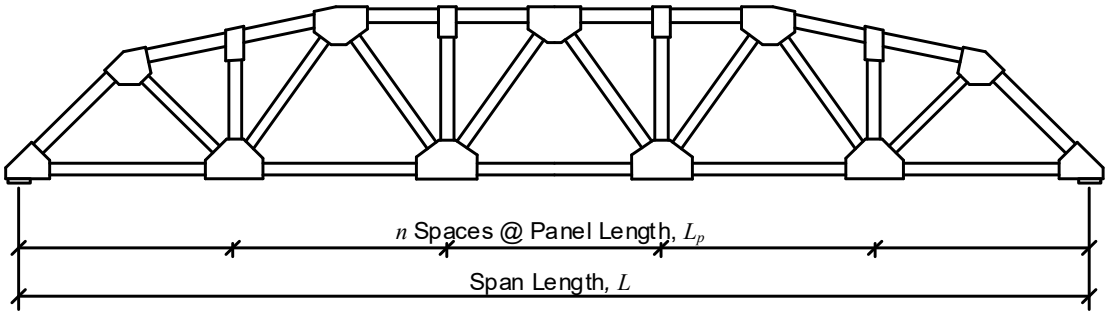

Figure 3-2: Span Length, Panel Length, and Depth Dimensions of PTBs

Truss bridges typically divide the span length of the bridge, L, into a number of panels, each having an equal panel length designated as L_p as shown in Figure 3-2 for the Bloody Bridge. A photo of the Bloody Bridge is shown in Figure 3-3. The primary difference between a pony-truss bridge and through-truss bridge is that the pony-truss bridge lacks framing members above the roadway between the two trusses that a through truss would have. Thus pony-trusses have a similar load carrying mechanism as a through-truss but have a slightly different mechanism for maintaining stability of the compression chord. While a through-truss bridge relies on the connecting members above the roadway to provide lateral bracing to the top chord that is in compression, a PTB must rely on the flexural support of the floor beams and web members to keep the top chords of the trusses stable under compressive load.

Older PTBs employ members built-up from plates using rivets. Top chords are typically three or four sided box members, diagonals and verticals are typically I-shaped, and bottom chords are made up of pairs of plates, pairs of angles, channels, or pairs of channels as is shown in Figure 3-4. Newer PTBs employ rolled sections of a modest weight in the range of 20 to 40 lbs per ft. Members are typically arranged such that the webs of the sections are perpendicular to the plane of the truss. In this arrangement, strong-axis buckling of the top chord members is perpendicular to the plane of the truss, placing the highest buckling resistance in line with the less stable direction. Weak-axis buckling of the top chord members is in the plane of the truss and corresponds to unbraced lengths approximately equal to the panel length of the trusses. Additionally, arranging the verticals with their webs perpendicular to the plane of the truss allows them to provide bracing to the top truss chord through strong axis bending, which provides much more stiffness than the alternative.

3.1.1: Super Structure Description:

An inventory was obtained from ODOT on Nov 7, 2014, and includes 873 structures in the State of Ohio defined as steel pony truss structures with fracture critical members that are inspected by county agencies. Figure 3-5 shows the statistical distribution of the year that the pony-truss bridges in the ODOT were constructed.

Figure 3-3: Bloody Bridge, in St. Mary's, OH[1]

Figure 3-4: Typical Cross Sections Used for Bottom Chords of PTBs

The typical span-to-depth ratio of a pony-truss bridge is on the order of 10:1. Thus a practical upper limit on span length would be approximately 160' since longer trusses would be sufficiently deep to permit framing between the top chords without obstructing the passage of vehicles on the roadway. Pony-truss bridges shorter than approximately 30 to 40' in span are not economical compared to alternative bridge types. Figure 3-6 shows the statistical distribution of the span lengths of PTBs in the ODOT inventory. The longest bridge has a span of 160', the shortest has a span of 16', the average span length is approximately 81', the median span length is 77', and the standard deviation is 27.8', which means that approximately 68% of the PTB inventory is between approximately 53' and 109' in span.

PTBs are generally designed for two lanes of traffic, though some older bridges can accommodate only a single lane using modern lane widths. In some cases, PTBs are designed to accommodate more than two lanes. The ODOT inventory data indicates that

[1] http://www.karenmillerbennett.com/ accessed on June 7, 2015.

all of the bridges are currently carrying one or two lanes. Figure 3-7 shows the statistical distribution of the deck widths, which includes one bridge with a deck width of 55' that would, by current specifications, be designed for four lanes of traffic.

More than 70% of the PTBs in the ODOT inventory have zero skew. Figure 3-8 shows the statistical distribution of skew angle for the remaining 249 bridges. For skewed bridges, the maximum skew angle is 60°, the average and median skew angles are 26° and 25°, respectively, and the standard deviation is 12.7°. When PTBs are skewed, floor beams are often oriented parallel to the skew, but sometimes, the panel points of the two trusses can be located such that the floor beams can be detailed perpendicular to the truss framing into different panel points on each truss.

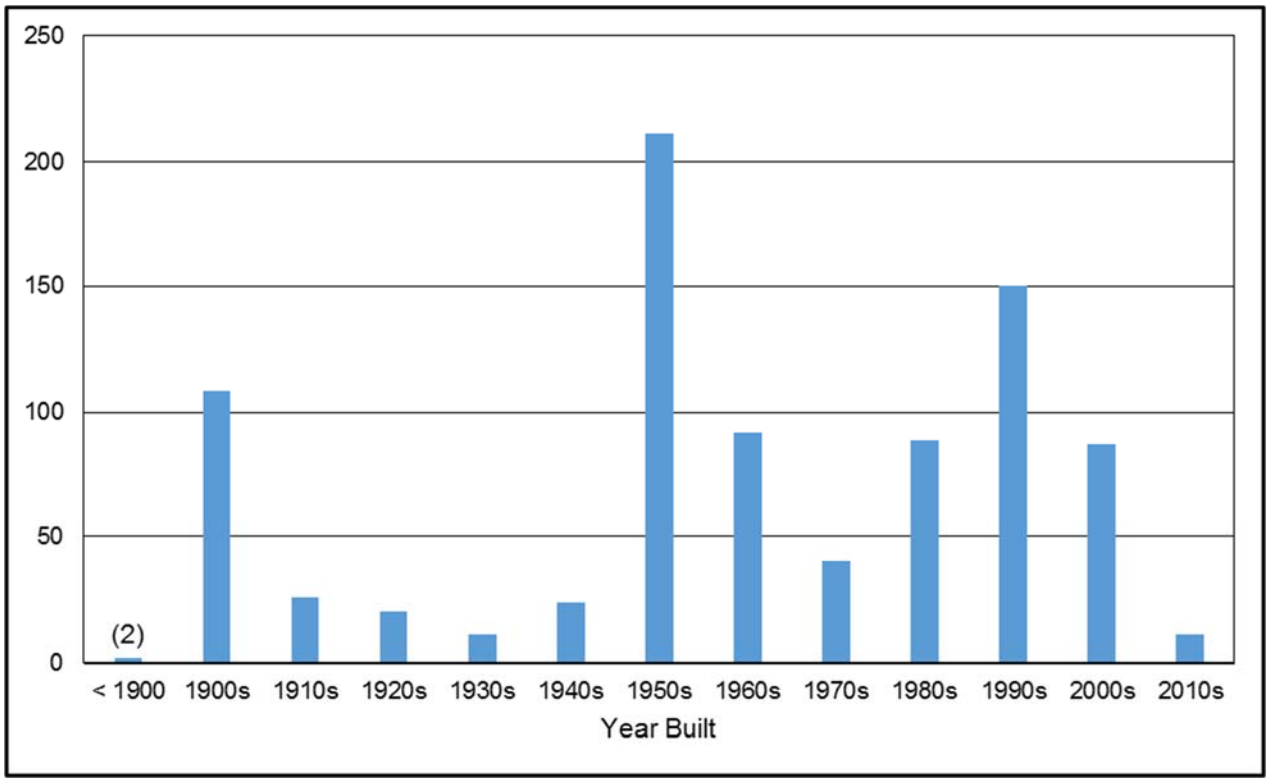

Figure 3-5: Year Built for Pony-Truss Bridges in the ODOT Inventory

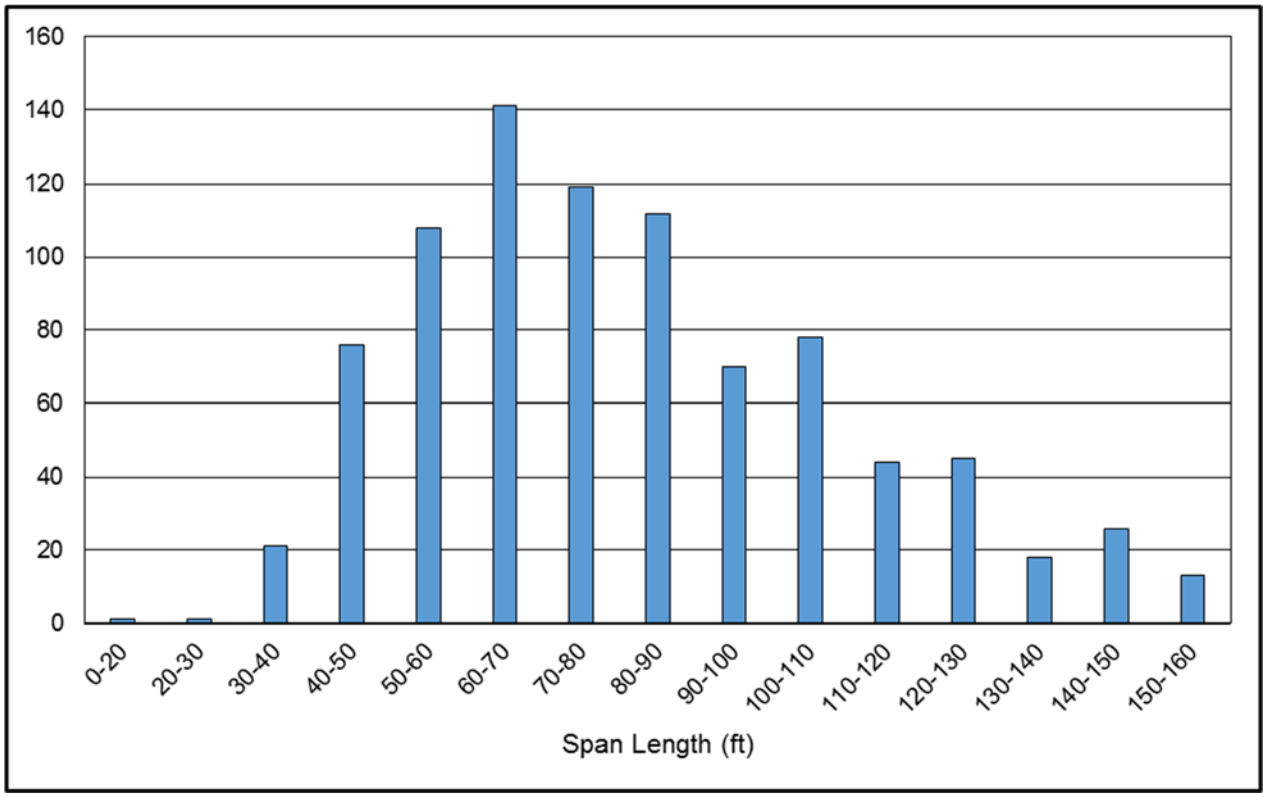

Figure 3-6: Span Lengths of Pony-Truss Bridges in the ODOT Inventory

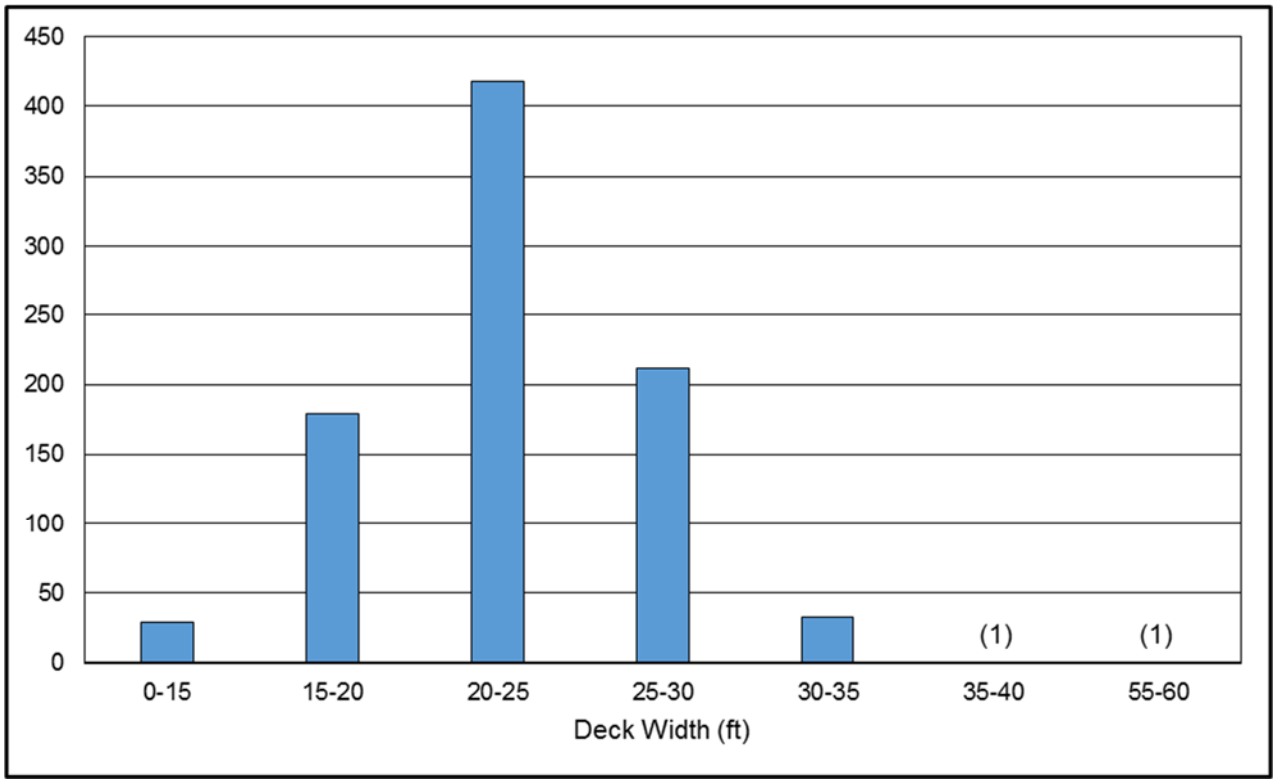

Figure 3-7: Deck Widths of Pony-Truss Bridges in ODOT Inventory

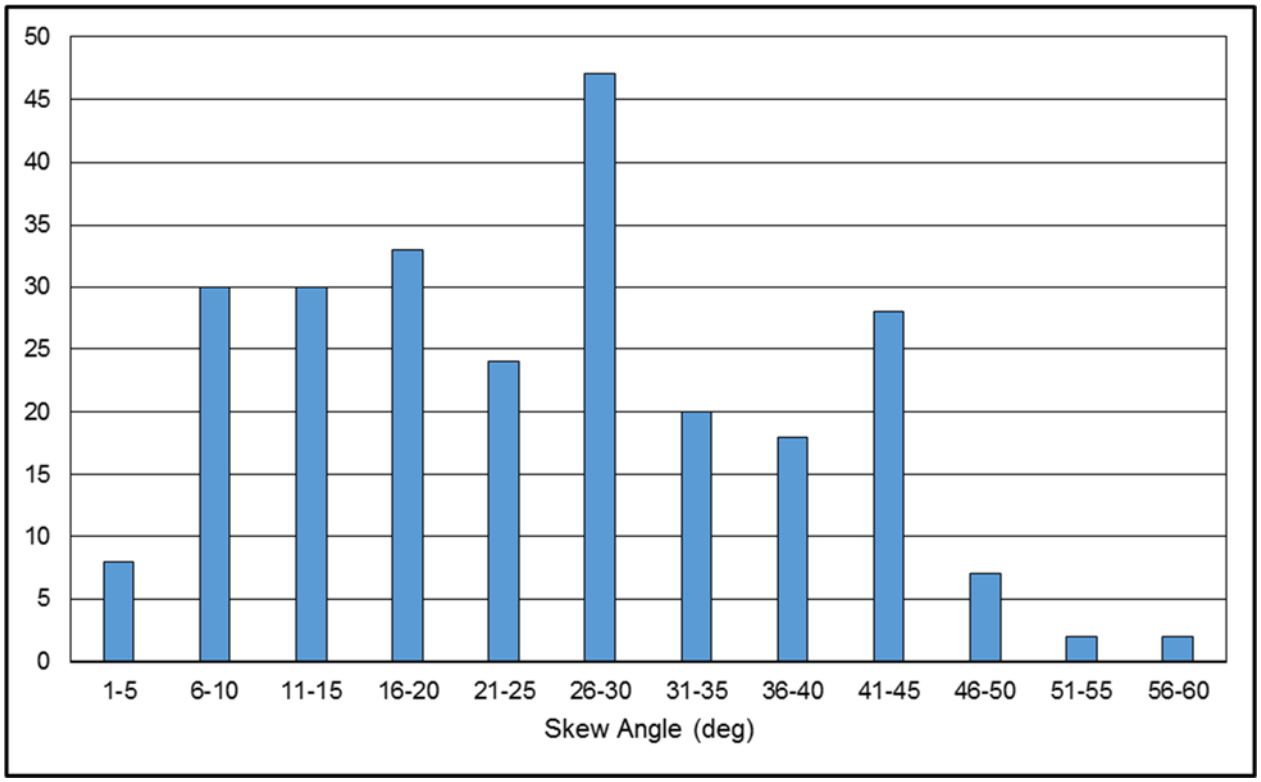

Figure 3-8: Skew Angle of Pony-Truss Bridges in ODOT Inventory

3.1.2: Floor Systems:

Framing for the floor systems of PTBs generally consists of a deck supported by stringers running parallel to the trusses, which are in turn supported by floor beams that span transversely between the lower panel points of the trusses. In an "underslung" configuration shown as case (a) in Figure 3-9, the stringers are situated such that they sit on top of the floor beams - the bottom flange of the stringers bear on the top flanges of the floor beam. Stringers are often designed as simply-supported and span from one floor beam to the next without continuity. In some cases, stringers are arranged such that they span two consecutive panels and are continuous across the intermediate floor beam. A pair of bolts or small fillet welds are often used at each end of the stringer members to secure the stringer to the floor beam.

In some cases, the floor system is detailed such that the top of steel of the stringers is at the same elevation as the top of steel of the floor beams in a so-called "framed" configuration, as is shown as case (b) in Figure 3-9. Framed floor systems require more fabrication than underslung floor systems, including coping of the top flange of stringers, fabrication of angle components, and drilling of additional holes, but offers the advantage of a more compact floor system which can be advantageous when vertical clearance is an issue. In one case, the authors observed a framed PTB floor system where the stringers were lowered relative to the floor beams such that the top flange of the stringers did not need to be coped.

In end panels of PTBs, stringers are sometimes detailed to bear directly or through bearing plates on the abutment, they sometimes bear on sill members such as a small

square or rectangular HSS member, or sometimes they are supported by an end floor beam that may span from truss to truss or may be supported intermediately along its length by the abutment. Depending on the deck type, deck width, and panel length, stringer members are typically W12 to W16 members ranging in weight from 30 to 60 lbs. per ft. spaced at 2'-4" to 6'-0" center to center.

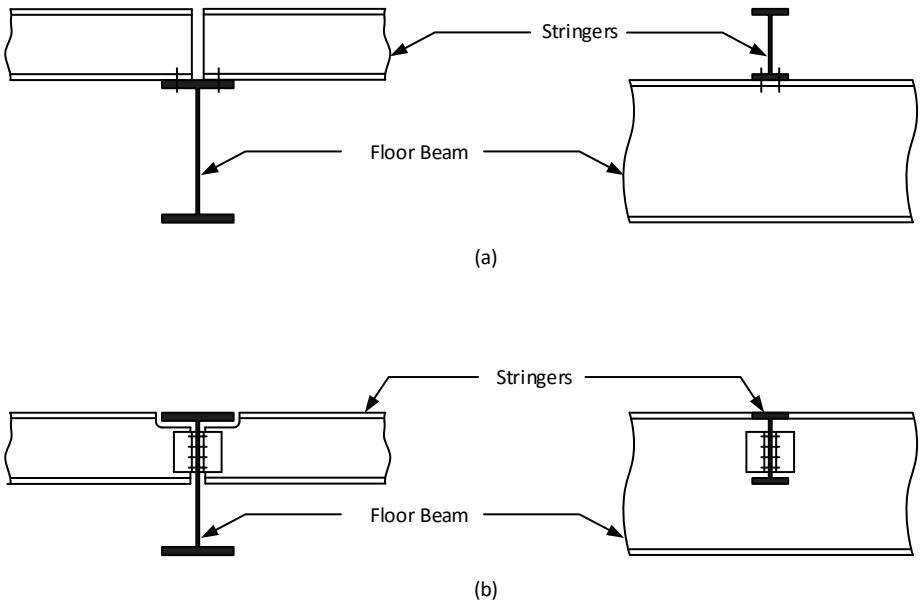

Figure 3-9: (a) Underslung and (b) Framed Floor System Configurations

Depending on the width of the bridge (or length of the floor beams) and the panel length of the trusses, floor beams can range in size from W16 to W36 members ranging in weight from 50 to 130 lbs. per ft. Floor beams frame into panel points at their ends with some level of rotational restraint. Common end connection details for floor beams are shown in Figure 3-10. Case (a) shows a vertical that is extended below the gusset connection with the bottom chord and diagonals to allow a header plate connection to the inside flange of the vertical member. Case (b) is very similar to case (a) with the exception that a double web angle connection is made from the floor beam to the inside flange of the vertical member. This connection, though more flexible than the header plate connection in case (a), still has some rotational stiffness. Case (c) is again similar to case (a), but in this case the floor beam extended instead of the vertical and an endplate and knee brace are used to connect to floor beam to the truss. The endplate and knee brace are sometimes incorporated into the gusset connection of the truss. In Case (d), a header plate is used to connect the floor beam to the truss, which often becomes part of the gusset connection within the truss. This last case has the benefit of raising the floor system relative to the bottom chord, which coupled with a framed floor system, can be advantageous when vertical clearance below the bridge must be preserved.

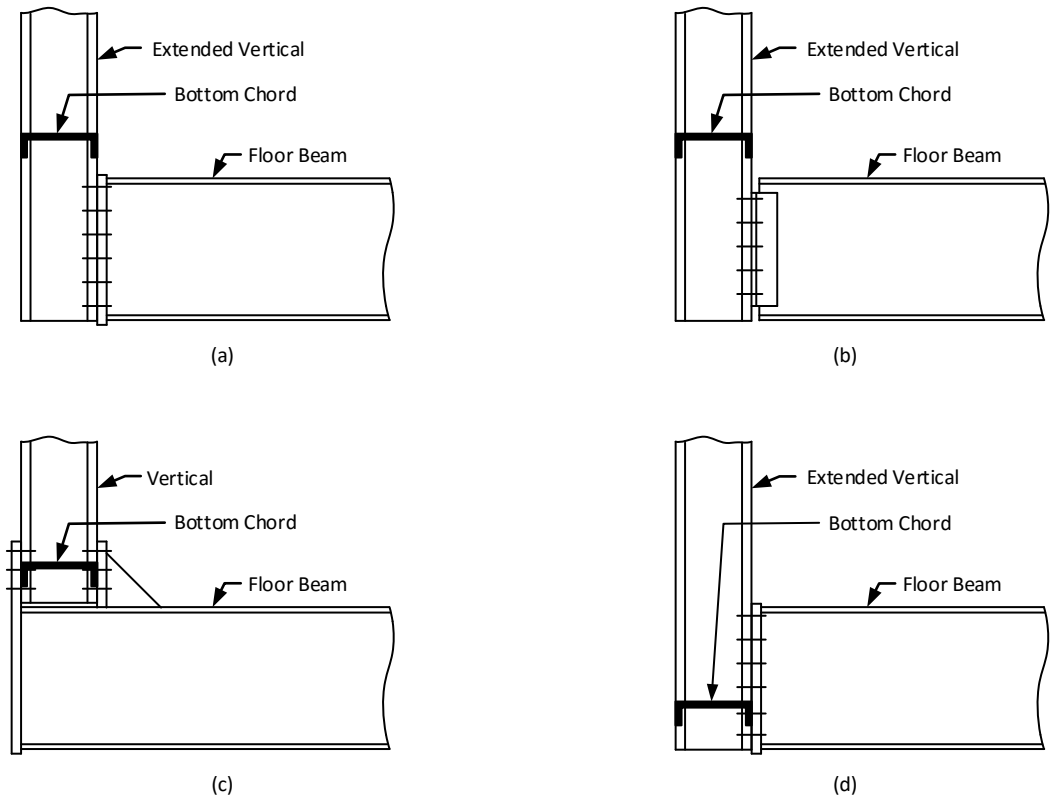

Figure 3-10: Common Details for End Connections of Floor Beams in PTBs

3.1.3: Bridge Decks:

Figure 3-11 shows the distribution of deck types for PTBs in the ODOT inventory. As is shown, the vast majority of PTBs, 84%, have corrugated steel plate decks that are typically filled with asphalt or sometimes gravel. A detail of the decking that is often used is shown in Figure 3-12. This decking is generally attached to the stringers using metal clips that clamp to the top flange of the stringer to the deck using structural bolts, as is shown in Figure 3-12.

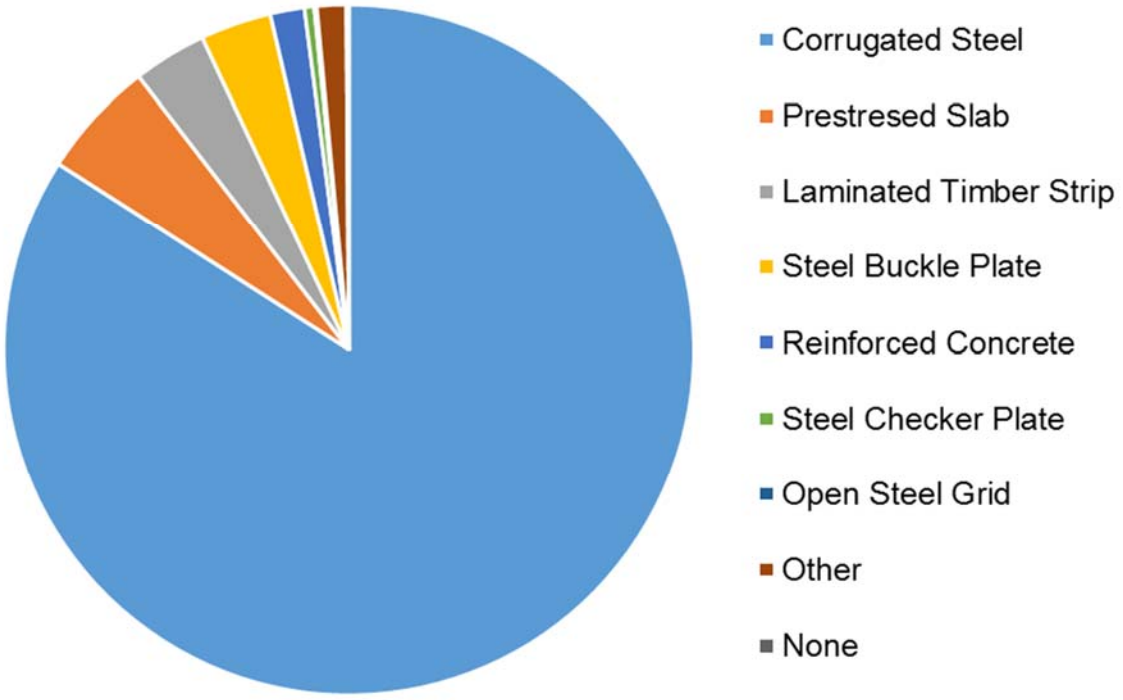

Figure 3-11: Types of Bridge Decks on Pony-Truss Bridges in ODOT Inventory

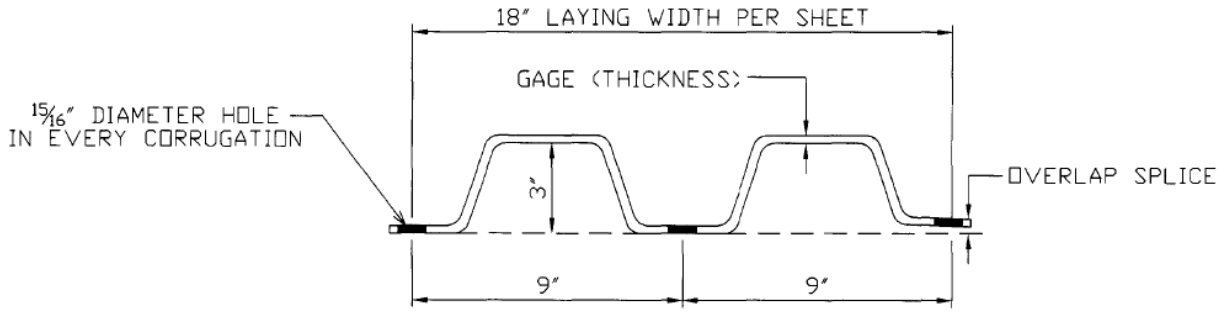

Figure 3-12: 3" x 9" Corrugated Metal Flooring

Prestressed slabs are another option for bridge decks, representing approximately 5% of ODOT PTBs. Wooden decking represents approximately 3% of ODOT PTBs. Wooden timbers are arranged transversely spanning perpendicular to the stringers. Metal clips are used to secure the timbers to the top flanges of the stringers but these clips likely have little strength. An asphalt overlay is often placed on top of the wooden decking. Reinforced concrete decks are found on approximately 2% of ODOT PTBs.

Figure 3-13: Typical Attachment of Asphalt-Filled Metal Decking to Stringers

3.2: Design Assumptions for Pony-Truss Bridges:

A simple analysis and design of a point truss bridge is generally completed using a 2D analysis approach assuming pinned connections.

Lateral buckling of the top chord can be analyzed in several ways. The process of finding the critical buckling stress for a top chord member that has discrete elastic lateral restraints is cumbersome and therefore conservative estimations are often made. A complete analysis would involve a full 3D model of the framing system, thus allowing a realistic lateral restraint of the top chord to be considered. However, due to computational time needed, the following assumptions (or combination thereof) are commonly made and often arrive at a conservatively stiff bracing system of the top chord.

1) Lateral support stiffness can be provided equal to a predetermined percentage of compressive capacity in the top chord. Using 2.5% of the chord compressive capacity is commonly referred to from AREMA Chapter 15 (AREMA, 2015). The lateral deflection of web members can be conservatively calculated and limited to a reasonable amount to ensure stiffness. This method is simplistic and has been shown to be adequately conservative.

2) Analyzing the top chord as a compression member with lateral spring supports (equal to web member bending stiffness) to ensure global buckling is controlled is another method, but is more computationally challenging due to its indeterminate nature. Typically this is completed with a 2D finite element program. Neither of the previous alternatives take into account the stiffness of the floor beam, whose end rotation and connectivity

contribute to the lateral stiffness and deflection of the web members, so assumptions for lateral support stiffness are critical to either process.

3.2.1: Strength Design Approach for Pony-Truss Bridges:

Pony-Truss Bridges (PTBs) are generally designed using a 2D analysis approach, wherein a certain percentage of the gravity loads is assumed to be supported by one of the trusses, and then that truss is analyzed and designed as a planar structure. Live loads are assumed to enter through the deck, pass through the stringers, into the floor beams, and then enter the trusses as point loads at the panel pointed where the floor beam are attached. The trusses carry the loads through bearing or seats to the abutments. The load path for dead loads is very similar aside from the assumption that the self-weight of the truss members, which actually acts vertically along the length of each member, is assumed to be concentrated at the truss nodes at each end of each member. Lateral loads, primarily from wind in Ohio, are rarely substantial and are resisted by “lateral rods” or “lateral angles” that are typically arranged in an X below the stringers in each panel of the floor system.

Lateral stability of the trusses is maintained by moment connections between the floor beams and the trusses. Verticals, which are essentially zero-force members, connect to the floor beams at their lower ends and frame from the lower panel points of the truss to the top chord to stiffen the top chord against lateral displacements. Verticals also provide mid-length bracing to members in the top against in-plane, weak-axis member buckling.

Truss members are designed to carry tension, compression, or both. In tension, members are designed for limit states of gross-section yielding, net-section fracture, and are checked to insure adequate stiffness to prevent vibrations. It is preferable to design tension members such that gross-section yielding governs over net-section fracture, either at the nominal strengths or factored strengths. This can be challenging, however, considering that I-shaped members are often attached only through their flanges, which creates a shear lag issue that reduces the net-section fracture strength. Detailing chord member to be continuous at panel points helps with the situation but can be challenging when extended verticals are used or in other cases.

In compression, members are designed for flexural buckling, typically using an effective length factor of 0.75 as suggested in the 7th Edition of AASHTO LRFD Section 4.6.2.5 (AASHTO 2015).

End connections of truss members can be bolted or welded, depending primarily on the era during which the truss was built or depending on owner, engineer, and fabricator preferences. In some case a combination of bolting and welding is employed, employing shop-welded connections with field-bolted splices. Bolts are designed for simple shear, whilst members and gussets are designed for bearing strength, tear out, and block shear. Newer guidance suggests checking gussets for gross section yielding, net section fracture, block shear rupture, and buckling in tension, compression, and shear as appropriate (FHWA 2009).

Although floor beams are usually connected at their ends with moment connections, they are designed assuming that they are simply supported. This comes from the reality that even though there is rotational restraint between the floor beams and trusses, the trusses

themselves are free to rotate out of their plane, thus providing little end restraint to the floor beams. 3D analyses of PTBs - even with fully restrained floor beam to truss connections - show very little end moments developed in the floor beam. Although floor beams are assumed to carry loads from the floor system to the trusses, they are not assumed during design to carry loads from one truss to the other.

Stringers, too, are designed as simply-supported beams. In some uncommon cases, stringers are detailed to continuously span two or more panels (three or more floor beams). Stringers are sometimes connected to the floor beams using bolts or welds, but in some cases, generally in underslung floor systems, the stringers may not have a positive connection to the floor beams aside from simple bearing. During design, stringers are not assumed to carry axial forces.

Bridge decks in PTBs are designed to carry wheel loads transversely through flexure to the stringers. During design, decks are not typically assumed during design to carry in-plane forces or to provide strength to the stringers or floor system. If they are to assist in global strength, they will be in tension due to being below the neutral axis of the structure. Furthermore, there will be a lag in lateral force transfer from the tension flange of the truss to the tension in the deck.

Bearings and seats are designed for the vertical reactions of the trusses and to allow longitudinal movement due to thermal expansion and contraction of the system. Stringers and trusses are typically all either fixed or expansion at each substructure. Stringer fixity varies, but truss fixity is typically through anchor bolts through a masonry and/or sole plate.

3.2.2: Fracture Critical Members in Pony Truss Bridges:

Truss members that are in tension or experience tension are generally considered to be fracture critical during design because, based on the 2D design approach described earlier, there is no load path redundancy in the system. This typically includes members in the bottom chords and most of the diagonal members.

Floor beams are also often considered to be fracture critical members. Some states consider all floor beams to be fracture critical members, others consider them to be fracture critical when one or more of the following conditions exist (FHWA-NHI 12-049, 2012):

1. The floor beam has flexible or hinged connections at its ends,
2. The spacing of the floor beams is greater than 14’-0”,
3. There are no stringers in the floor systems, or
4. The stringers are detailed as simply-supported beams.

It is important to keep in mind, however, that the conditions listed above are taken from FHWA-NHI 12-049, which is an inspection manual and not a specification. Thus those conditions should be interpreted as suggestions and not as strict rules. It is speculated that the floor-beam spacing of 14’-0” has roots in the Pennsylvania DOT inspection guidelines since the primary authors of FHWA-NHI 12-049 were engineers from an engineering firm that have strong ties to PennDOT.

Stringers are not typically considered to be fracture critical since there are usually several of them across the width of the deck, they are typically closely spaced, and the deck is generally designed to be continuous flexurally across several or all of the stringers.

3.3: Secondary Load Paths and System Redundancy in Pony-Truss Bridges:

While pony truss bridges are generally designed using 2D analysis methods that often result in non-redundant load paths, secondary load paths do exist in the finished bridges. These secondary load paths often depend on the details of the design, such as connections between floor beams and stringers, connections between the stringers and deck, connections between stringers and the abutments, etc. Further, the secondary load paths are often less stiff than the primary load paths meaning that they usually participate little in carry loads until larger deformations are experienced, or when the primary load path is interrupted.

The following sections address different secondary load paths that may exist in pony truss bridges.

3.3.1: Internal Member Redundancy:

Internal member redundancy can be considered within a couple of different contexts. On one hand, it can be considered within the context of member redundancy since all of the cross sectional elements making up an internally redundant member share load and thus if a member in the primary load path, then all elements of that member also participate in the primary load path. Simply having an internally redundant member is not sufficient to declare that that member is not facture critical, however. It still has to be shown that in the event of the fracture of one of the elements making up that member, that the remaining element(s) will have sufficient strength, stiffness, and fatigue life to keep the structure safe from collapse until the fracture in the fractured element can be discovered.

The analysis needed to show that the loss of an element in an internally redundant member will not result in a collapse is very similar to analysis that is required for the loss of an entire member. When considering the loss of entire member, the member is removed from a structural model, a nonlinear analysis is performed, and the results are evaluated to determine if sufficient load carrying capacity remains. In the former case, a 2D analysis of one truss is sometimes sufficient if (a) the internally redundant member is designed with enough extra capacity or if (b) the internally redundant member is composed of several redundant elements. If a 2D analysis is not sufficient, then a 3D analysis can be performed. In the latter case, a 2D analysis is rarely sufficient and a 3D analysis accounting for the potential benefits of other load paths provided by the floor system or other 3D framing in the system is almost always needed.

3.3.2: Axially Continuity of Stringers:

One of the most obvious secondary load paths in a pony truss bridge is the ability of the floor system to carry longitudinal loads and stresses. Depending on the type of floor system, the end connections of the stringers, and connections of the floor beams to the trusses, axially continuity in the stringers may provide a viable secondary load path to

provide redundancy for members in the bottom chords of the trusses. Several conditions must exist, however, before this load path can develop.

In order for the stringers to act as a secondary load path that is redundant with bottom chord members of the truss, loads that would otherwise be carried by a bottom chord member must first be transferred from the truss to the floor beam, then be transferred from the floor beam to the stringer(s), and then either (i) be transferred from the stringers, through another floor beam and back into the truss or (ii) in the case of an end panel in the truss, transferred from the stringers into the abutments. Figure 3-14 shows two stringers that have been spliced in their webs to provide axial continuity over a floor beam.

Figure 3-14: Welded Web Splice Plates in Stringers to provide Axial Continuity

Table 3-1 shows the level of load carried by the bottom chord members in the trusses and stringers in the Bloody Bridge under a number of different conditions based on finite element analyses. In all cases, the load applied was the unfactored dead load including future wearing surface. Case A represents a model with axial releases in all stringers. Case B represents a model with axial continuity in all stringers and roller supports for stringers at the abutments. Case C represents a model with axial continuity in all stringers and pinned supports for stringers at the abutments. Case D is similar to Case C expect that one of two channels making up the bottom chord of the right truss was removed. Case E is similar to Case D except that both channels making up the bottom chord of the right truss were removed. As is shown, the stringer lines closest to the trusses - the exterior stringers - carry the highest axial loads while the other stinger lines - the interior

stringers - carry much less, or almost no axial load. In some cases, the interior stringers actually carry a low level of compression.

Table 3-1: Bottom-Chord and Stringer Forces in the Bloody Bridge

	Left Chord	S7	S6	S5	S4	S3	S2	S1	Right Chord	Total
	(kip)	(kip)	(kip)	(kip)	(kip)	(kip)	(kip)	(kip)	(kip)	(kip)
Case A	110.48	0.00	0.00	0.00	0.00	0.00	0.00	0.00	110.48	220.96
	50%	0%	0%	0%	0%	0%	0%	0%	50%	
Case B	86.33	27.41	-1.93	-1.38	0.11	-1.38	-1.93	27.41	86.33	220.97
	39%	12%	-1%	-1%	0%	-1%	-1%	12%	39%	
Case C	64.19	14.04	-2.29	-0.25	0.18	-0.25	-2.29	14.04	64.19	151.56
	42%	9%	-2%	0%	0%	0%	-2%	9%	42%	
Case D	63.50	14.41	-2.24	-0.26	0.20	-0.22	-3.51	19.06	55.59	146.53
	43%	10%	-2%	0%	0%	0%	-2%	13%	38%	
Case E	58.83	16.83	-1.91	-0.35	0.30	-0.02	-11.64	52.42	0.00	114.46
	51%	15%	-2%	0%	0%	0%	-10%	46%	0%	

3.3.3: Flexural Continuity of Stringers:

In cases where the stringers are detailed as continuous over one or more intermediate floor beams, flexural continuity can provide a secondary load path that can help in the event of a floor beam fracture. This secondary load path would be largely dependent on the strength of the stringers as well as the connection between the stringers and floor beams. An example of this is illustrated in Figure 3-15 where the two-span stringers are laid out in a staggered arrangement such that along any given floor beam, continuity is provided at every other stringer. A photo of a continuous stringer from the Whitewater Ave Bridge in New Paris, OH, is shown in Figure 3-16. As was mentioned earlier, web splices are also provided at the simply-supported stringer ends, which would provide axial continuity in addition to the flexural continuity.

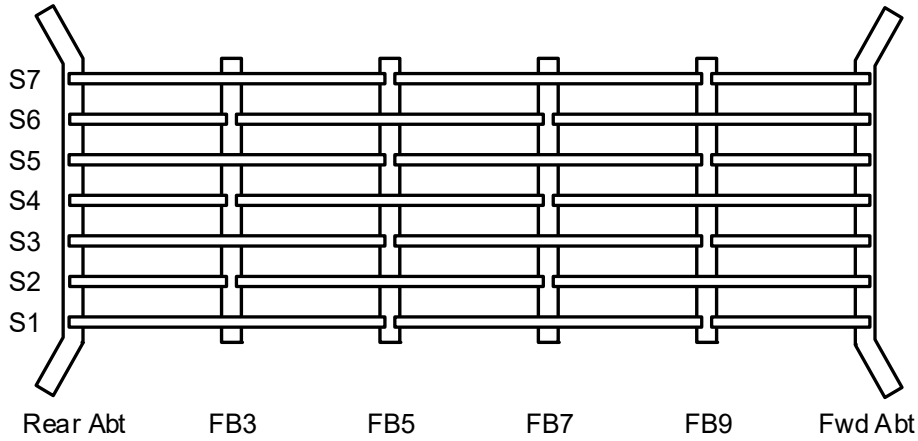

Figure 3-15: Stringers Detailed to be Continuous over One Intermediate Floor Beam

3.3.4: Longitudinal Continuity of the Deck:

As was stated previously, one of the most obvious secondary load paths in a pony truss bridge is the ability of the floor system to carry longitudinal loads and stresses. Depending on the type and condition of deck used, the deck or decking can provide longitudinal redundancy to help carry unintended loads in the event of the loss of a bottom chord member in one of the trusses. To supplement the load path in the trusses, there would have to be a means of transferring the forces in the truss through the floor beams, to the stringers, and into the deck, similar to that described in Section 3.3.2. Additionally, this secondary load path would depend significantly on the type and condition the deck as well as the connection between the deck and stringers.

3.3.5: Flexural Continuity of the Deck:

If the bridge deck and/or decking are properly attached to the stringers, and the stringers are properly attached to the floor beams, then flexure of the deck and/or decking in the transverse direction (perpendicular to the stringers) can be used as a secondary load path to help carry load in the event of a fracture in a stringer or floor beam. This is not terribly important for stringers since they are rarely categorized as fracture critical members, but in the case of floor beams, this can be quite beneficial. Clips, like those shown in Figure 3-16, are sometimes used to connect decking to the top flanges of stringers. The decking, designed to carry truck loads through flexure transverse to the stringers, also acts in parallel with the strength of the floor beams. In extreme cases, the flexural strength of the decking can be accounted for to provide additional strength to the floor beams.

Figure 3-16: Continuous Floor Beam in a Bridge in Preble County, OH

3.3.6: Moment Connections in the Trusses Instead of the Assumed Pins:

Trusses are generally modeled assuming that end connections of the members are pinned, permitting free rotation within the plane of the truss. In practice, however, these connections are either welded, riveted, or bolted with two or four rows of welds or fasteners creating what most would consider to be a “fixed” or fully restrained connection. Comparing the forces in the truss members from the Bloody Bridge Road Bridge shows that modeling the truss with pinned ends vs fully restrained ends (technically, a 2D “frame” model) results in a maximum percent difference of 1% for all of the members (excluding zero-force members). These results were obtained from two 2D linear and elastic analyses of the truss under dead load.

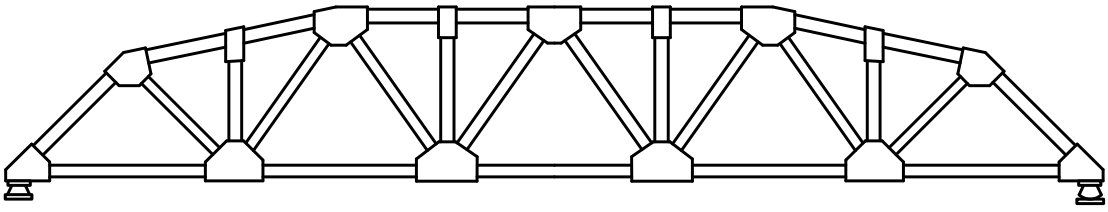

Figure 3-17: Bloody Bridge Truss

If the bottom chord member is removed from the center panel of the truss, the 2D truss model incorporating pinned connections becomes unstable and is unable to carry any load whatsoever. A 2D frame model incorporating fully restrained connections is able to carry a small amount of load through frame action, but this is generally not significant since the members in the truss will be bent about their weak axes and their weak axis moment capacity is very low. In the case of the Bloody Bridge Road Bridge, the 2D frame model subjected to a nonlinear analysis with plastic hinges defined at each end of the members was able to carry 17.46^{kip} of dead load before developing a collapse mechanism in the frame. This represents approximately 20% of a total dead load on the bridge of 84.54^{kip}, not to mention the live loads.

Based on these arguments, it seems that the added computational cost of modeling trusses as frames in not justified. It is simpler and slightly conservative to model the truss superstructures as analytical trusses instead of analytical frames.

3.3.7: Transfer of Force / Displacement from One Truss to the Other:

Another source of redundancy that is rarely utilized during design is the ability of one truss to assist the other by transferring forces and displacements through the floor beams. This load path requires end-connections of the floor beams to be fully restrained. Even then, the flexibility associated with this load path limits its usefulness. Since the top chords of the trusses in PTBs are rarely braced laterally, the full restraint of the connections at the ends of the floor beams is undermined by rotation of the trusses out of their plane. Still, transferring loads and displacements from one truss to the other can be helpful in the event of the loss of a primary load path member.

3.3.8: Indeterminate Support Conditions at Bearings and Seats:

Superstructures that are modeled as analytical trusses with pinned members are generally regarded as determinate structures inasmuch as the removal of a single member will result in an internally unstable system. If a truss is modeled with a pinned support at one end and a roller at the other, as is shown in Figure 3-17, then those supports will be externally determinate. If a pinned connection is provided at both ends of the truss, however, then the structure becomes externally indeterminate by one degree. This external redundancy can offset an internal instability, however. Considering Figure 3-18 where a bottom chord member is removed from the truss, if the horizontal displacement at the right support is restrained as is shown in Figure 3-19, then a stable system results. The stability of this system depends on many factors but a system designed with this contingency in mind can use indeterminate supports as a secondary load path.

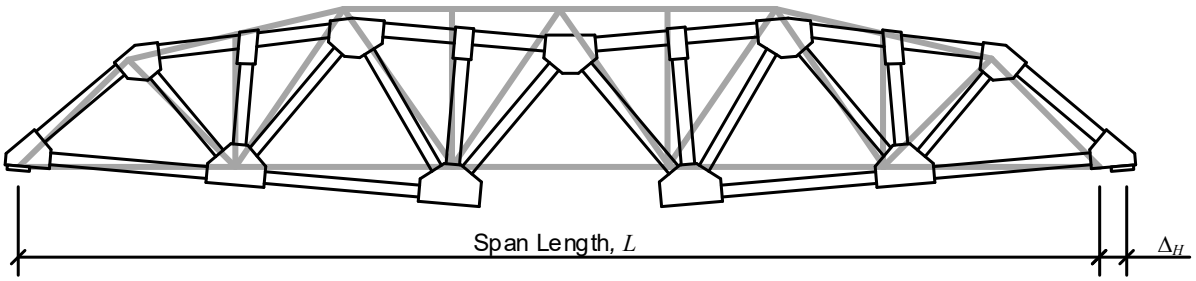

Figure 3-18: Indeterminate Support Conditions

Thermal expansion and contraction of the bridge has to be accommodated, either through expansion joints or integral abutments, but displacements due to thermal actions are 3 to 10 times smaller than the displacement corresponding to a collapse associated with the loss of a bottom chord member. Figure 3-19 shows a truss seat that is bearing horizontally against the back wall on a summer day at approximately 80°F. Additionally, bottom chord members that are designed to act exclusively in tension under in normal situations are put into a state of compression when the supports are engaged as a secondary load path. The level of compression increases as the magnitude of the displacement at the support increases. Thus balancing the need for to accommodate thermal actions with the need to restrict displacements associated with collapse is a challenge.

Figure 3-19: Truss Seat Bearing Horizontally with the Back Wall (Temp ≅ 80°F)

Chapter 4 - Redundancy Analysis of Structures

4.1: NCHRP 406:

As was noted in the literature review, NCHRP Report 406 represents a comprehensive work outlining methods for quantifying redundancy of structures based on a reliability approach. The document applies not just to fracture critical members, but to reliability in general. The document defines four critical limit states, (a) member failure, (b) ultimate capacity, (c) functionality, and (d) damaged conditions, and uses these limit states with a live-load margin defined as the amount of live load capacity of the structure remaining after dead loads have been applied. The live load margin is conceptually presented as

$$\text{LL Margin} = R_n - DL \tag{4-1}$$

where R_n is the nominal capacity and DL is the dead load. NCHRP 406 recommends using two side-by-side HS-20 trucks as the live load noting that, although other live load models were available, the widespread use of the HS-20 truck made it an easy-to-implement solution.

The live load margins are expressed as load factors, which, conceptually, are factors representing the number of live loads that are needed to reach a limit state after the dead loads are applied to the structure. The load factors are then used to compute reserve ratios, which are in turn used to determine levels of redundancy by comparing them to limits that are determined based on predetermined levels of reliability.

4.1.1: Member Failure Limit State:

The member failure limit state is defined as the capacity of the structure to resist first member failure. A member failure is defined as the exceedance of strength as computed using AASHTO equations for strength without resistance factors where the demand is computed using a linear-elastic model. This is generally expressed as the number of HS-20 trucks that are needed in addition to dead loads to cause a failure of any member in the structure, as

$$LF_1 = \frac{R_n - P_{DL}}{P_{LL}}, \tag{4-2}$$

where R_n is the nominal capacity of the member, P_{DL} is the member force or moment resulting from unfactored dead loads, and P_{LL} is the member force or moment resulting from unfactored live loads. As an example, suppose the nominal capacity of a member is $R_n = 550^{\text{kip}}$, the force present in that member due to dead load is $P_{DL} = 180^{\text{kip}}$, and the force in that member due to one instance of live load is $P_{LL} = 120^{\text{kip}}$. With these assumed values, the load factor associated with failure of that member is

$$LF_1 = \frac{550^{\text{kip}} - 180^{\text{kip}}}{120^{\text{kip}}} = 3.083 \tag{4-3}$$

which means that the member would be capable of supporting more than 3 instances of the live load before reaching its limit. If that member is the first member to fail as the live load is incrementally increased, then that load factor is LF_1.

An "instance" of live load is "one" of whatever live load model is chosen for the evaluation. If the recommendations of NCHRP 406 are selected, then one instance of live load would be two HS-20 trucks, positioned side-by-side in the critical position, without impact factors applied.

4.1.2: Required Member Strength Limit State:

The required member load factor, $LF_{1,req}$, is similar to the member failure load factor but is computed based on the strength required of the member instead of the strength actually provided by the member, which is generally larger than that required. The required member load factor is calculated as,

$$LF_{1,req} = \frac{R_{req} - P_{DL}}{P_{LL}}, \tag{4-4}$$

where R_{req} is the member strength required based on the design specification. Based on the AASHTO-LRFD specification, assuming that the Strength I load combination governs, and using the member yielding as the member limit state,

$$0.95R_{req} \geq 1.25DC + 1.50DW + 1.75(LL + IM), \tag{4-5}$$

The member strength reserve ratio can be calculated as,

$$r_1 = \frac{LF_1}{LF_{1,req}}, \tag{4-6}$$

4.1.3: Ultimate Strength Limit State:

The ultimate limit state is collapse of the structure. The load factor associated with collapse, LF_u, can be calculated by analyzing the structure under the effect of the dead loads and a designated live load using a nonlinear structural model of the bridge. The live load is incrementally increased until the system collapses and the number of instances of the live load at collapse is taken as LF_u. Mathematically, LF_u can be expressed as,

$$LF_u = \frac{L_u - DL}{LL}, \tag{4-7}$$

where DL and LL are the total applied dead load and one instance of live load, respectively, and L_u is the collapse load, i.e. the total applied load that causes a collapse mechanism to form in the structure. The reserve ratio associated with the ultimate capacity limit state is,

$$R_u = \frac{LF_u}{LF_1}. \tag{4-8}$$

A reserve ratio for the ultimate limit state of $R_u \geq R_{u,req} = 1.30$ is required for the bridge to be considered redundant.

4.1.4: Functionality Limit State:

The functionality limit state is defined based on the deflection of the structure. NCHRP 406 addresses several considerations associated with deflection criteria that could be considered to affect the serviceability of bridges. Ultimately the authors recommend a live load deflection limit of $L / 100$ as a practical limit on deflection, where L is the span length of the bridge. The load factor associated with this limit is

$$LF_f = \frac{L_f - DL}{LL}, \tag{4-9}$$

where L_f is the applied load resulting in a deflection equal to $L / 100$. The reserve ratio associated with the functionality limit state is,

$$R_f = \frac{LF_f}{LF_l}. \tag{4-10}$$

A reserve ratio for the functionality limit state of $R_f \geq R_{f,req} = 1.10$ is required for the bridge to be considered redundant.

NCHRP 406 recommends that, "*because redundancy is concerned with the performance of the structure, the displacements are checked in the main members only. The displacements of the slab or secondary members are not checked for this functionality limit state."* This recommendation and its applicability to pony truss bridges will be revisited in a later section.

4.1.5: Damage Limit State:

The damage limit state is meant to be included as a measure of the bridge's resiliency in the presence of unintended distress in the structure. This damage might result from an impact from a vessel or vehicle, loss of a member due to fracture, or the loss of a member due to terrorist activity. The damage is generally simulated by removing one or more members from a structural model of the bridge and simulating its behavior in that damaged condition by applying the dead load and then incrementally increasing the live load until a collapse mechanism forms in the nonlinear inelastic model of the bridge. The load factor associated with the damaged condition is taken as

$$LF_d = \frac{L_d - DL}{LL} \tag{4-11}$$

where DL and LL are the total applied dead load and one instance of live load, respectively, and L_d is the collapse load of the structure in its damaged state, i.e. the total applied load that causes a collapse mechanism to form in the damaged structure. The reserve ratio associated with the damaged structure can be expressed as

$$R_d = \frac{LF_d}{LF_l}. \tag{4-12}$$

A reserve ratio for the damaged limit state of $R_d \geq R_{d,req} = 0.50$ is required for the bridge to be considered redundant in its damaged state.

4.1.6: Reliability Considerations:

Appropriate safety margins can be determined based on reliability considerations, similar to what had been originally used in the development of AASHTO's LRFD specifications (AASHTO-LRFD, 2015). The reliability factor β is the measure of safety used to evaluate the reliability at the system level, as well as the member level.

The reliability factor can be cast to represent the number of standard deviations that separate the nominal (expected) resistance value from failure. In other words, the reliability factor incorporates the assumptions made in the design procedure as well as the uncertainties related to the evaluation of material and component strength and to the estimation of the applied loads. Typical values for the reliability factor range from 3.0 to 4.5, depending on the specific detail or component being considered. AASHTO LRFD specifications were calibrated to a reliability index of approximately 3.5. It is an advantage of LRFD approaches that a uniform level of safety, i.e. of the reliability factor, can be attained. Classical LRFD approaches have been developed under the hypothesis of lognormal distributions of the random variables considered. In this case, in order to calculate the reliability factor, the coefficients of variation of the variables of interest are also needed. If A and B are two random variables (for example, say that A represents the capacity and B the demand on a member), associated to coefficients of variation V_A and V_B, the reliability factor for that member can be calculated as:

$$\beta = \frac{\ln\left(\frac{A}{B}\right)}{\sqrt{V_A^2 + V_B^2}} \qquad (4\text{-}13)$$

Previous research (Nowak,1992) indicated that the probability density functions of maximum live loads are better represented by a Gumbel distribution than a lognormal distribution. A different approach is necessary in this case to estimate the reliability factor. This approach requires mapping the distribution of each random variable into equivalent normal distributions around the point at which failure is most likely to occur. This approach is more general and can be used for any type of probability distribution, but it requires specialized software or a spreadsheet to be applied.

Reliability factors can be calculated for all levels of performance of a structure, a member, or a component. Assuming that the coefficients of variation of the system are of the same size as those at member and component level can compensate for the approximations that are inevitable in a nonlinear analysis. For instance, reliability factors can be calculated at the system level for ultimate limit state (A can be taken as the ultimate load factor and B as the live load factor) or for the serviceability limit state (A can be taken as the serviceability load factor and B once again as the live load factor). Additionally, one could calculate a system-level reliability factor using for random variable A the load factor corresponding to the achievement of the ultimate capacity of the damaged condition of

the system. Finally, a member- or component-level reliability factor can be calculated using the random variables that relate to those members of component.

While an LRFD approach produces uniform levels of member reliability factors, allowing to use them directly in the evaluation of the system relative reliability factors, LFD methods do not produce uniform values of reliability factors. In this case, values of relative reliability factors between two given limit states need to be calculated as the difference of the natural logarithms of the ratios random variables A and B for one limit state and those of the ratios of random variables A' and AB'. Similarly to what discussed before, the A and A' variables represent capacity (for example, A could be the ultimate capacity of the system and A' that of a member or component) and B and B' represent demand (for example, for the application of interest, both could be the live load). Furthermore, assuming that the coefficients of variation for capacity and for demand are the same for the various limit states, the equation for the relative reliability factor (using once again lognormal distributions) can be written as:

$$\Delta\beta = \frac{\ln\frac{A}{B} - \ln\frac{A'}{B'}}{\sqrt{V_A^2 + V_B^2}}^{B=B'} = \frac{\ln\frac{A}{A'}}{\sqrt{V_A^2 + V_B^2}} \qquad (4\text{-}14)$$

The A/A' ratio can be defined as a system reserve ratio, representing the capacity margin at the various limit states. Once again, if the random variable distributions are not lognormal a more involved approach is necessary to calculate the relative reliability factors, but the results discussed do not lose generality.

By investigating the response of an adequate number of structures, by means of high definition nonlinear analysis, it is possible to build a set of results that allows the calculation of the reliability factors. Results in literature (NCHRP 406) show that relative reliability factors for ultimate, serviceability, and damaged states are at least 0.85, 0.25, and -2.70, respectively. Also, the same literature reference shows that the results obtained by assuming lognormal distribution when compared to those using a Gumbel distribution for live loads are quite similar. System reserve ratios resulting from that research have been shown to be at least 1.30, 1.10, and 0.50 for ultimate, serviceability, and damaged states, respectively. These values imply that the margin between capacity and demand should be at least 30 percent higher than that at the failure of the first member. Similarly, the margin between capacity and demand at the serviceability limit state is 10 percent higher than that at the failure of the first member. Finally, these show that a damaged bridge should carry at least half of the demand corresponding to failure of the first member. These system reserve ratios represent a direct measure of the redundancy of a structure, as they provide an overall picture of the expected structural response at the failure of one member.

The values presented by (NCHRP 406) are used in the current project, based on the similarity of the approaches used for the system-wide and element- (and component-) based evaluations of the response of pony truss bridges. With particular focus on the damaged limit state, the recommended system reserve ratio has been used and confirmed as part of this project.

4.1.7: Step-By-Step Procedure in NCHRP 406:

1) A three-dimensional nonlinear model of the bridge is constructed including dead loads. Primary members within the bridge are defined using a bilinear elastic-plastic material model.

2) Two side-by-side HS-20 trucks are applied incrementally to the 3D model and an analysis is performed by incrementing the HS-20 loading until a member in the structure reaches its limiting strain. The number of truck loadings required to reach the strength of any member (taken as the yield strength in NCHRP 406) is defined as LF_1, the member failure load factor. The number of truck loadings required to reach a maximum displacement in the bridge of $L/100$ is defined as LF_f, the functionality load factor. The number of truck loadings required to reach a member ultimate limit (defined as a strain of 0.02 in NCHRP 406) is defined as LF_u, the ultimate strength load factor. This load factor is the assumed to represent the maximum capacity of the bridge before collapse.

4) Damage is simulated in the bridge by removing a member and the bridge is loaded again using the HS-20 loading. The number of truck loadings required to reach the limiting strain of 0.02 in any remaining member is defined as LF_d, the damaged load factor.

5) System reserve ratios are computed, R_u, R_f, and R_d, corresponding to the ultimate strength limit, functionality limit, and damaged limit of the bridge are computed and are then normalized by dividing by their respective required values.

$$r_u = \frac{R_u}{R_{u,req}}, \quad r_f = \frac{R_f}{R_{f,req}}, \quad r_d = \frac{R_d}{R_{\mathrm{d},req}} \tag{4-15}$$

6) The required member strength load factor, $LF_{1,req}$, is computed based on the governing design specification, and then the member strength reserve ratio, r_1, is computed.

7) The redundancy factor, Φ, is computed as,

$$\Phi = \min(r_1 r_u, r_1 r_f, r_1 r_d) \tag{4-16}$$

If the redundancy factor, Φ, is greater than 1.00 then the bridge is said to be redundant.

4.2: ASCE 41-13:

ASCE 41-13 is a standard for the seismic evaluation and retrofit of existing buildings. The purpose of the standard, which had its roots in the FEMA 356 guidelines proposed by the Structural Engineering Associate of California (SEAoC), and the plethora of research work performed in years following the 1994 Northridge Earthquake, is to provide engineers with methods of assessing the seismic integrity of structures that were designed to meet codes and standards that are not as rigorous as current codes. The document is organized with a general description of the evaluation procedures in criteria in Chapters 1-8, material specific guidance is found in Chapters 9-12 (steel structures are covered in Chapter 9), and the remaining chapters address issues like seismic isolation systems, architectural considerations, mechanical and electric systems in buildings, etc.

4.2.1: ASCE 41-13 Evaluation Procedure:

The general procedure for an ASCE 41 evaluation is as follows:

1. Define Building Performance Levels.
2. Define Seismic Hazards and Levels of Seismicity
3. Obtain As-Built Information
4. Perform an Analysis of the Structure
5. Evaluate the Structural Components
6. Identify Deficiencies and Implement Retrofit Strategies.

Performance levels that are defined in Step 1 describe the desired behavior of the structure and are defined in ASCE 41-13 as “collapse prevention,” “life safety,” “immediate occupancy,” and “operational.” These are defined in detail in Section 2.3 of ASCE 41-13. Collapse prevention, for example, means that the structure will be extensively damaged, there will be some risk to life within and around the structure, and the building will likely need to be demolished after a seismic event. However, the structure will not likely collapse during the event. Immediate occupancy, on the other hand, means that there is little damage to the structure and there is little risk to life, but that the mechanical equipment within the structure may not be operational immediately following the event.

The seismic hazards and levels of seismicity determined in Step 2 correspond to the peak ground accelerations, or in some cases, ground motions that result from the seismic hazards, which are the geologic faults.

Four different analysis procedures are detailed in ASCE 41-13. The linear static procedure (LSP) is a linear elastic analysis of the structure subjected to gravity loads and static lateral loads determined based on the seismicity of the building’s location and the building’s natural period of vibration. The linear dynamic procedure (LDP) is a linear elastic time history analysis of the structure subjected to acceleration records that are representative of the seismicity anticipated for the building’s location. The nonlinear static procedure (NSP) includes an analysis of the structure where the nonlinear load-deformation responses of the structural components are accounted for. The NSP analysis, also called a push-over analysis, is conducted under gravity loads and a monotonically increasing lateral load pattern that is representative of the distribution of inertial forces resulting from an earthquake. In the nonlinear dynamic procedure (NDP) a time history analysis of a structural model similar to that used in the NSP analysis is conducted with gravity loads and acceleration records.

A general depiction of the nonlinear load-deformation response of structural components is shown in Figure 4-1. The actual response curve and its idealization represent first the linear-elastic portion of the response, then nonlinear yielding of component, and finally deterioration and failure. While the general shape of component responses are common, the specific parameters associated with this curve are highly dependent on the type of material used for the construction.

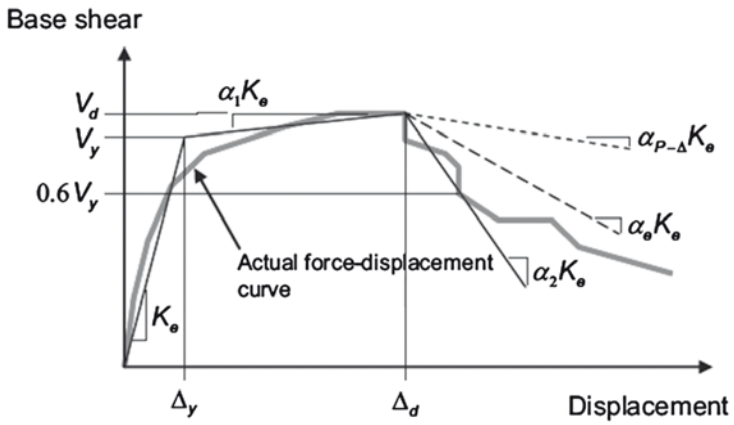

Figure 4-1: Nonlinear Component Behavior in the NSP (ASCE 1-13 Figure 7-3)

ASCE 41-13 defines primary and secondary structural components as well as deformation-controlled (ductile) components and force-controlled (nonductile) components. The Type 1 and Type 2 curves shown in Figure 4-2 represent the behavior of two slightly different ductile components whereas the Type 3 curve represents the behavior of a nonductile component. When properly designed and detailed, steel is generally considered to be a ductile material and its specific load deformation response is characterized as shown in Figure 4-3(a). The specific points and parameters are defined in Chapter 9 of ASCE 41-13 based on the type of component (steel beam (M-θ), tension member (P-Δ), or compression member (P-Δ), for example). The same curve is depicted in Figure 4-3(b) where the performance levels associated with immediate occupancy (IO), life safety (LS), and collapse prevention (CP) are also indicated.

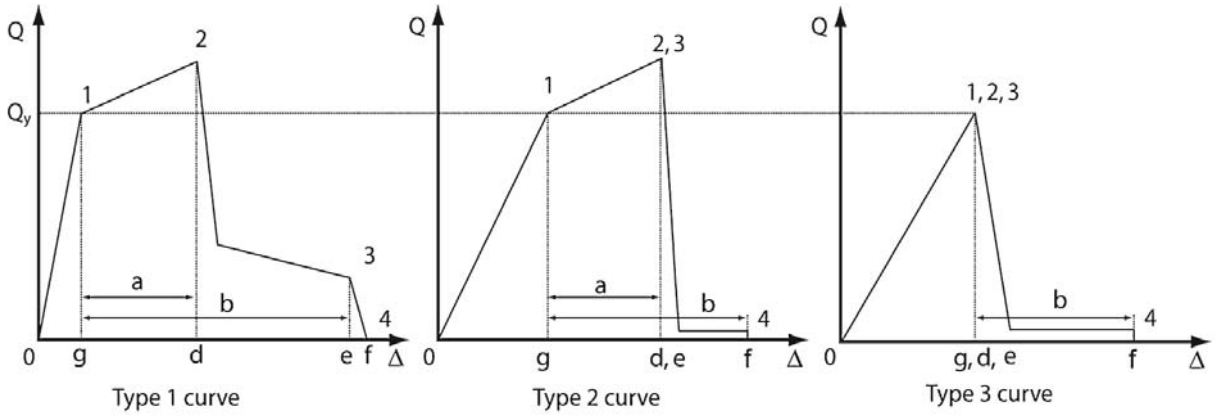

Figure 4-2: Load-Deformation Responses for Components (ASCE 42-13 Figure 7-4)

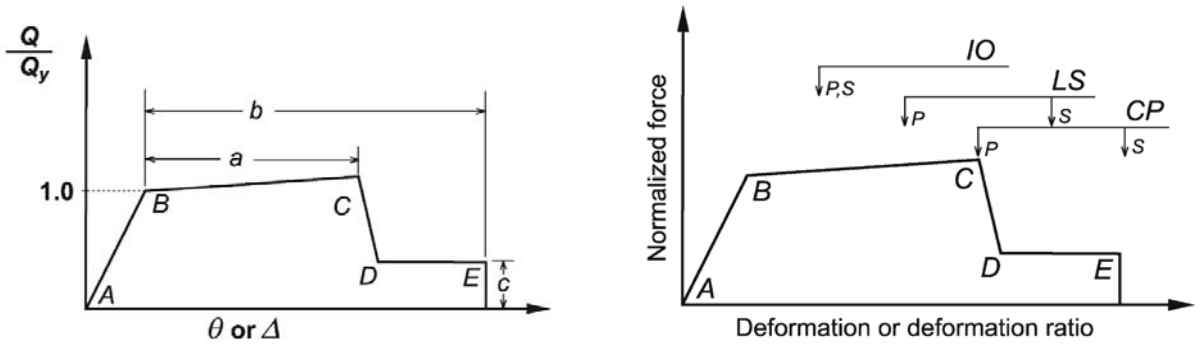

(a) (b)

Figure 4-3: Load-Deformation Responses for Steel Components (ASCE 41-13 Figure C7-3)

4.2.2: Analogy to Bridge Structures:

If one were to apply the ASCE 41-13 evaluation procedure directly to an FCA for bridge structures, Step 1 would be analogous to setting a performance criterion such as, for example, "the bridge must not experience a collapse or partial collapse under a given loading in the event that any one tension member experiences a brittle fracture." Step 2 would be to define what loading is to be used when determining if the performance criteria in Step 1 is satisfied. In the state of Ohio, and particularly for pony truss bridges, the seismic risk is low. Thus the loading will likely be defined as a gravity load consisting of dead load and some level of truck loading, likely less than the full design truck load. Step 3 would be analogous to conducting a field inspection of the bridge wherein the actual condition of structure can be surveyed and assessed, and refined dead loads can be determined (actual deck thickness, wearing surface thickness, etc). Going a step further, refined live load data could also be acquired, including truck counts and weights. In regions of low seismicity, and for smaller bridges with lighter traffic demands, Step 4 would be analogous to either a linear static analysis, a nonlinear static analysis, or a combination of both.

4.3: Application to Fracture Critical Analyses of Pony-Truss Bridges:

The approach developed and recommended in NCHRP 406 was intended to address the overall redundancy of bridge structures. The goal of the study described in this report is, in part, to develop a method and criteria that can be used to evaluate fracture critical members in pony truss bridges. As such, some but not all of the developments in NCHRP 406 are directly applicable to the current goals.

Historically a member is defined as fracture critical if its removal from the structure would result in the collapse of the structure or a part of the structure. Therefore the evaluation of a bridge's redundancy in a damaged state is directly applicable to the goals of the current study. The evaluation of redundancy in the other conditions - ultimate limit state and functionality limit state - is of lesser importance than the evaluation of an existing structure. As such LF_u, R_u, LF_f, and R_f have limited applicability to the current study. The evaluation of an existing structure for fracture criticality proposed in this work is based primarily on redundancy in damaged conditions, i.e. LF_d and R_d will be used directly.

Further, NCHRP 406 was developed at a time when nonlinear structural analysis techniques were primitive by comparison with current technology. The limit states assessed in the analyses performed in NCHRP 406 were defined as stress and strain limits both in tension and compression and made no accommodation of ductile versus nonductile behavior, strain hardening, or the strength of connections.

Since most modern finite element packages are capable of nonlinear push-over analyses and have ASCE 41 / FEMA 356 hinges built into the software, it is proposed herein that the fracture critical analysis (FCA) - the "refined analysis" cited in the 2012 FHWA memorandum - be based on the procedures outlined in ASCE 41 using the loading and performance criteria outlined in NCHRP 406.

4.3.1: Appropriate Limits for Reserve Ratio:

A straightforward performance objective for an FCA would be to simply stipulate that a bridge must be able to sustain its full design loading in a condition where the member under consideration has been removed. Although this is simple, it is also quite conservative and may lead to unnecessary design, retrofit, and maintenance costs for the bridge owner.

Basically, setting the requirement for a reserve ratio in the damaged state of $R_d \geq 0.5$ is loosely equal to requiring that the bridge be capable of supporting its unfactored dead load plus approximately half of the unfactored live load. There is precedent for this in ASCE 7-10 where, when conducting a time history analysis of a building subjected to seismic ground motions, it is stipulated that the building should be subjected to gravity loads consisting of full dead load and 30% of the live load. Additionally, the analyses that are proposed in ASCE 41-13 conducted with gravity loads consisting of full dead load, 25% of the unreduced live load, and the snow load, all multiplied by an arbitrary load factor of 1.1.

4.3.2: Functionality Limit:

Functionality in a damaged state is of importance but will be handled differently than is proposed in NCHRP 406. Whereas functionality as addressed in NCHRP 406 was considered in the undamaged structure, for a fracture critical analysis, functionality should be addressed in potential damaged states. Thus a displacement limit of $L/100$ is imposed in the determination of L_f when calculating R_d. Specifically, the value of L_{cd} is taken as the applied load leading to a collapse mechanism in the damaged structure, or the applied load leading to a displacement in excess of $L/100$ in the damaged structure, whichever is smaller.

In NCHRP 406, it is recommended that displacements only be evaluated in the main members. In the current study, however, the fracture criticality of floor beams is also considered. Thus floor beams are considered to be main members in this work. As a result, when considering the displacement limit of $L/100$ used in some cases to define L_{cd}, the length, L, that is used should be appropriate to the component under consideration. If the FCA is of a member within one of the trusses, then L should be taken as the span length of the truss. On the other hand, if the FCA is of a floor beam, then L should be taken as the span length of the floor beam.

Chapter 5 - Evaluation of Pony Truss Bridges for Load-Path Redundancy

An implementation of the advanced redundancy analyses described in Chapter 4 tailored directly to the application of fracture critical analyses (FCAs) of pony truss bridges is presented here. While this approach was developed for use with the SAP2000 or MIDAS software packages, other finite element structural analysis packages may also be suitable. This chapter is written in terms that are not specific to a particular software package, but examples are presented in the appendices illustrating implementation of the procedure in both SAP2000 and MIDAS. Any structural analysis software package can be used so long as it supports the appropriate nonlinear material responses in its analyses. Specifically, the implementation of axial and flexural "FEMA" hinges as defined in ASCE 41-13 (2013) and the ability to customize those hinge responses is preferred. Further, support for moving loads and predefined truck load patterns is also preferred.

5.1: Overview of the Evaluation Procedure

5.1.1: Step 1 - Create the FE Model

A finite element model of the bridge is created in the software package chosen. The model should preferably be a three-dimensional model including at least the trusses and floor beams. As is described later in this chapter, stringers and decking can also be included in the model if it is expected that they will provide a secondary load path or if they are desired for ease of applying live loads.

5.1.2: Step 2 - Definition of Live-Load Patterns - LL

Step 2 is to determine the dead load of the bridge and live-load patterns that are critical for the member being evaluated. This is accomplished by conducting an analysis of the bridge to determine the location of the live load that creates the maximum response for the member under consideration. This analysis can be a moving load analysis in a software package or can be based on an influence line analysis for the structure. In the latter case, this analysis will likely be completed on a 2D model of the truss and consists of an influence line analysis for each member and truck configuration considered. The results of the influence line analysis may then be verified by conducting a moving load analysis in the FE software package.

It is recommended that both HS-20 and H-20 load patterns be considered during the fracture critical analysis (FCA) evaluation for PTBs. Additional load patterns were considered in the development of this report including ODOT Legal Loads 2F1, 3F1, 4F1, and 5C1, and PennDOT Legal and Permit Loads ML-80, TK-527, and P-82 (PennDOT DM-4, 2012). It was found that these load patterns gave similar results to the HS-20 and H-20 load patterns but at considerable additional computational complexity.

As is discussed in Chapter 4 and recommended in the literature, it is recommended that all loads and load cases be defined with load factors and impact factors set to unity.

5.1.3: Step 3 - Define the Nonlinear Behavior of the Members

Nonlinear behavior of the members is defined next in the model. Two types of FEMA 356 / ASCE 41 hinges can be included in the model to capture member failures; axial hinges in members to capture the failure modes of tension and compression failures, and flexural hinges to represent flexural failures.

5.1.3.1: Axial Hinge Definitions:

Axial hinges are used to capture failure modes such as gross section yielding, net section fracture, and compression buckling of the truss members. Different hypothetical axial responses are depicted in Figure 5-1. Case (a) represents an Elastic Perfectly Plastic (EPP) response, case (b) represents an Elastic Plastic Hardening (EPH) response, case (c) represents an Elastic Plastic Fracture (EPF) response, case (d) represents an Elastic Plastic Hardening Fracture (EPHF), and case (e) represents an Elastic Plastic Buckling (EPB) response. Within these hinge definitions, P_y is the yield force of the member, P_u is the tensile strength, and P_{cr} is the buckling load (critical load) of the member. δ_y is the axial deformation corresponding to the yield force, δ_h is the axial deformation corresponding to the onset of strain hardening, and δ_u is the deformation corresponding to failure.

Cases (a) and (b) are felt to be too rudimentary to be useful in the current study but are included in this discussion since much of the work upon which this study is based was initially implemented using those material models (NCHRP 406). It is expected that Cases (c) and (d) would be most appropriate for tension failures and that Case (e) would be most appropriate for compression buckling failures. Case (e) is depicted in Figure 5-1 in the first quadrant, though if compression was taken as a negative force and a shortening of the member was taken as a negative elongation, then the EPB behavior would be expected to occur in the third quadrant.

Combining the EPHF response in tension with the EPB response in compression results in the full tension/compression, or bi-directional behavior shown in Figure 5-2. This hinge definition is recommended for nonlinear axial behavior of members in the FCA procedure. Alternatively, a bi-directional model consisting of the EPF response in tension with the EPB model in compression can be implemented, which would provide a slightly more conservative result that would not include additional reserve system capacity in the form of strain hardening.

It should be noted that the bi-directional hinge model shown in Figure 5-2 is appropriate only when end connections of the member are detailed such that the full yielding capacity of the member can be reached in tension and the buckling strength can be reached in compression. For truss members these conditions will generally be satisfied, though the net-section fracture strength of a member in tension may govern over the gross-section yielding strength. When either or both of these conditions is not satisfied, then a hinge model representative of the expected connection behavior should be implemented, or, more conservatively, the member should be released axially. This is generally encountered in the floor systems with connections between stringers and floor beams. An example would be an axial hinge with a tensile capacity equal to the shear strength of the bolts connecting the bottom flange of a stringer to the top flange of a floor beam.

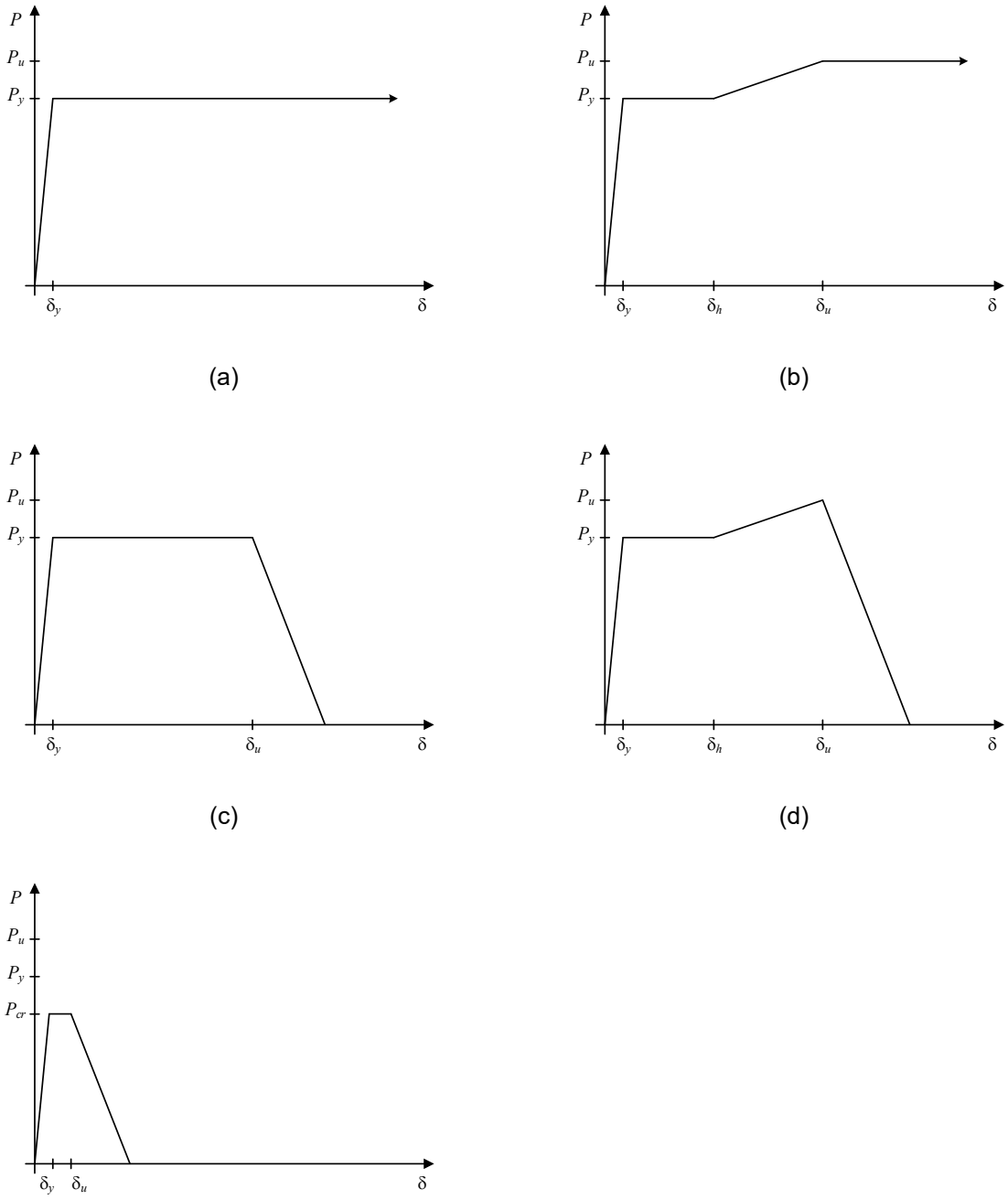

Figure 5-1: (a) EPP, (b) EPH, (c) EPF, (d) EPHF, and (e) EPB Hinge Behavior

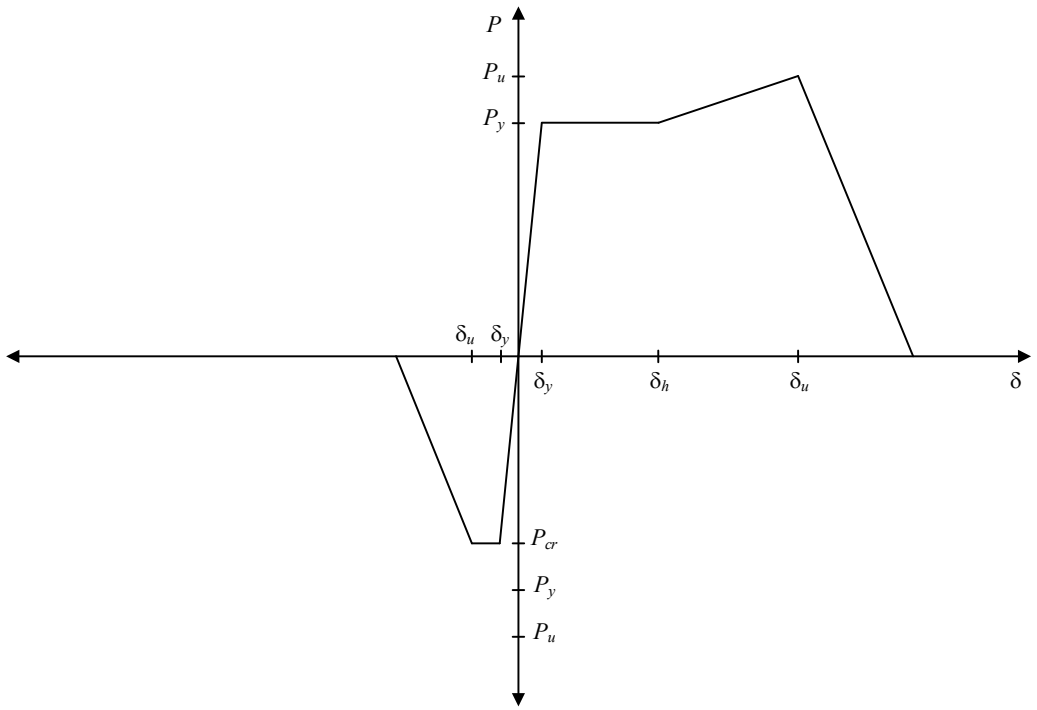

Figure 5-2: Recommended Bi-Directional Axial Hinge Model for Members

5.1.3.2: Flexural Hinge Definitions:

Flexural hinges are used to capture failure modes such as first flexural yielding and plastic moments in beam members. Flexural hinges defaulting to the ASCE 41 / FEMA 356 are generally adequate.

5.1.4: Step 4 - Conduct an Analysis of the Undamaged Bridge:

After the model has been created, an analysis of the bridge in its undamaged state is conducted. The purpose of this analysis is to determine the load factor associated with member failure, LF_1, which is used to determine which member will govern the strength of the undamaged bridge. This analysis is generally a linear and elastic analysis as LF_1 is defined based on the first member in the system reaching its strength.

When conducting an FCA of a member within one of the trusses, maximum and minimum member forces (maximum tension and maximum compression) are determined for all truss members for both dead load (P_{DL}) and live load (P_{LL}) wth load factors, γ_{DL}, set to unity. The factor LF_1 is computed for each member as is shown in Equation 5-1 and the lowest value is the governing value for the truss. R_n in Equation 5-1 is the governing member strength based on the design specification chosen (typically the current edition of the AASHTO-LRFD bridge specification) and is computed using resistance factors, ϕ, set to unity. LF_1 is computed using concurrent forces and capacities. That is, governing

values of P_{DL}, P_{LL}, and R_n for tension are used concurrently, and then governing values of P_{DL}, P_{LL}, and R_n for compression are used concurrently.

$$LF_1 = \frac{R_n - P_{DL}}{P_{LL}} \tag{5-1}$$

When conducting an FCA of a truss member, the analysis used to determine LF_1 can be based on a two-dimensional model of the structure, even if the analysis used in Step 5 to determine LF_d is based on a three-dimensional model. This is true since the distribution of loads to and between the two trusses is generally well predicted by simple lever-rule calculations used for distribution factors in a 2D analysis. This can save computation time, particularly when considering multiple load positions for trucks and/or when moving loads are used. Alternatively, LF_1 can be taken as LF_{1S},which can be based on the nonlinear system response of the undamaged model, as is discussed in Section 5.2.2

When conducting an FCA of a floor beam, maximum and minimum bending moments are determined for the member at each candidate cross section (i.e. each potential fracture location to be considered) for both dead load (M_{DL}) and live load (M_{LL}) with load factors, γ_{DL}, set to unity. M_n in Equation 5-2 is the governing member capacity based on the design specification chosen and is computed using resistance factors, ϕ, set to unity. The factor LF_1 is computed as is shown in Equation 5-2 at each candidate cross section of the floor beam and the lowest value obtained is the governing value for the member.

$$LF_1 = \frac{M_n - M_{DL}}{M_{LL}} \tag{5-2}$$

Figure 5-3 shows a hypothetical load deformation response for an undamaged truss or floor beam. This curve represents the full nonlinear response of the structure starting in the unloaded condition, through the application of dead load, through the application of full live load, then through the application of additional live load using the same pattern until the first member fails, and then finally through the development of a collapse mechanism. The independent variable, "Δ," is the vertical displacement of the node in the structure that is expected to displace the most. The dependent variable, "Load," is the total load applied to the structure as determined by a summation of the vertical reaction forces. The load, "L_1," is the total applied load that is needed to cause the first member force, P_{DL} + P_{LL}, to reach its capacity R_n. The load, "L_u," is the total applied load that results in a collapse mechanism. The displacement "Δ_{DL}" is the displacement of the undamaged structure resulting from dead loads.

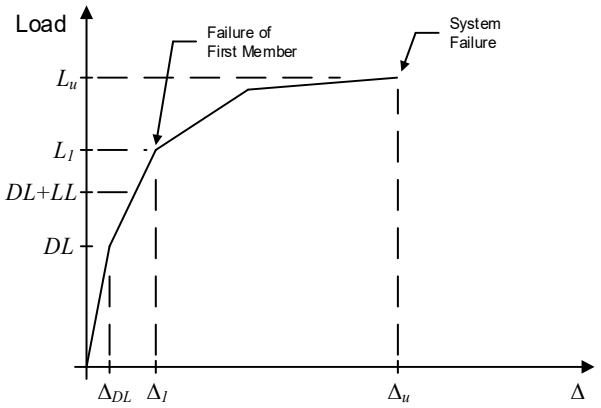

Figure 5-3: Load-Displacement Results from a Nonlinear Analysis of the Undamaged Bridge

5.1.5: Step 5 - Conduct an Analysis of the Damaged Bridge:

In Step 5, an analysis is conducted to determine the capacity of the system when the member being evaluated has sustained a fracture. When conducting an FCA of a truss member, this is accomplished by simply removing the member being evaluated from the model. When conducting an FCA of a floor beam, a fracture is modeled by imposing a rotational hinge in the floor beam at the location of the hypothetical fracture. This approach is analogous to stating that in the event of a tension flange fracture in a floor beam, the floor beam will no longer be able to transfer moment at that location but will still be able to transfer shear forces. The analysis is conducted and the values of LCD, DL, and LL from the results are used to compute LF_d, as is shown in Equation 5-3.

$$LF_d = \frac{L_d - DL}{LL} \tag{5-3}$$

The FCA procedure implemented herein is based on the procedure in ASCE 41-13. In an ASCE 41 NSP evaluation (a nonlinear pushover analysis), the analysis is conducted in displacement control and the results are presented as reference load as a function of a reference displacement. For an NSP pushover analysis, the reference load is the total horizontal shear at the base of the building (the base shear) and the reference displacement is the lateral displacement at a reference node, often at the roof level of the building. As a result, the software package will likely present the results of the nonlinear bridge analysis in those terms as well. In defining the analysis parameters, however, the reference displacement is generally chosen as the vertical displacement at the node that has the largest vertical deflection and the reference load is the sum of the vertical reactions at the bridge supports.

Figure 5-4(a) shows a hypothetical load-deformation response for a damaged truss or floor beam. This curve represents the full nonlinear response of the structure starting in the unloaded condition, through the application of dead load, through the application of live load until the first member fails, and then finally through the development of a collapse mechanism. The independent variable, "Δ," is the vertical displacement of the node in the structure that is expected to displace the most. The dependent variable, "Load," is the total load applied to the structure as determined by a summation of the vertical

reaction forces. The load, "L_d," is the total applied load that results in a collapse mechanism, $DL + (LF_d)(LL)$. The displacement "Δ^*_{DL}" is the displacement of the damaged structure resulting from dead loads and the displacement "Δ_d" is the displacement when a collapse mechanism forms in the damaged structure.

In some rare cases, it may be found that the bridge in its damaged state can support the full dead load and 100% of the live load. If this is the case, then no further analysis is required as a fracture of the member under consideration does not result in a structural collapse and thus the member is not fracture critical. It is unlikely, however, that 100% of the live load will be applied prior to the development of a collapse mechanism in the structure. In fact, in some cases, a collapse mechanism may develop before the full dead load can be applied, which results in a negative value of LF_d. In other cases, the deflection of the damaged structure can be excessive and the load, L_d is defined by the functionality limit, redefined here as a displacement of $\Delta_f = \Delta_{DL} + Span / 100$ due to live load, as is illustrated in Figure 5-4(b).

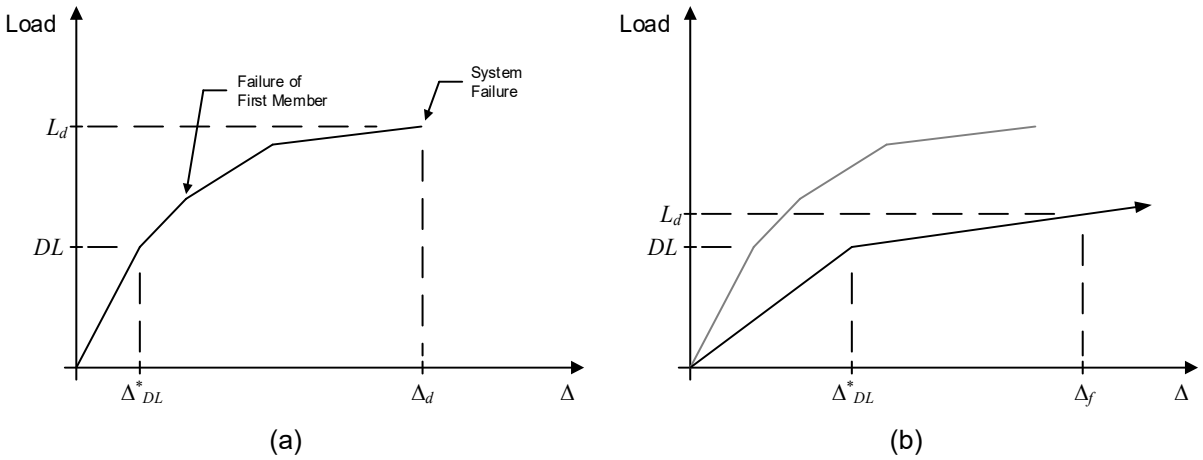

Figure 5-4: Load-Displacement Results from a Nonlinear Analysis of the Damaged Bridge

5.1.6: Step 6 - Calculate the Reserve Ratio for the Member Being Evaluated:

The last step of the procedure is the calculation of the reserve ratio, R_d, as shown in Equation 5-4. If R_d is not less than 0.5, then the member under consideration can be classified as not fracture critical.

$$R_d = \frac{LF_d}{LF_1} \quad \text{or} \quad R_d = \frac{LF_d}{LF_{IS}} \tag{5-4}$$

If the owner elects to employ the member strength reserve ratio, r_1, as defined in Equation (4-6), then the load factor $LF_{1,req}$ is computed as defined in Equation (4-4). R_d can then be factored as

$$R'_d = r_1 R_d . \tag{5-5}$$

$R_d' = r_1 R_d$, which will increase the reserve ratio.

5.2: Additional Considerations

5.2.1: Finite Element Topology:

Creating a three-dimensional nonlinear finite element model involves many decisions regarding the idealization of an actual structure in computer model. Striking an appropriate balance between accuracy and complexity can be challenging. This section aims to address some issues that an engineer might be faced with during the process of assembling the FE model.

5.2.1.1: End Connections in the Truss Members:

The construction of the trusses in PTBs invariably involves connections between the truss members and gusset plates that are either welded or bolted. This observation leads to the notion that perhaps the trusses should be modeled as frames with rigid in-plane end connections instead of trusses with pinned in-plane behavior. This approach was investigated by the research team and it was found that modeling the trusses as frames had little effect on the member forces in the trusses within the elastic range of behavior and that negligible in-plane bending moments were developed in the truss members. To adequately capture behavior of the frame members beyond the elastic range of response, default ASCE 41-13 weak-axis flexural hinges were defined at both ends of each W shape in the truss. This approach had very little impact on the overall strength and behavior of the undamaged bridge and increased the strength of the damaged bridge by less than 5%, which does not justify the added effort required for modeling. As a result, the research team recommends modeling the truss members with pinned ends with respect to in-plane bending. The truss members are modeled with fixed ends with respect to out-of-plane bending.

5.2.1.2: Modeling the Floor System:

Floor systems of pony-truss bridges invariably consist of floor beams spanning between panel points of the trusses. The floor beams support stringers that span parallel to the trusses. The stringers in turn support decking of one sort or another that spans perpendicular to the stringers.

Floor beams are generally attached to the truss panel points using moment connections. These moment connections in reality, however, are often not detailed with sufficient strength to carry the full moment capacity of the connected floor beam. Since the ability of the trusses to resist the end moment of the floor beams is limited, this is not a critical concern. Still, an engineer should be cognizant of the potential for failure of the moment connections between the floor beams and trusses during the fracture critical analysis process. This can be accommodated by manually checking the end moments in the floor beams and comparing those to estimated or calculated moment capacities for the connections, or additional nonlinear hinges can be added to the model at these locations that will force the software to make those checks automatically.

In cases where the stringers and decking are not expected to contribute to the response of the structure, these elements need not be included in the model. These cases include

bridges where the stringers are simply supported at each floor beam, where stringers lack a robust connection to the floor beams, when the decking lacks strength or stiffness, and/or cases where the decking lacks a robust connection to the stringers. In those cases, the engineer may model the live load as directly applied to the floor beam elements, or for the sake of convenience, may model the stringers and/or decking with appropriate structural releases for ease of loading.

When they are expected to contribute to the overall response of the structure, elements representing the stringers and decking should be added to the model. In those cases, element discretization and nonlinear properties should include expected nonlinear responses of the members, decking, and the connections between adjacent members. The authors of this report employed two primary means of modeling the stringers and decking. The first approach, which was used most often, was to model the decking using a strip approach as is illustrated in Figure 5-5. The second approach, which was used primarily in the high-resolution modeling, was to employ shell elements to capture the behavior of the decking. In the former case, capturing longitudinal diaphragm responses of the deck is not practical but this was not felt to be a significant limitation since very few of the decks in the Ohio inventory actually possess a deck capable of developing that behavior. Further, using the strip modeling approach facilitated the ability to capture nonlinearities in the decking of robustly connected floor systems by including nonlinear hinges in the deck elements adjacent to each stringer.

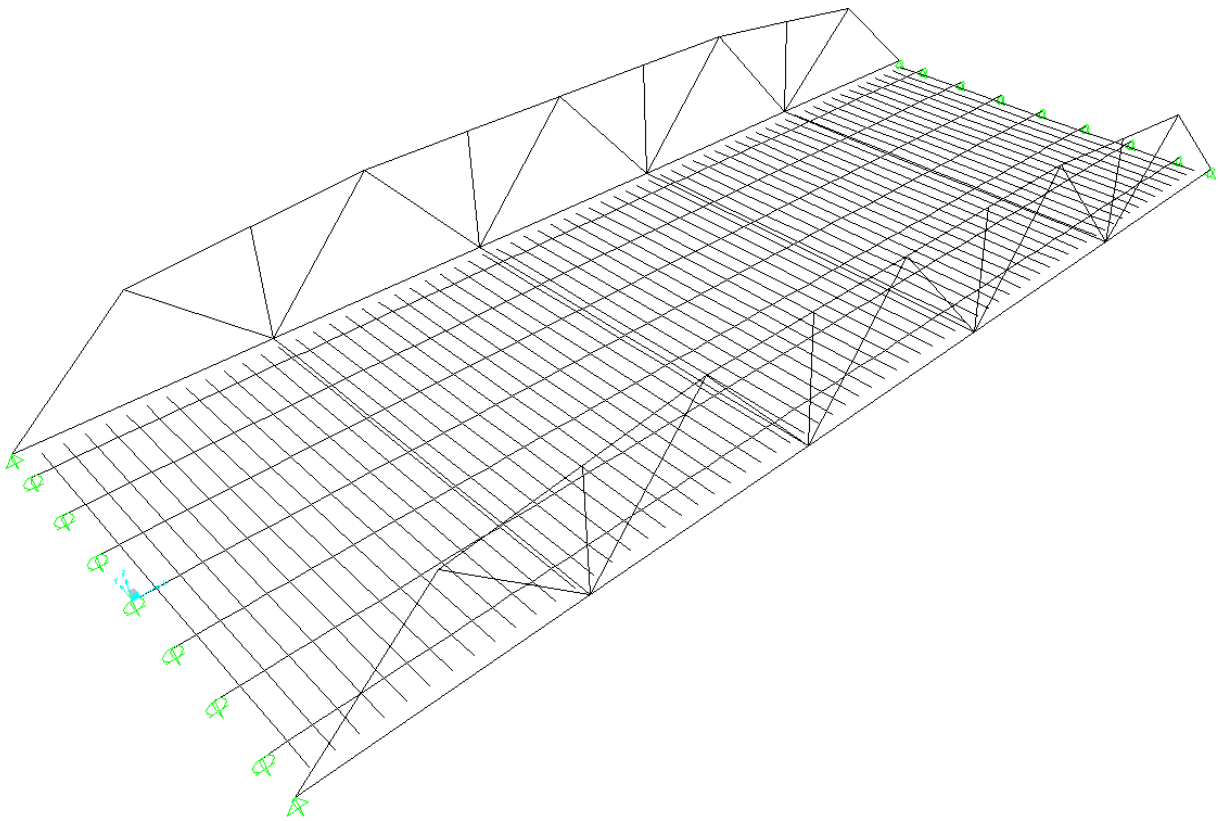

Figure 5-5: Strip Approach to Modeling the Floor System

5.2.1.3: Bridge Railings:

Although they were not considered explicitly in this study, bridge railings have the potential to contribute to the strength of a bridge as secondary elements.

5.2.2: Alternate Determination of LF_1:

The method outlined to determine the member failure load factor, LF_1, in Equation 4-2 is based on a linear model of the bridge wherein the member dead load force, P_{DL}, and member live load force, P_{LL}, are determined. LF_1 is then determined based on the nominal capacity, R_n, of the critical member in the structure. It is shown in Appendix A that the critical member failure load factor for Bridge #1 (as described in Appendix A) due to an HS-20 loading is,

$$LF_1 = \frac{440.0^{\text{kip}} - 92.33^{\text{kip}}}{112.2^{\text{kip}}} = 3.099 \quad (5\text{-}6)$$

Since a linear and elastic model is used to determine member forces in the calculation of LF_1, it can be shown that P_{DL} is proportional to total dead load applied to the structure, DL, and P_{LL} is proportional to the total live load applied to the structure, LL. As a result, it is permissible to derive the load factor, LF_1, as the first nonlinearity in the response of a structure so long as the software used to determine that response is capable of accounting for codified limit states for the members. This is illustrated in Figure 5-6.

The traces shown in Figure 5-6 represent the nonlinear response from a 2D FE model for Bridge #1 from Appendix A. The first load step up to approximately $DL = 104^{\text{kip}}$ represents the application of dead load. Beyond that is the application of two HS-20 trucks side-by-side representing a live load, $LL = (1.157)(72^{\text{kip}}) = 83.30^{\text{kip}}$ wherein 1.157 is the distribution factor for the trusses in the bridge and 72^{kip} is the weight of one HS-20 truck. The nonlinearity at approximately $L_1 = 372.8^{\text{kip}}$ represent the failure of a bottom chord member in tension at the code prescribed level. This response can be used to determine the member failure load factor, LF_{1S}, so notated to indicate that it was determined based on system response instead of based on member response as indicated in Equation 4-2.

$$LF_{1S} = \frac{L_1 - DL}{LL} = \frac{372.8^{\text{kip}} - 104.0^{\text{kip}}}{83.30^{\text{kip}}} = 3.227 \quad (5\text{-}7)$$

Using LF_{1S} based on the system response offers advantages in efficiency of the fracture critical analysis procedure and is employed in the examples presented in the original NCHRP 406 report.

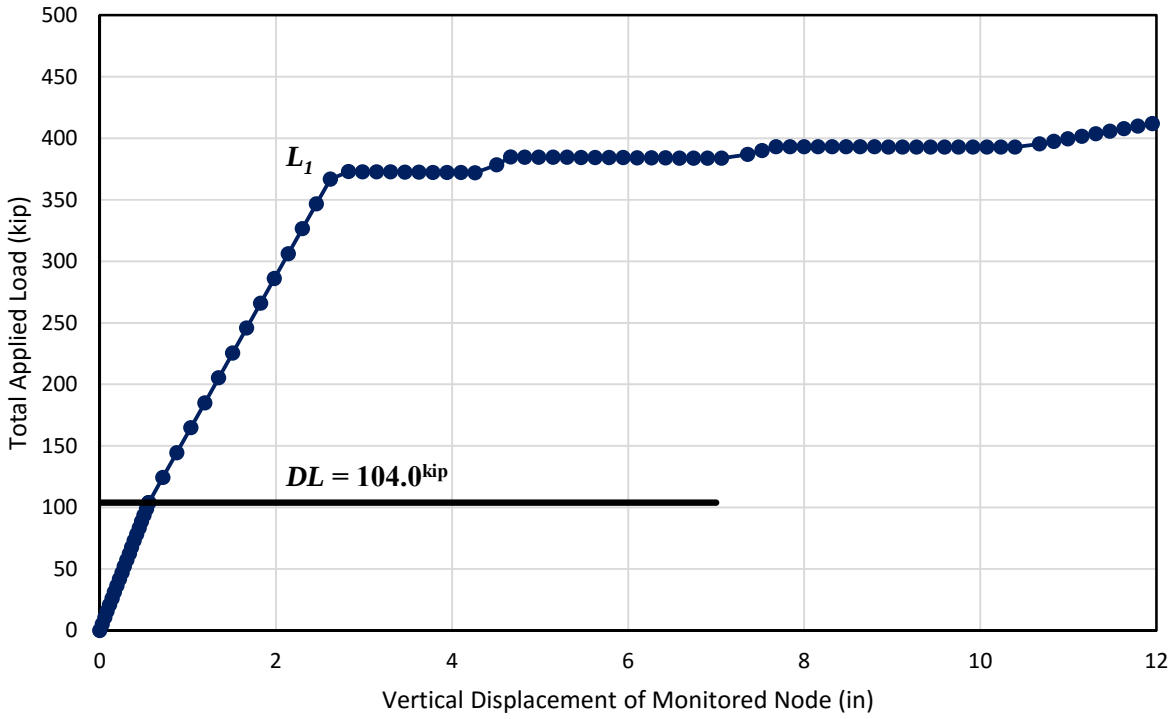

Figure 5-6: Nonlinear Response of an Undamaged Structure 2D Model

Chapter 6 - Supplemental Case Studies

This chapter is meant to highlight case studies of the fracture critical assessment procedure that was described in Chapter 5. Topics include general observations from fracture critical assessment of the superstructure, observations regarding the truck configurations that were implemented, case studies investigating redundancy in floor systems, and a discussion of high-resolution finite element modeling that was performed.

6.1: Fracture Critical Assessments of Truss Superstructures:

Several analyses of select bridges were conducted as part of this study. Two bridges were studied extensively as discussed in Appendix A and Appendix B. Bridge #1 has a span length of 66'-0", is made up of 5 panels, each roughly 13.20' in length. The top chord and diagonal members of the trusses are made up of wide flange sections and bottom chords of the trusses are made up of single channels, though a modified version of the bridge, Bridge #1M, was considered with pairs of channels for the bottom chord. Bridge #2 has a span length of 160'-0", is made up of 10 panels, each 16.00' in length. The top chord and diagonal members of the trusses are made up of wide flange sections and bottom chords of the trusses are made up of pairs of channels.

When longitudinal floor system continuity was neglected, it was found that the bottom chords made up of single channels and diagonal members generally were not able to be reclassified as not fracture critical. It was found, however, that bottom chords made up of pairs of channels were able to be reclassified as not fracture critical when one of the two channels was removed simulating a fracture in one of the two elements.

When longitudinal floor system continuity was added by assuming connections between the stringers and floor beams that were able to develop the full axial strength of the stringers, the system redundancy was improved, but not as much as was expected. Providing restraint for the floor beams at the abutments in the axial direction of the stringers further improved redundancy. Decking continuity was not considered widely in the study since few pony truss bridges in Ohio feature decks capable of developing appreciable in-plane forces.

6.2: Fracture Critical Assessment Truck Loading:

NCHRP Report 406 (NCHRP 406) recommends the use of the HS-20 truck configuration for redundancy analyses. As part of this study, ten different truck loadings were investigated, including the H-20, HS-20, Tandem, 2F1, 3F1, 4F1, 5C1, P-82, ML-80, and TK-527as illustrated in Figure 6-1. These truck configurations were used for fracture critical assessments of all members that experienced tension in the Modified Bridge #1 and Bridge #1 as described in Appendix A and Appendix B, respectively. The HS-20 truck was applied with a rear axle spacing fixed at 14' and all axles were considered to be active as long as they within the limits of the bridge when the truck was in its critical

position for each member, even in cases where an axle created a load that was opposite in sign from the overall effect of the truck.

Reserve ratios, R_d, were computed for each tension member for each truck configuration and are shown in Table 6-1 and Table 6-3. Table 6-2and Table 6-4 show the percent above the minimum reserve ratios for each member in Table 6-1 and Table 6-3, respectively. For the 21 members analyzed in the two bridges, it was found that the tandem and the 2F1 governed in 11 of the cases. The H-20 governed in none of the cases and the HS-20 governed in one case. When assumptions regarding modeling floor system continuity and other issues were changed, it was found that the truck load governing individual members changed. It is also noted that the reserve ratio for Member T01R in each of the two bridges - the bottom chord member closest to the abutment - had a high level of variability with respect to the truck loading used.

While the H-20 and HS-20 did not govern in many cases, it is observed that when the H-20 and HS-20 are considered together (i.e. the lesser reserve ratio from two analyses considering those two trucks) that the reserve ratio was only 4% and 6% above the minimum when all ten trucks were consider for Bridge #1M and Bridge #2, respectively. If Member T01R is excluded, then the reserve ratio was only 2% and 3% above the minimum of all ten trucks, respectively. An obvious conclusion is to simply include all ten truck configurations in all FCAs (or all conceivable truck configurations). This would result in an overall analysis time that was felt by the researchers to be excessively burdensome and impractical. As a result, the researchers recommend using the lesser of the H-20 and HS-20 trucks for the FCA procedure.

Table 6-1: Reserve Ratios for 3D FCA of Bridge #1M for Various Truck Configurations

	Truck										
Member	**H-20**	**HS-20**	**Tandem**	**2F1**	**3F1**	**4F1**	**5C1**	**P-82**	**ML-80**	**TK-527**	**Min**
T01R	1.709	1.639	1.686	1.684	1.666	1.665	**1.443**	1.451	1.657	1.689	**1.443**
T02R	0.858	**0.845**	0.859	0.848	0.878	0.860	0.905	0.914	0.862	0.893	**0.845**
T03R	1.017	0.895	1.024	0.913	0.953	0.903	0.909	1.108	0.906	**0.876**	**0.876**
T16R	-0.449	-0.458	-0.445	-0.454	**-0.461**	-0.460	-0.268	-0.290	-0.460	-0.446	**-0.461**
T18R	1.096	1.096	1.096	1.096	1.096	1.096	1.096	**1.076**	1.096	1.096	**1.076**
T19R	0.338	0.326	0.331	**0.306**	0.311	0.315	0.311	0.335	0.313	0.319	**0.306**
T21R	1.106	1.225	**1.103**	1.115	1.249	1.236	**1.103**	1.224	1.233	1.236	**1.103**

* Bridge modeled as a theoretical truss with no floor system continuity

Table 6-2: Percent above Minimum Reserve Ratio for 3D FCA of Bridge #1M for Various Trucks

	Truck										
Member	**H-20**	**HS-20**	**Tandem**	**2F1**	**3F1**	**4F1**	**5C1**	**P-82**	**ML-80**	**TK-527**	**H/HS-20**
T01R	18%	14%	17%	17%	15%	15%	0%	1%	15%	17%	14%
T02R	2%	0%	2%	0%	4%	2%	7%	8%	2%	6%	0%
T03R	16%	2%	17%	4%	9%	3%	4%	26%	3%	0%	2%
T16R	2%	1%	3%	2%	0%	0%	42%	37%	0%	3%	1%
T18R	2%	2%	2%	2%	2%	2%	2%	0%	2%	2%	2%
T19R	11%	7%	8%	0%	2%	3%	2%	10%	3%	4%	7%
T21R	0%	11%	0%	1%	13%	12%	0%	11%	12%	12%	0%

Table 6-3: Reserve Ratios for 3D FCA of Bridge #2 for Various Truck Configurations

	Truck										
Member	**H-20**	**HS-20**	**Tandem**	**2F1**	**3F1**	**4F1**	**5C1**	**P-82**	**ML-80**	**TK-527**	**Min**
T01R	2.630	1.792	2.469	2.725	1.860	2.175	**1.255**	1.265	2.098	1.712	**1.255**
T02R	1.085	1.080	1.069	**1.043**	1.158	1.047	1.122	1.095	1.087	1.100	**1.043**
T03R	1.173	1.196	1.116	**1.088**	1.146	1.174	1.170	1.279	1.226	1.217	**1.088**
T04R	1.154	1.218	1.155	1.218	**1.138**	1.163	1.197	1.163	1.180	1.226	**1.138**
T05R	1.230	1.220	1.232	1.202	1.193	1.200	1.216	1.190	1.232	**1.181**	**1.181**
T31R	-0.267	-0.143	-0.271	**-0.273**	-0.176	-0.192	-0.094	-0.099	-0.191	-0.139	**-0.2729**
T33R	2.233	2.263	**2.201**	2.273	2.309	2.349	**2.201**	2.221	2.346	2.338	**2.201**
T34R	0.888	0.903	**0.869**	0.876	0.948	0.914	1.015	1.006	0.895	0.948	**0.8695**
T36R	1.229	1.182	1.258	**1.162**	1.243	1.320	1.258	1.290	1.302	1.328	**1.162**
T37R	0.891	0.935	**0.884**	0.974	0.973	0.911	0.997	0.996	0.901	0.974	**0.8843**
T39R	1.051	1.147	1.035	**1.034**	1.045	1.112	1.258	1.317	1.096	1.097	**1.034**
T40R	0.877	0.871	0.879	0.862	0.875	**0.850**	0.966	0.947	0.915	0.879	**0.8500**
T42R	0.973	1.093	**0.956**	1.043	0.964	0.987	1.169	1.054	0.968	1.000	**0.9555**
T43R	0.922	0.957	0.908	0.924	0.912	0.920	0.945	0.928	**0.879**	0.925	**0.8786**

* Bridge modeled as a theoretical truss with no floor system continuity

Table 6-4: Percent above Minimum Reserve Ratio for 3D FCA of Bridge #1M for Various Trucks

	Truck										
Member	**H-20**	**HS-20**	**Tandem**	**2F1**	**3F1**	**4F1**	**5C1**	**P-82**	**ML-80**	**TK-527**	**H/HS-20**
T01R	109%	43%	97%	117%	48%	73%	0%	1%	67%	36%	43%
T02R	4%	4%	3%	0%	11%	0%	8%	5%	4%	5%	4%
T03R	8%	10%	3%	0%	5%	8%	7%	18%	13%	12%	8%
T04R	1%	7%	1%	7%	0%	2%	5%	2%	4%	8%	1%
T05R	4%	3%	4%	2%	1%	2%	3%	1%	4%	0%	3%
T31R	2%	48%	1%	0%	36%	30%	65%	64%	30%	49%	2%
T33R	1%	3%	0%	3%	5%	7%	0%	1%	7%	6%	1%
T34R	2%	4%	0%	1%	9%	5%	17%	16%	3%	9%	2%
T36R	6%	2%	8%	0%	7%	14%	8%	11%	12%	14%	2%
T37R	1%	6%	0%	10%	10%	3%	13%	13%	2%	10%	1%
T39R	2%	11%	0%	0%	1%	7%	22%	27%	6%	6%	2%
T40R	3%	2%	3%	1%	3%	0%	14%	11%	8%	3%	2%
T42R	2%	14%	0%	9%	1%	3%	22%	10%	1%	5%	2%
T43R	5%	9%	3%	5%	4%	5%	8%	6%	0%	5%	5%

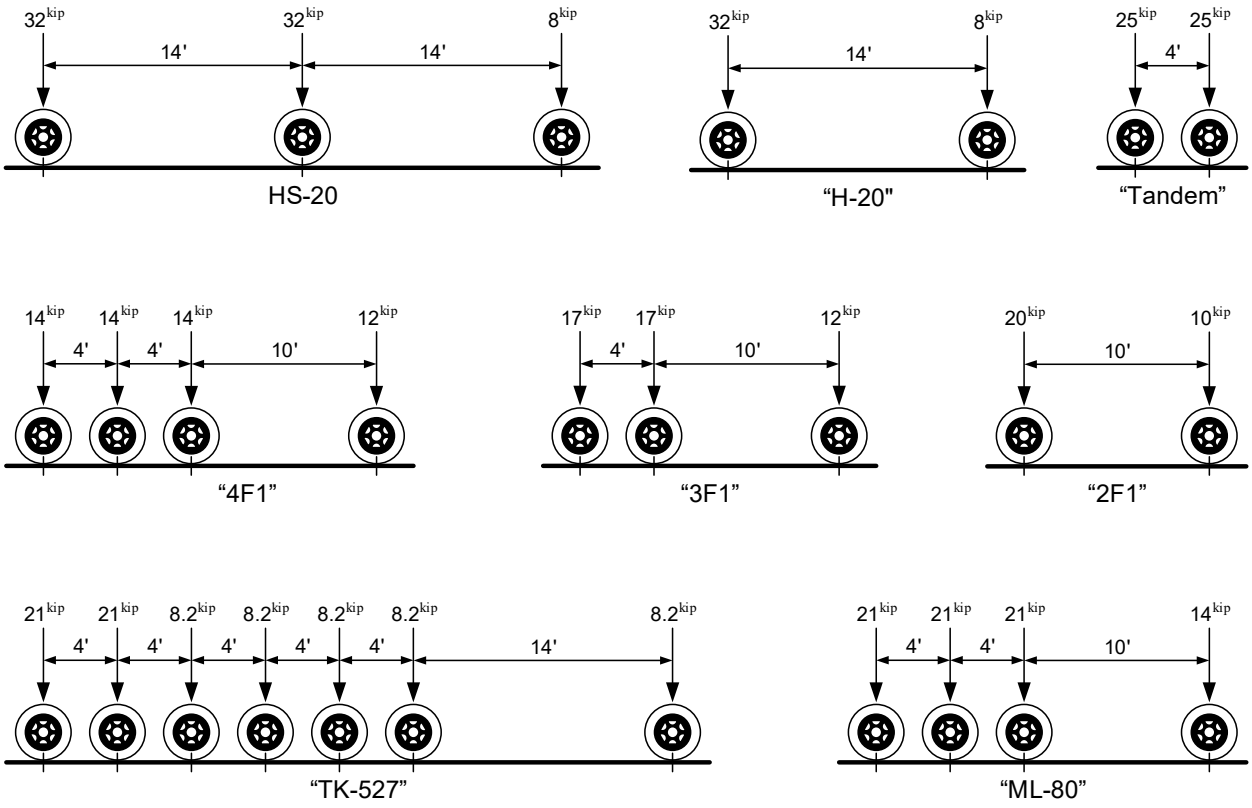

Figure 6-1: Axle Configurations for Trucks Considered

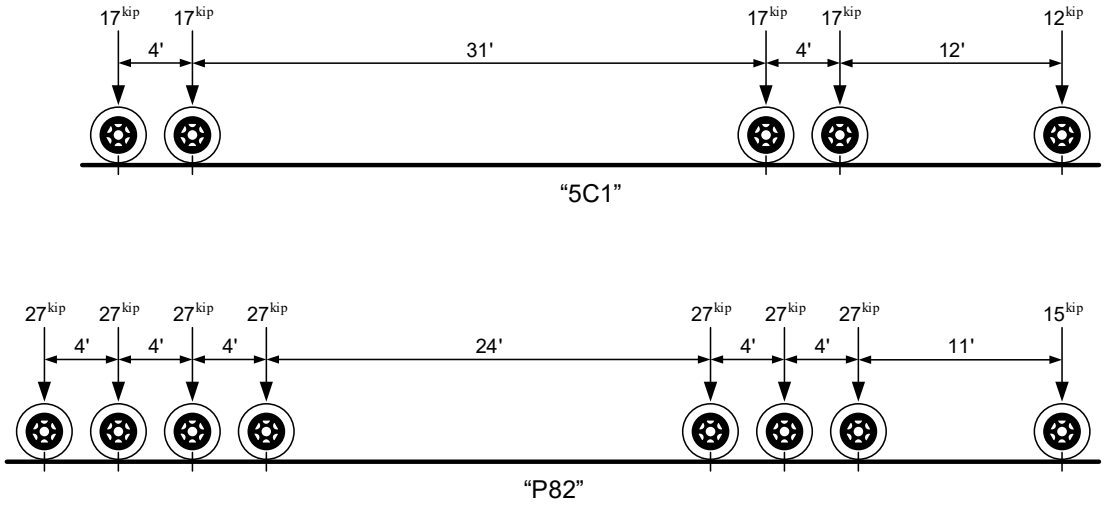

Figure 6-1: Axle Configurations for Trucks Considered (cont)

6.3: Flexurally Continuous Stringers:

Steel bridges with underslung floor beams may have stringers spanning more than one panel. These continuous stringers are often staggered as is shown in Figure 3-15 and in Figure 6-2 so that half of the stringers will be attached and supported at their midlength to any given floor beam. An investigation into the possibility of stringers supplying redundancy to a floor beam that has fractured was performed. A simple two-dimensional model of a floor beam from Bridge #1 from Appendix A (the Bloody Bridge in Auglaize County Ohio) was created in SAP2000 with linear-elastic springs placed at the location of the stringers, as is shown in Figure 6-3, to represent the stiffnesses of the stringers. The ends of the floor beam supported by the trusses were modeled as pinned even though moment connections were detailed in the bridge. Even with moment connections, it was felt that the end rotations would be appreciable due to the flexibility of the trusses. Thus the conservative approach of modeling the ends of the floor beam as pinned was adopted.

The analyses that were conducted were performed by assuming that a fracture occurred in one of the floor beams. To simulate a fracture event in a floor beam, a moment release was introduced in the floor beam at the hypothetical damage location. Modeling damage as an internal pin is intended to represent the situation where a fracture initiates in the tension flange and propagates through the web but does not affect the compression flange. In this state, the floor beam is expected to transfer shear but not bending moment. During the analyses, fractures at various locations along the length of the floor beams were simulated by placing internal hinges at each stringer location.

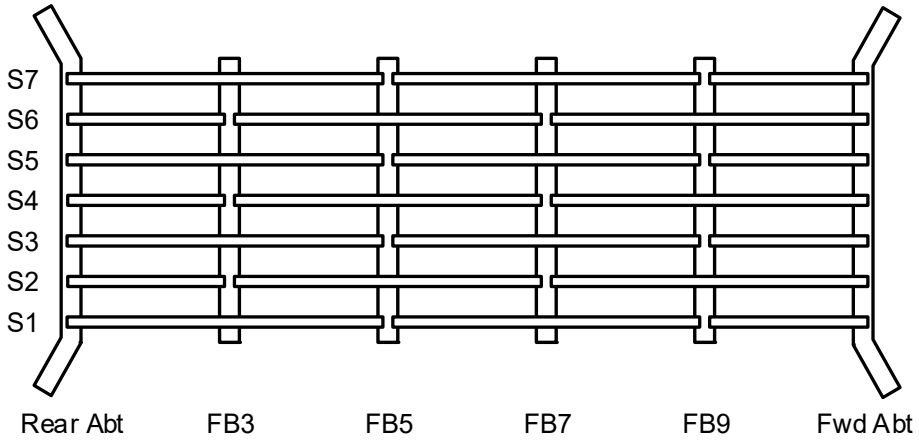

Figure 6-2: Staggered Continuous Stringer Arrangement for Bridge #1

The stiffnesses of the springs shown in Figure 6-3 were determined as the stiffnesses of the stingers assuming that they are loaded at the location of the damaged floor beam and are pinned at the locations of the other two floor beams. Three cases exist with respect to the stringers. In the first case, the damaged floor beam is at the mid-length of the stringer as shown in Figure 6-4, which, for example, would be representative of stringer lines S5 over the first and second panels. The spring stiffness associated with each stringer in this case would be K_{mid}, as shown in Equation 6-1. In the second case, the damaged floor beam is at one end of the stringer as shown in Figure 6-5, which, for example, would be representative of stringer line S4 spanning the second and third panels. The spring stiffness associated with each stringer in this case would be K_{end}, as shown in Equation 6-2. In the third case, a few stringers would span only the end panel and would be simply supported offering no stiffness to the floor beam in its damaged state; stringer line S4 in the first panel is an example of the third case. As can be seen, the midlength configuration is much stiffer than the end-load configuration.

$$K_{mid} = \frac{6EI}{L_p^3} \tag{6-1}$$

$$K_{end} = \frac{3EI}{2L_p^3} \tag{6-2}$$

Considering the staggered configuration of the stringers and the potential to have a stringer spanning only one panel connected to the first or last floor beam, there are four permutations of the floor beam model to be considered. First, there are both exterior floor beams and interior floor beams. The interior floor beams, FB5 and FB7 as shown in Figure 6-2, are supported by two adjacent stringers in the end-loaded configuration shown in Figure 6-5, which together offer a total stiffness of $2K_{end}$. The exterior floor beams, FB3 and FB9 as shown in Figure 6-2, are supported on one side by a stringer in the end-loaded configuration shown in Figure 6-5 and by a simply-supported stringer on the other side, which offer a total stiffness of $1K_{end}$. Second, when there are an odd number of stringer lines, a floor beam may be supported at its midspan (a) by a stringer in either the

midlength configuration, or the floor beam may be supportes at its midspan (b) by a stringer or two stringers in the end-loaded configuration. As it turns out, each of the four floor beams in the Bridge #1 as shown in Figure 6-2 represents one of the four possible unique configurations.

Given the four floor beam configurations and assuming that a fracture can occur in the floor beam at any of the seven stringer locations, taking advantage of symmetry, there are 16 different analyses to consider for Bridge #1.

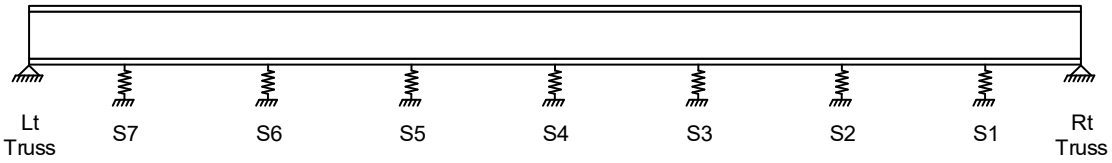

Figure 6-3: Modeling the Stiffness of Stringers as Springs Connected to a Floor Beam

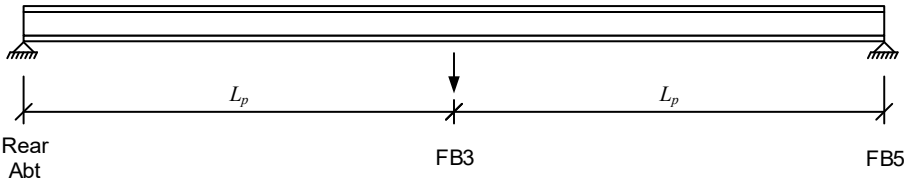

Figure 6-4: Two-Span Continuous Stringer Supporting a Floor Beam at Midlength

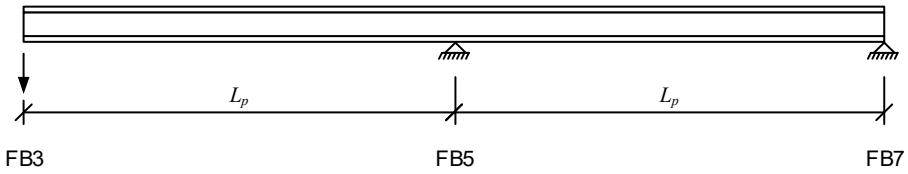

Figure 6-5: Two-Span Continuous Stringer Supporting a Floor Beam in an End-Loaded Configuration

Dead loads were modeled as point loads located at the stringer locations. Live loads were applied as point loads of 16 kips each to represent one axle in each of two trucks, with six foot axles both positioned one foot from the center of the floor beam.

The reaction forces in the springs and at the truss locations as well as deflections at each stringer location were recorded. The decision was made to define yielding as a failure criterion in the stringers. Thus, the force necessary to induce yielding was computed and compared to the reaction forces in the springs. The deflections recorded from the analyses were compared to the length of the floor beam as well to determine whether the floor beam should be considered redundant.

6.3.1: Bridge #1

The stringers of Bridge #1 are W12x30s, which is a common stringer size. Seven stringer lines are present and they are spaced at 42" center-to-center. The floor beams are W24x94s with a theoretical length of 25'-6$^3/_8$" spaced at 13'-2$^3/_8$". Calculations for the equivalent spring stiffnesses are shown as Equations 6-3 and 6-4 for stringers corresponding to Figure 6-4 and Figure 6-5, respectively.

$$K_{mid} = \frac{6EI}{L_p^3} = \frac{(6)(29{,}000^{\text{ksi}})(238\ \text{in}^4)}{(158.4'')^3} = 10.43\frac{\text{kip}}{\text{in}} \tag{6-3}$$

$$K_{end} = \frac{3EI}{2L_p^3} = \frac{(3)(29{,}000^{\text{ksi}})(238\ \text{in}^4)}{(2)(158.4'')^3} = 2.606\frac{\text{kip}}{\text{in}} \tag{6-4}$$

The reaction force in the spring that would cause first yielding can be computed from the moment diagram corresponding to Figure 6-4 and Figure 6-5 as is shown in Equations 6-5 through 6-8, where F_y and S_x are the yield strength and section modulus of the stringer.

$$M_{mid} = \frac{R_{Spring}L_p}{8} \le M_y = F_y S_x \tag{6-5}$$

$$\rightarrow \qquad R_{Spring} = \frac{8F_y S_x}{L_p} = \frac{(8)(50^{\text{ksi}})(38.6\ \text{in}^3)}{(158.4'')} = 97.47^{\text{kip}} \tag{6-6}$$

$$M_{end} = R_{Spring}L_p \le M_y = F_y S_x \tag{6-7}$$

$$\rightarrow \qquad R_{Spring} = \frac{F_y S_x}{L_p} = \frac{(50^{\text{ksi}})(38.6\ \text{in}^3)}{(158.4'')} = 12.18^{\text{kip}} \tag{6-8}$$

The dead load and live load definitions are shown in Figure 6-6 and Figure 6-7, respectively.

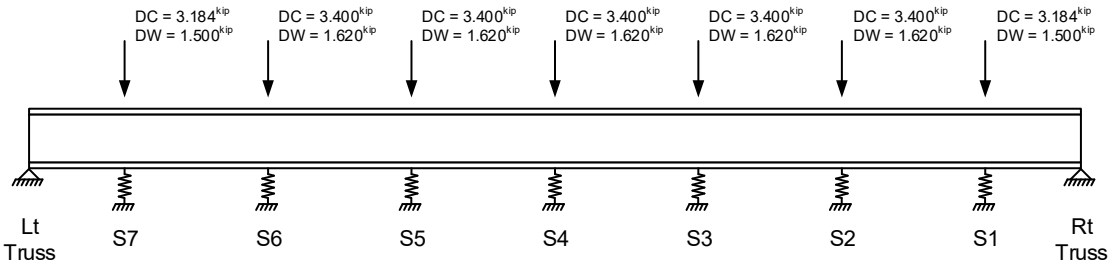

Figure 6-6: Dead Loads for Bloody Bridge Floor Beam

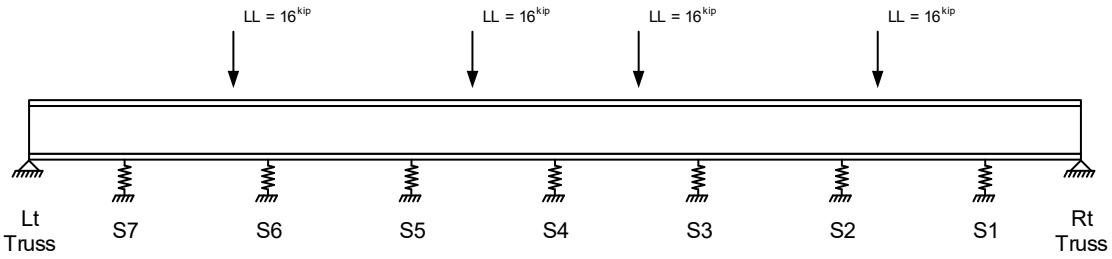

Figure 6-7: Live Loads for Bloody Bridge Floor Beam

For Bridge #1, it was determined that FB3 with a fracture at the midspan of the floor beam was found to be the critical case. FB3 represents the case of an exterior floor beam with the end-loaded stringer configuration at its midspan. For this case, it was found the maximum moment in the connected stringers due to unfactored loads was 81% of their yield moment and the deflection due to unfactored loads was L / 80. Based on this series of analyses, it can be stated that the floor beams in Bridge #1 would not be fracture critical if they were arranged in a staggered flexurally continuous configuration.

6.3.2: Additional Bridges

The study that is summarized in the previous section for Bridge #1 with staggered flexurally continuous stringers was conducted for the five additional bridges shown in Table 6-5 with panel lengths ranging from 12'-2 5/8" to 16'-0". In all cases, the floor beams with hypothetical cracks at any one stinger location were stable under unfactored dead load and unfactored H-20 loads without impact. Deflections in the damaged state under the same loading were found to be in the range of L / 100 to L / 30.

Based on this series of analyses, it can be stated that under all conditions considered, floor beams in pony truss bridges that have staggered flexurally continuous stringers that are robustly attached to the floor beams can be classified as not fracture critical.

Table 6-5: Bridges Considered in the Continuous Stringer Study

Bridge	S_T	Floor Beam	L_P	Stringer	S_S
Bloody Bridge	25'-6 3/8"	W24x94	12'-2 5/8"	W12x30	3'-6"
Beisner Rd	30'-10 3/8"	W30x124	14'-3"	W12x30	3'-3"
Deep Cut Rd	29'-6 3/8"	W27x102	14'-7 1/4"	W12x30	3'-6"
Twp Road 365	18'-3/8"	W18x55	15'-1 3/4"	W12x30	3'-4"
Glywood Rd	25'-6 3/8"	W24x84	15'-6"	W12x30	3'-6"
Campbell Ave	31'-3 5/8"	W36x135	16'-0"	W16x45	6'-0"

6.3.3: Three-Dimensional FE Floor Beam Modeling:

To corroborate the two-dimension floor-beam analyses that were described previously a series of three-dimension models of Bridge #1 was created with the express purpose of examining floor beam behavior. Default ASCE 41 flexural hinges were included in the

floor beams to the left and right of each stringer location. Dead loads as described in Appendix A were applied to the decking members and a live load consisting of two HS-20 trucks were centered transversely on the bridge deck with 2'-0" distance between the wheels. The trucks were position facing forward with their rear axles over floor beam #3.

Two different stringer configurations were considered; the first included stringers that were simply supported at each floor beam while the second considered a staggered continuous arrangement like that shown in Figure 6-2. In both cases, the decking was considered to contribute nothing to the strength of the floor system. As was the case with the two-dimensional analyses described previously, a crack was simulated by introducing a moment release in the floor beam. This case study focused on floor beam #3 and the crack was presumed to form at midspan of the floor beam. Figure 6-8 shows the load vs centerline deflection response of the floor beam in the bridge without stringer continuity and Figure 6-9 shows the response with staggered stringer continuity (labeled every other, or "EO", in the figure). Responses for the floor beam centerline deflection are shown for both the undamaged and damaged cases in each figure.

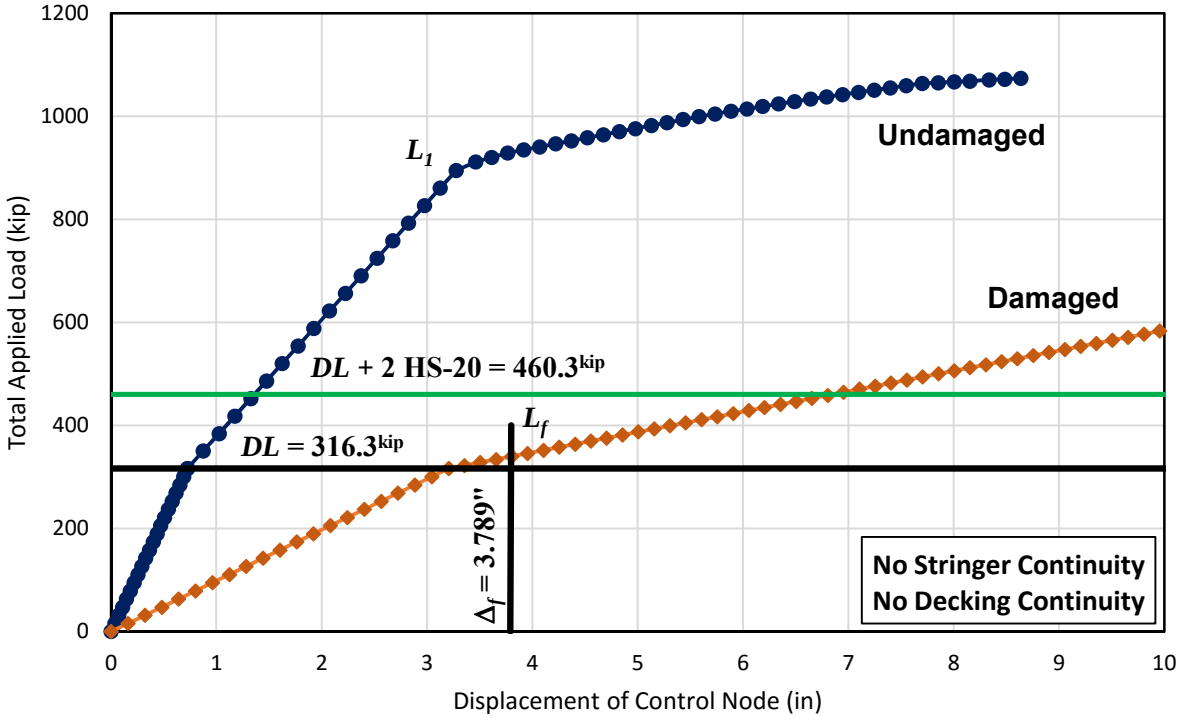

Figure 6-8: Load-Deformation of Floor Beam #3 - No Stringer Continuity

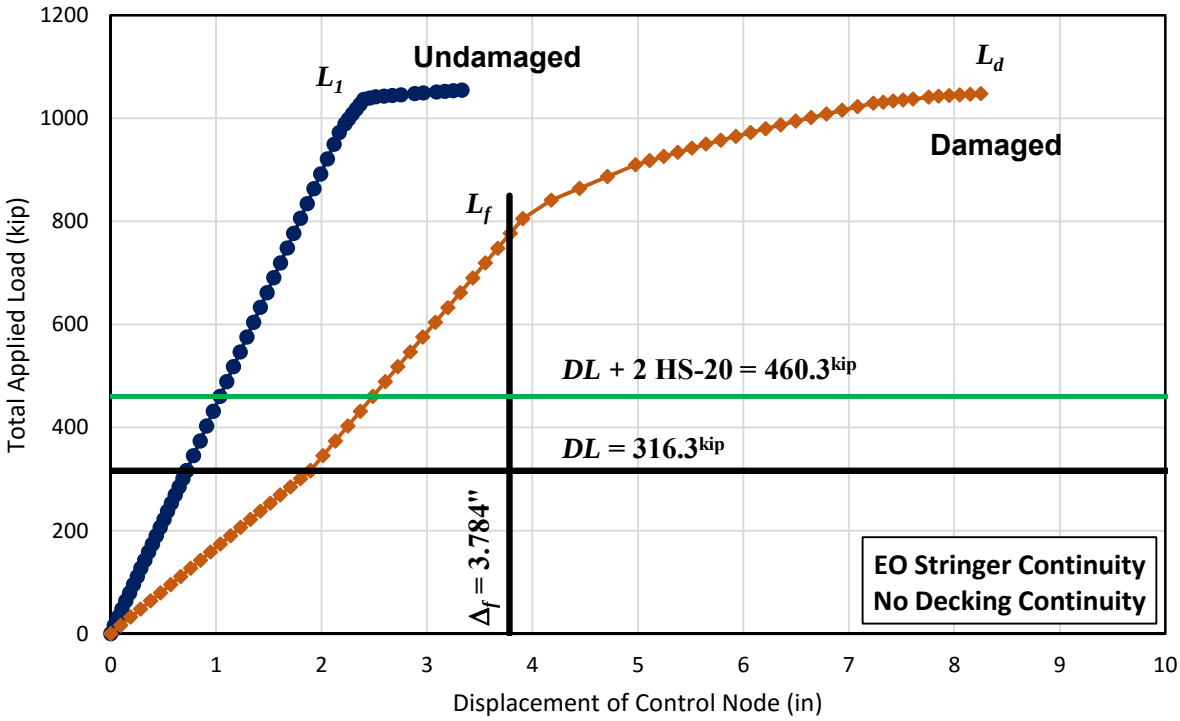

Figure 6-9: Load-Deformation of Floor Beam #3 - Staggered Stringer Continuity

In the case where the stringers are assumed to have no flexural continuity, the fractured floor beam remains stable under both dead load and live load, but experiences significant deformation and the functionality limit governs. L / 100 = 25.53' / 100 = 3.064". The dead load deflection of the undamaged beam is 0.7252", thus the functionality limit is Δ_f = 3.789". The reserve ratio of the model in this state, calculated below, is $R_d = 0.03078$ indicating that the floor beam should be treated as fracture critical. If the deflection limit is relaxed to Δf = 10.56", the L_f would equal 606.9^{kip} and R_d would be 0.5024 and the floor beam could be classified as not fracture critical. This would correspond to a deflection of roughly L / 30, which is fairly large. Note in Figure 6-8 however, that at a deflection of 6.955" the floor beam is able to carry full dead load and live load (load factors and impact factors = 1.00).

In the undamaged model, first yielding occurred in floor beam #3 followed by yielding in floor beam #5 before compression buckling of the top truss chord occurred indicating the ultimate limit state for the bridge under this loading. In the damaged model, yielding is noted in floor beam #5 at a total applied load of 612^{kip} and the analysis was terminated when the deformation of the control node reached approximately 18", before an ultimate limit state was observed.

$LL = 144^{\text{kip}}$, $DL = 316.3^{\text{kip}}$, $L_{1S} = 894.7^{\text{kip}}$, and $L_f = 334.1^{\text{kip}}$

$$LF_{IS} \simeq \frac{894.7^{\text{kip}} - 316.3^{\text{kip}}}{144^{\text{kip}}} = 4.017 \qquad LF_d = \frac{334.1^{\text{kip}} - 316.3^{\text{kip}}}{144^{\text{kip}}} = 0.1236$$

$$R_d = \frac{LF_d}{LF_{IS}} = \frac{0.1236}{4.014} = 0.03078$$

In the case where the staggered continuous stringer arrangement was assumed, the fractured floor beam remains stable under both dead load and live load and sustains a limited deformation. The functionality limit governs but at a much higher load than in the case with no stringer continuity. The dead load deflection of the undamaged beam is 0.7204", thus the functionality limit is Δ_f = 3.784". The reserve ratio of the model in this state, calculated below, is $R_d = 0.6852$ indicating that the floor beam could be treated as not fracture critical. The deformation corresponding to full dead load and live load (load factors and impact factors = 1.00) is Δ = 2.368", which corresponds to a deflection of roughly L / 186.

In the undamaged model, first yielding occurred in floor beam #3 followed by yielding in floor beam #5 at a total applied load of 834kip before compression buckling of the top truss chord occurred indicating the ultimate limit state for the bridge under this loading. In the damaged model, yielding is noted first in stringers 3 and 5 over floor beam #3 at a total applied load of 910kip and yielding was observed in floor beam #5 at a total applied load of 987kip. After more yielding in floor beam #5, the bridge was able to sustain a total applied load of 1,048kip before the floor system was not able to carry any additional load.

$$LL = 144^{\text{kip}},\ DL = 316.3^{\text{kip}},\ L_{IS} = 988.1^{\text{kip}},\ \text{and}\ L_f = 776.6^{\text{kip}}$$

$$LF_{IS} \simeq \frac{988.1^{\text{kip}} - 316.3^{\text{kip}}}{144^{\text{kip}}} = 4.665 \qquad LF_d = \frac{776.6^{\text{kip}} - 316.3^{\text{kip}}}{144^{\text{kip}}} = 3.197$$

$$R_d = \frac{LF_d}{LF_{IS}} = \frac{3.197}{4.665} = 0.6852$$

At the limit of each model, moments at the end of the floor beams were checked and found to be below the expected moment strength of the connection to the truss panel points. Further, the shear developed at the ends of the stringers was low enough to be accommodated with typical connections (i.e. two or four bolts in tension).

Based on this case study, the conclusion drawn from the two-dimensional analysis is corroborated. Floor beams of pony truss bridges that have continuous stringers that are robustly attached to the floor beams can be treated as not fracture critical.

6.4: Flexurally Continuous Decking:

In bridges where the deck or decking has a robust attachment to the stringers and stringers have robust attachments to the floor beams, there exists a potential for the decking to provide additional strength to the floor system. To investigate this potential, additional three-dimensional FE models of Bridge #1 were created building on what was discussed in Section 6.3.3. This case study was conducted based on a 5 gauge 3”x9” metal decking attached to the stringers with bolted clips or plug welds, but could also be extended to a reinforced concrete deck attached via shear studs. In the case of the metal decking, the asphalt was considered to not add any strength to the decking.

Two additional models were created to supplement the two models described in Section 6.3.3. In the third model, the stringers were assumed to be simply supported and in the fourth model, the stringers were assumed to be arranged in the staggered continuous arrangement. In both the third and fourth model, the decking was made continuous across the width of the deck and rotational hinges were defined to the right and left of each stringer. Figure 6-10 shows the load vs centerline deflection response of the floor beam in the bridge without stringer continuity and Figure 6-11 shows the response with staggered stringer continuity (labeled every other, or “EO”, in the figure). Responses for the floor beam centerline deflection are shown for both the undamaged and damaged cases in each figure.

As can be seen in both figures, the continuous decking substantially adds to the strength of the floor system, and in all cases the strength was limited by yielding and then buckling of the compression chord of the trusses. Although significant yielding in the decking was noted, the floor beam deformations in both models was drastically reduced by the presence of the decking. Force transfer between the deck and stringer was highest in the vicinity of the fracture and was found to be in the range of 5 to 6 kips per foot (in the width direction of the decking), which can easily be accommodated with bolted clips or plug welds.

Based on this, it can be observed that the presence of decking with a robust connection to the strength and when the stringers are robustly attached to the floor beams, can add substantial reserve capacity to the floor system and eliminate the need for classifying floor beams as fracture critical.

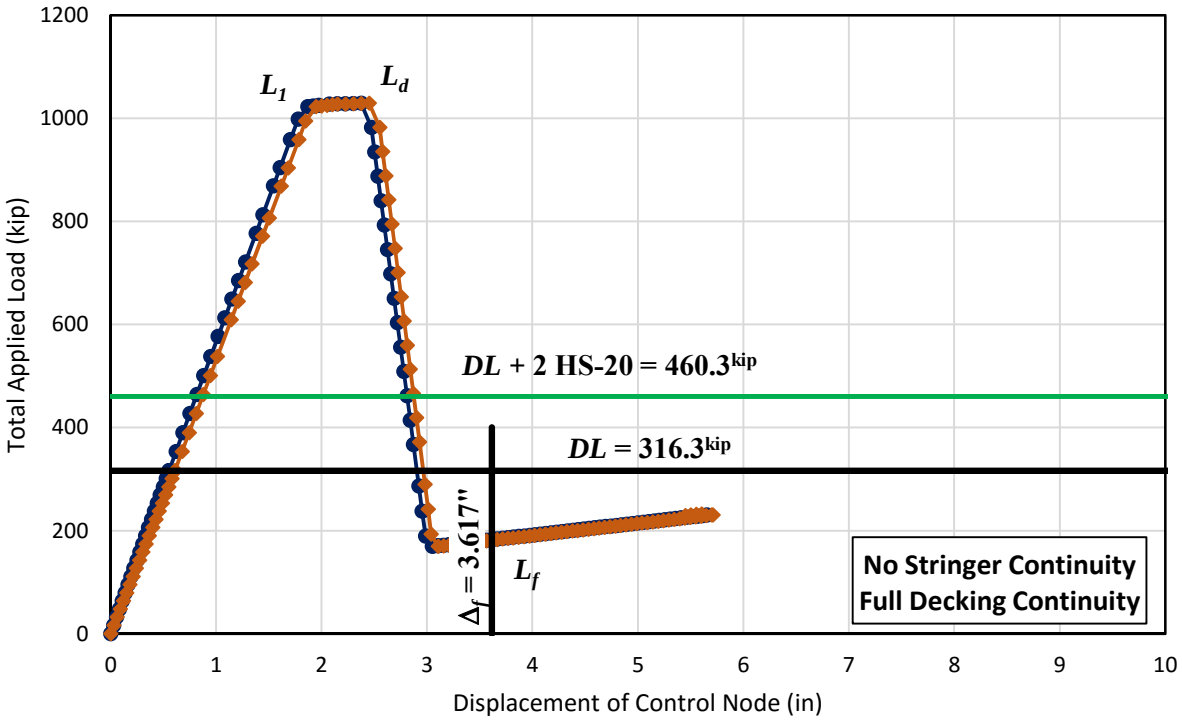

Figure 6-10: Load-Deformation of Floor Beam #3 with Continuous Decking- No Stringer Continuity

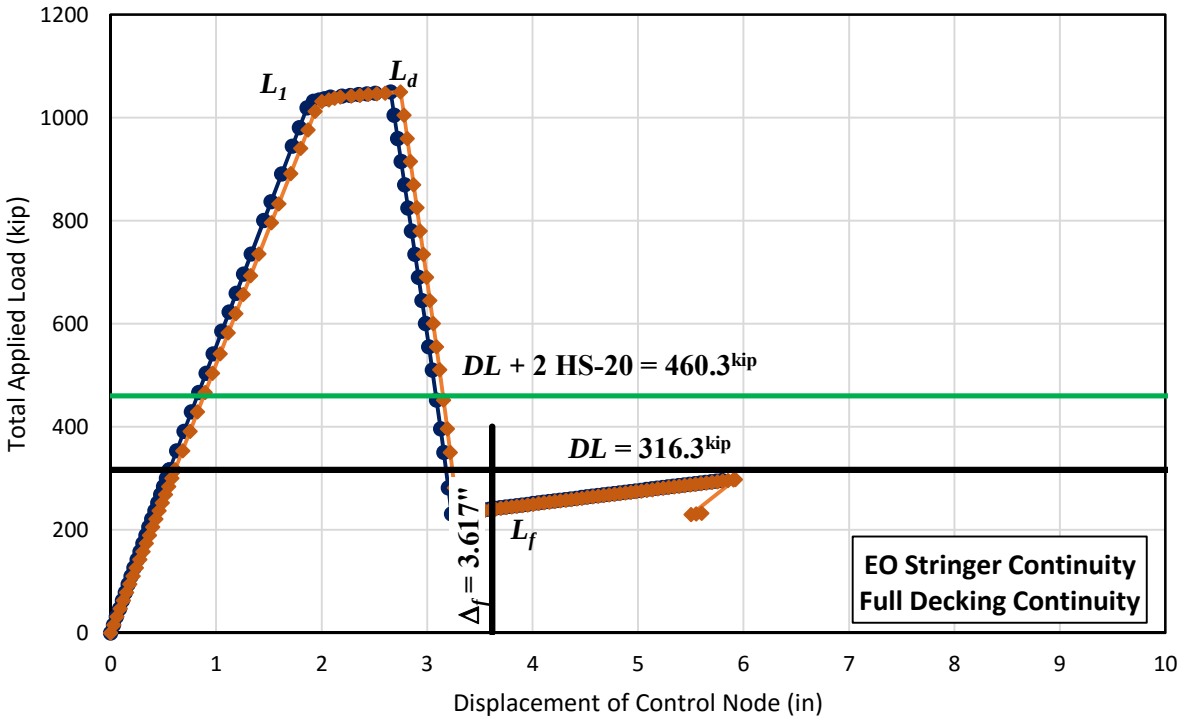

Figure 6-11: Load-Deformation of Floor Beam #3 with Continuous Decking- Staggered Stringer Continuity

6.5: High Resolution Finite Element Case Studies:

To verify the results of more commonly available finite element software, a highly detailed finite element model of the Campbell Avenue pony truss bridge over Wills Creek was created using the software package ABAQUS/CAE Version 6.13 (Dassault Systèmes, 2010). A perspective view of the model is shown in Figure 6-12.

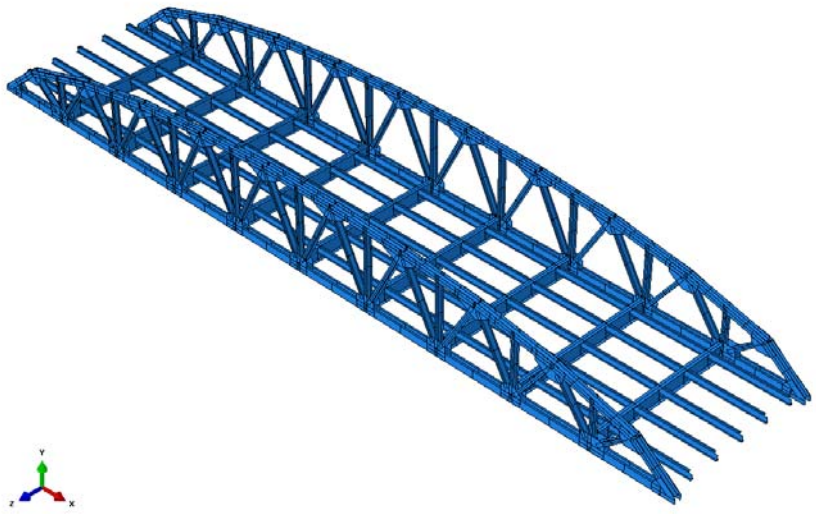

Figure 6-12: High-Resolution FE Modeling Image from ABAQUS

There were two element types used in this model, shell elements and beam elements. The shell element type used was the general purpose shell S4R, a 4-node doubly curved shell with reduced integration, hourglass control and finite membrane strains. The beam element type used was B31, a 2-node linear beam in space. The shell elements were used to model almost all of the structural components of the bridge with the exception of the lateral rods which were modeled as beams. The steel members have shell offset applied such that the elements of the webs run the full depth of the member, as is illustrated in Figure 6-13.

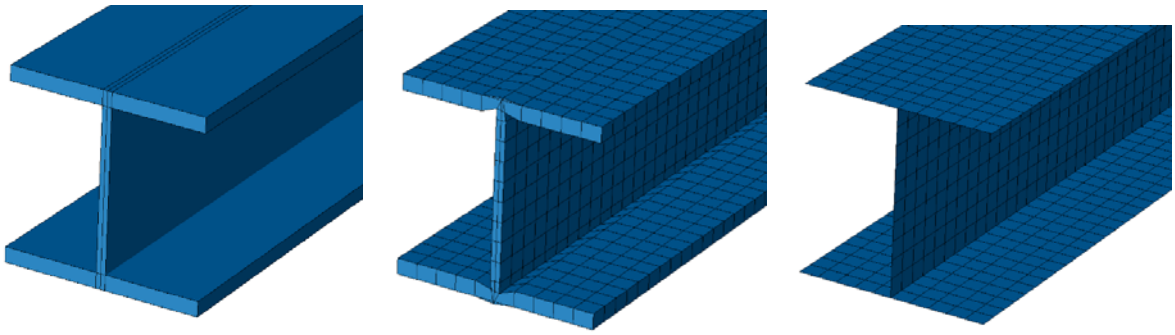

Figure 6-13: Shell Thickness, Mesh with Thickness, and Mesh without Thickness (left to right)

Two materials were used, in the detailed model, A572 grade 50 steel and 4[ksi] concrete. Though the steel parts of the bridge include plates, channels, and angles; all these parts are specified in the plans as A572 grade 50 steel. Young's modulus was taken as 29,000[ksi] and 0.3 was used as Poisson's ratio. For the plastic behavior nominal steel values were used as shown in Figure 6-14.

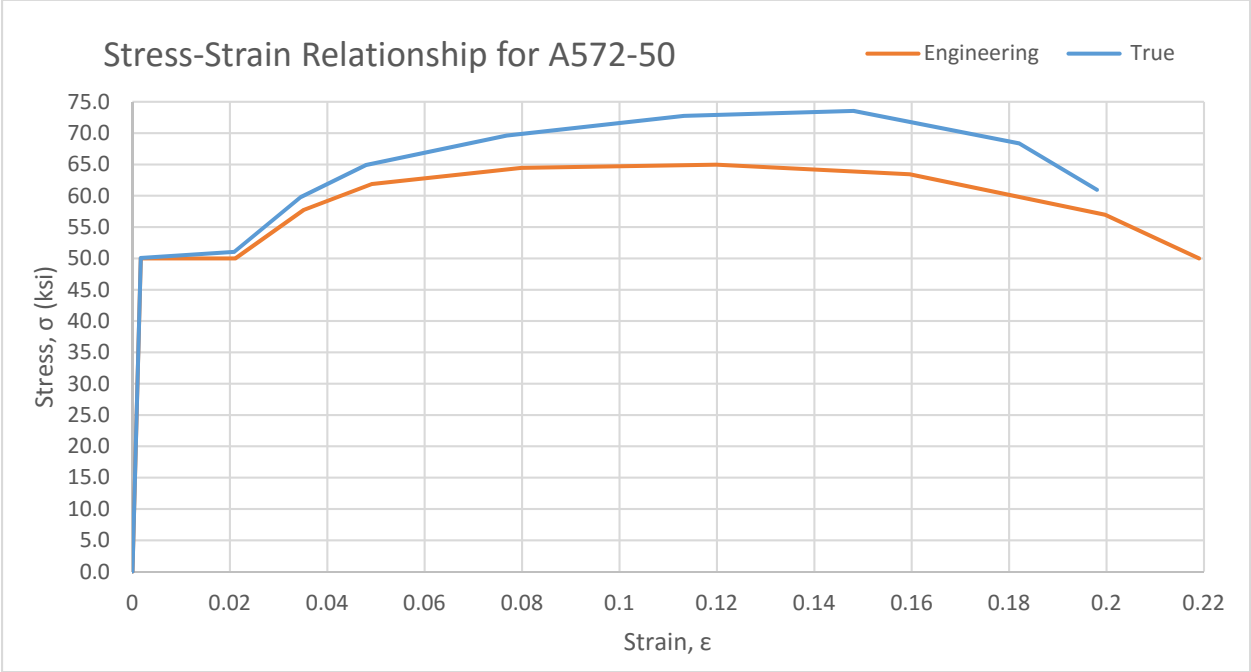

Figure 6-14: Stress-Strain Relationship used in High-Resolution Modeling

The concrete was modeled using the Concrete Damaged Plasticity material behavior. The values used for this concrete were modified from study by Jankowiak and Lodygowski (2005) in the same manner as was done by McConnell (2012), scaling the stress relative to the desired maximum stress. McConnell was able to obtain good results with this method despite the concrete used by Jankowiak and Lodygowski being significantly stronger than their concrete (7.25[ksi] compared to 3.1[ksi]). The dilation angle used was 38°, the flow potential eccentricity used was 1, and the ratio of initial equibiaxial

compressive yield stress to initial uniaxial compressive yield stress was taken as 1.12, as was found by Jankowiak and Lodygowski. The hardening-damage parameter K_c was taken as 2/3 in accordance with the ABAQUS theory manual. The parameters are shown in Table 6-6.

Table 6-6: Concrete Material Properties used in High-Resolution Modeling

			Parameters for CDP	
			β	38
Kc	0.666666667		m	1
E [ksi]	3605		f = fb0 / f'c	1.12
Poisson	0.2		Γ	0.666
Compression Hardening			Compression Damage	
Stress [ksi]	Crushing Strain		Damage Parameter	Crushing Strain
1.1999997	0		0	0
1.615823916	7.47307E-05		0	7.47307E-05
2.40004812	9.88479E-05		0	9.88479E-05
3.224301674	0.000154123		0	0.000154123
4.00061436	0.000761538		0	0.000761538
3.218886395	0.002557559		0.015632156	0.002557559
1.618886795	0.005675431		0.047710548	0.005675431
0.420604455	0.011733119		0.071589182	0.011733119
Tension Stiffening			Tension Damage	
Stress [ksi]	Crushing Strain		Damage Parameter	Crushing Strain
0.15991436	0		0	0
0.227359943	0.00003333		0	0.00003333
0.149584763	0.000160427		0.032512872	0.000160427
0.069017823	0.000279763		0.055710386	0.000279763
0.018100315	0.000684593		0.073630382	0.000684593
0.004526079	0.00108673		0.07840742	0.00108673

The connections of members to gussets and connecting angles were modeled using mesh-independent fasteners with the rigid beam interaction. The fasteners were assigned a radius of 0.5”and were placed as bolts would be, the default coupling type “Continuum Distributing” was used for these fasteners. The deck and stringers were modeled as fully composite using the same method, however, for interaction between the steel deck and

floor beams a contact interaction was defined. This contact interaction was “hard” with a coefficient of friction defined as 0.2.

The lateral rod anchor plate was modeled as a part of the floor beam rather than a separate part welded to the floor beam. The lateral rods were tied to the anchor plate portion of the floor beam part. Each of the truss supports were constrained to a single point using a kinematic coupling constraint. Two of them at one end of the bridge were pinned, with all directions of translation restrained. The other two at the opposite end of the bridge, as well as the ends of the stringers, were defined as rollers, allowing translation in the direction of the roadway.

The loads were applied in two steps. The first step applied a gravity load to every part in the assembly (density of concrete and steel were defined in material properties as mass densities 0.0002835 kip/in^3 for steel 8.68×10^{-5} for concrete) except for the steel deck which was given a greater gravity load to account for asphalt and wearing surface, which were not included in the model.

The second step was the application of the truck live load, an HS-20 at the position previously found to be critical for the element being tested. The load was applied as pressure loads on 4, 10”x20” tire patches positioned 12” from the edge of the deck on the concrete deck, with another tire patch 72” center-to-center from the first one. On the steel deck it was distributed to the steel ribs at this position rather than projected onto the diagonals of the steel decking. The truck loading is increased beyond a regular loading while retaining the load ratio until the model failed to converge, indicating collapse.

Corrugated steel decks have little axial or in plane shear stiffness. While concrete decks have greater stiffness in both those directions, the location of decks makes the potential loading largely tensile with some shear. One potential load path for a lost bottom chord would be truss to floor beam to stringers and deck and then back. The distribution of tensile stress in a concrete deck is therefor of interest, as is the capacity of stringers to carry tension.

Figure 6-15 shows the distribution of the Maximum Principal stress in the deck as the dead load is applied for the case of a bottom missing chord member. The stress is quite low across the panel missing a member, indicating that the deck at least, is not acting as the bottom chord of a truss across the missing panel.

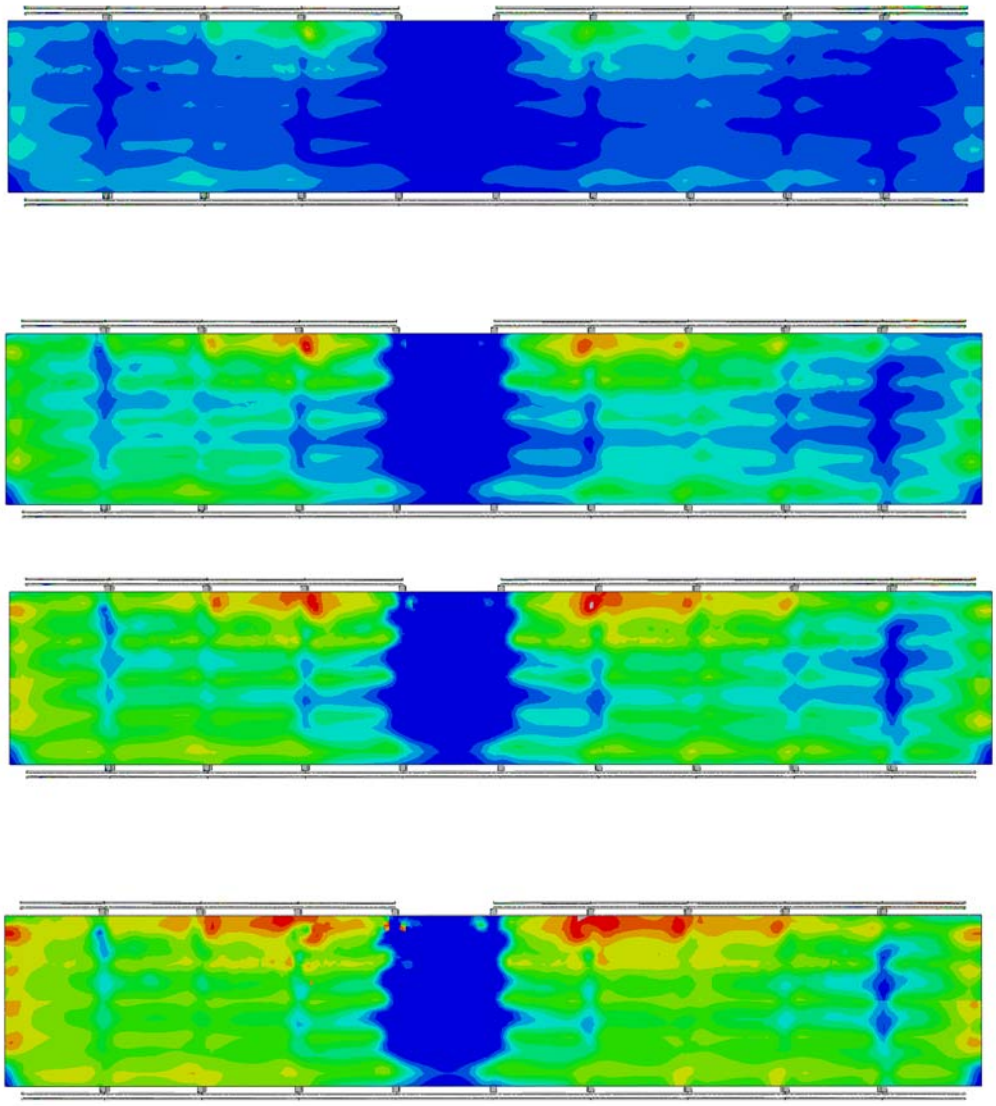

Figure 6-15: Max Principal Stresses in Concrete Deck with Bottom Chord Missing

6.6: High-Resolution Connection Modeling:

The high resolution modelling revealed some important notes about actions the less refined models must duplicate. First the connections of the stringers to the floor beams yielded first, even when the bridge was intact and had a concrete deck to share the load. The angles connecting the stringers to the floor beams yielded well before any other part. This indicates that while regularly designed as simply supported beams holding essentially no tension, stringers do pick up a portion of the bottom chord load that, in extreme situations such as overloading or loss of a bottom chord member, can be effective. Even the concrete deck was found to be insufficient for providing continuity across stringers and the steel deck should certainly not be counted on for providing much tensile strength.

Another revelation of the high-resolution modeling was that member yielding was often preceded by yielding of the gusset plates, and that the concrete of the deck endures some relatively minor cracking before collapse. From the way that the gussets yield, interaction between both bending directions and axial loads contribute significantly to the yield pattern.

Figure 6-16 shows connections used in the high resolution model. Figure 6-16(a) illustrates an end plate connection of a floor beam at a truss panel point. Figure 6-16(b) shows a gusset plated connection in the upper chord of one of the trusses, which features mesh-independent fasteners. Figure 6-16(c) shows a stringer-to-floor beam connection in the frame floor system.

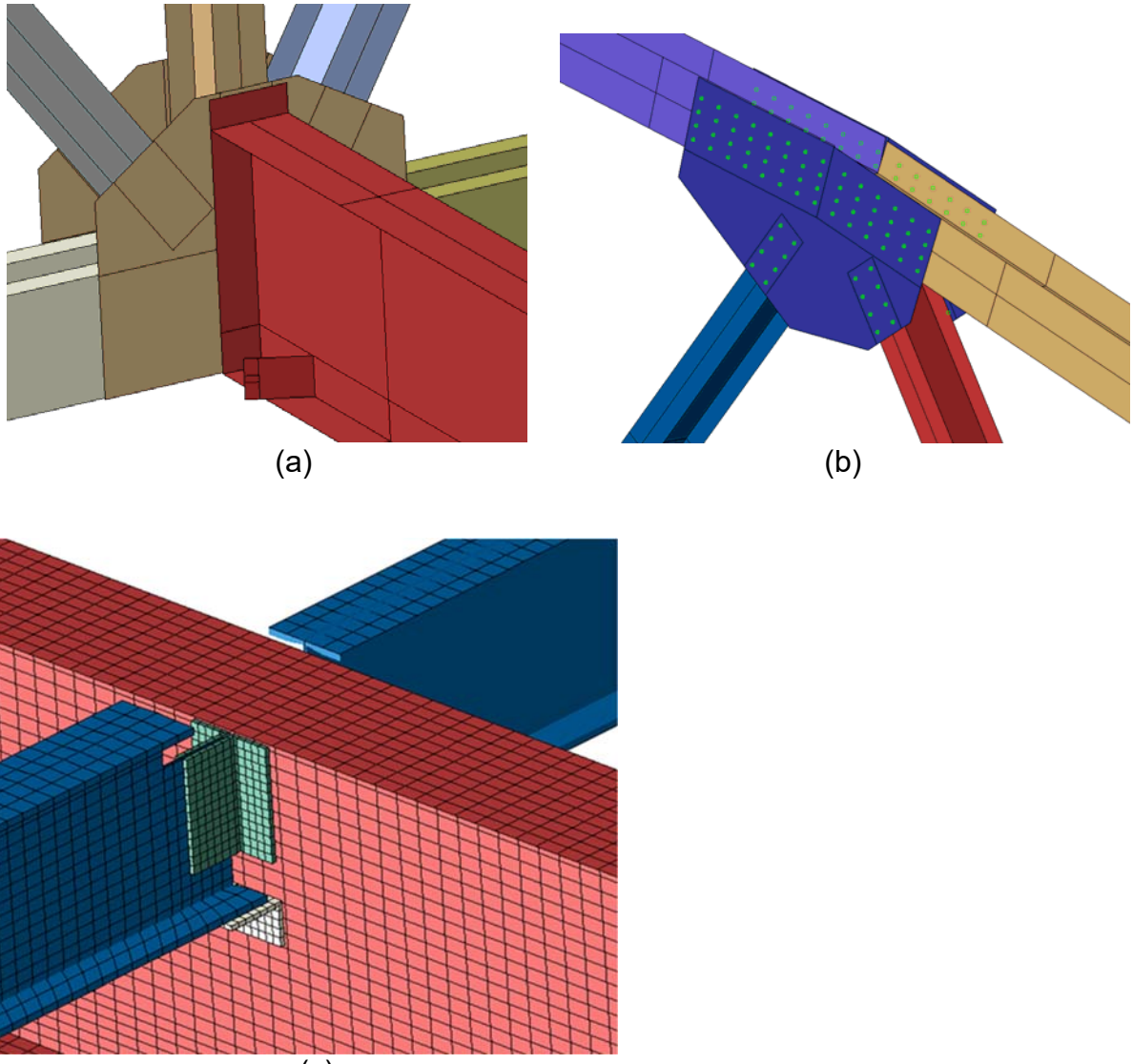

(a) (b)

(c)

Figure 6-16: High Resolution Modeling of PTB Connections

If the tensile force normally associated with the lost bottom chord member is not held by the deck then one of a few things may have happened. The gusset above the missing chord may be acting as a very stiff moment connection, or the stringers and floor beam may be holding that tension. Observing the high resolution model reveals that both of these phenomena are happening to a significant degree. The connections of the stringers to the floor beams however, are designed to be simply supported, holding essentially no tension. Figure 6-17 shows the connection of the stringer next to the missing chord member at the point of collapse illustrating the Von-Mises stress distribution. All three angles have yielded along their entire length, and this distribution of stress and yielding is reminiscent of the even higher resolution model of just this connection in tension, assembled from solid elements with bolts that was also modeled.

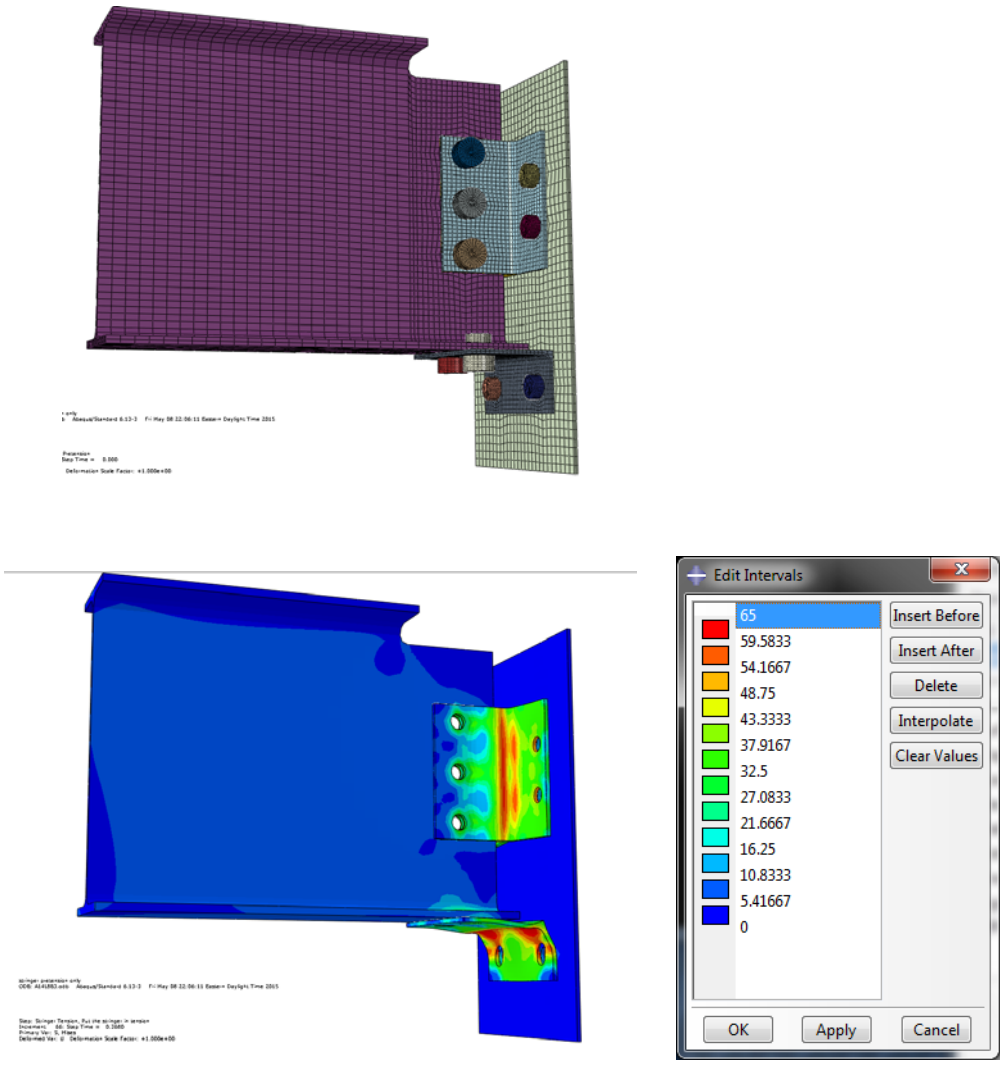

Figure 6-17: Von Mises Stresses in a Framed Stringer to Floor Beam Connection

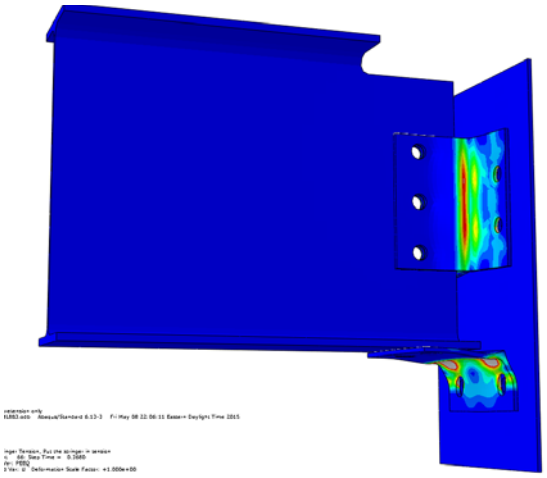

Chapter 7 - Conclusions and Strategies for Retrofit, Design, and Inspection of Pony-Truss Bridges

This chapter covers several strategies that can be used to eliminate or avoid fracture critical members in the retrofit of existing pony truss bridges and the design of new pony truss bridges. In the development of these strategies, much consideration was given to the cost of implementation, both within the context of the retrofit of existing structures and in the design of new structures. Adding flexural continuity to the stringers in a floor system, for example, might be easily accomplished with little extra cost in a new bridge design but could be rather challenging in a retrofit situation.

The cost of implementation must also be balanced with the potential savings in terms of increased inspection and maintenance costs associated with fracture critical members. Diagonal truss members, for example, can often be easily inspected since they are generally quite accessible from the deck of the bridge. Bottom chord members, too, are often fairly accessible, though less so than diagonal truss members. Floor beam inspections, on the other hand, can be more challenging and may require ladders, rigging, or even snoopers for access, therefore additional lifecycle cost savings can be achieved if fracture critical inspections of floor beams can be avoided.

7.1: Retrofit and Design Strategies for Pony Truss Bridge Superstructures

The superstructure is made up of the trusses and floor beams of the bridge. While the floor beams are undeniably also a part of the floor system, they do in fact provide stability to the trusses by means of moment connections at the truss panel points. For sake of this discussion, however, the inclusion of floor beams will be limited to their influence on the trusses. A discussion of floor beam redundancy will be presented in Section 7.2.

Taking account of the moment strength and rigidity inherently present in the connections within the trusses can be helpful. Although adding moment connections was shown to add only a marginal level of stiffness and strength to the system, doing so can contribute some additional strength and redundancy to the bridge, which in some cases might be enough to make a difference. In most cases, though, accounting for the moment strength in the truss connections will lead only to the development of plastic hinging in the members adjacent to the connections. Since the members are invariably bent about their weak axes in the plane of the truss, these plastic moments tend to be quite small, particularly when channels arranged with their flanges parallel to the plane of the truss are used.

Detailing supports of the bridge such that thermal expansion and contraction are accommodated but that larger displacements associated with a fracture can be resisted may be an effective way of adding redundancy to a bridge. The secondary load path associated with this mechanism, however, places the bottom chord of the truss in compression, and since the bottom chords are typically designed for tension only, and are thus typically slender, they generally have minimal strength in compression. If the

bottom chord was designed as an internally redundant member with sufficient intermediate connectors (such as a pair of channels braced against each other using bolted lacing) then this could be a solution worth investigating.

The members in the trusses can be classified as either compression members, tension members, or members subject to load reversals, which are typically the diagonal members of a truss. It is the tension members and members subjected to load reversals that are of interest here, and they will be addressed in the two following subsections.

7.1.1: Tension Chord Redundancy:

Members in the tension chords of the trusses are in general categorized as fracture critical. When tension chord members are analyzed as internally nonredundant members (i.e. a single channel or single wide flange) it was found that a refined analysis was generally not able to show sufficient system redundancy to justify reclassification as not fracture critical, even when the floor system was engaged as a secondary load path. When tension chord members were analyzed as internally redundant (i.e. pairs of angles, channels, or tees as shown in Figure 3-4), however, a refined analysis was generally able to show sufficient redundancy to reclassify these members as not fracture critical.

For the design of new structures, it is recommended that tension chord members be designed with internal redundancy. Further, it is recommended that the tension chord members be evaluated for fatigue assuming that one element of the tension chord is ineffective. This fatigue evaluation should, at a minimum, be conducted using the ADTT for the bridge over a period equal to the inspection interval of the bridge assuming that fracture-critical inspections are not required. A more conservative approach would be to design for infinite life of the member elements assuming that one element is ineffective.

For the retrofit of existing structures, replacement of existing tension chord members with internally redundant members is recommended, though it is recognized that this process will likely be invasive and costly, particularly for bridges with welded connections. As an alternative, post tensioning bars can be added to the tension chord members of the truss. Post-tensioning bars would be anchored at the panel points and pretensioned to a nominal level. PT bars should be designed to carry the full dead load and at least half of the design live load. As a rule of thumb, the PT bars should have about half the tensile strength of the full tension chord member that they are reinforcing. For smaller members in bridges of moderate length, this can likely be accomplished with just a pair of bars. For larger members in bridge of longer length, four or more bars may be required.

Anchorage of PT bars at panel points could be problematic depending upon truss details. As an alternative to mounting the bars to the gussets, PT bars can be mounted directly to the members so long as a continuous load path is maintained in the event of a member fracture, taking due consideration of the potential for fracture to occur at the connection of the member. An overlapping connection such as that illustrated in Figure 7-1 is a potential solution. Mounting the PT bars under the existing tension member may provide an additional measure of protection from corrosion.

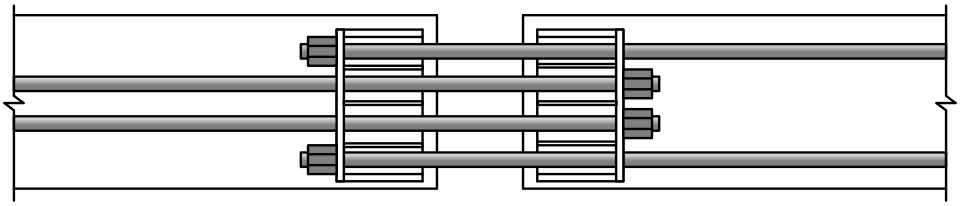

Figure 7-1: Overlapping PT Bar Connection Detail

7.1.2: Diagonal Member Redundancy:

Diagonal members in the trusses are also general categorized as fracture critical, even though they are in tension only under certain loading conditions. Diagonal members, though - to a greater extent than bottom chord members - can be easily inspected from the bridge deck. This retrofit of diagonal members may not be justified if a life cycle cost analysis is performed weighing the cost of retrofit versus the cost of more frequent inspections. Nonetheless, strategies similar to those outlined for the bottom chord members, such as providing internal member redundancy or external post-tensioning, can also be implemented for the diagonal members. It should be noted, though, that the vertical members provide stability to the top chord of the truss through flexure. To provide this stability those members must be detailed as a single member and not a pair of members with an equivalent area.

7.2: Retrofit and Design Strategies for Pony Truss Bridge Floor Systems

For sake of this discussion, the floor system of truss bridges will be considered to consist of the floor beams, stringers, and deck or decking. Furthermore, two types of redundancy can be considered, longitudinal and flexural. Longitudinal redundancy refers to transferring forces in the longitudinal direction of the bridge as a secondary load path acting, to some extent, in parallel with the superstructure. Flexural floor system redundancy refers to the moments developed about axes parallel to the plane of the deck, either parallel or perpendicular to the longitudinal direction of the bridge, such that secondary load paths are created in the floor system itself.

Standard practice with respect to inspection is to consider the decking and stringers to be not fracture critical. Floor beams supporting stringers spanning not more than 14’-0” are considered to be not fracture critical, but floor beams supporting stringers spanning more than 14’-0” are considered as fracture critical.

7.2.1: Floor Beam Details:

Internal member redundancy can be added to floor beams by bolting a cover plate to the bottom flange. It is unclear whether this approach will be recognized by FHWA and other agencies as providing sufficient redundancy to classify a floor beam as not fracture critical but it is the researchers’ opinion that a cover plate on the tension flange, if properly designed and detailed, will prevent collapse of the floor beam in the event of a fracture.

The cover plate should be sized such that it has a width approximately equal to the width of the beam flange and a thickness such that the strength of the plate is not less than the strength of the beam flange that it is reinforcing. The plate should be bolted to the flange since welding would provide a means for a fracture in the beam to propagate to the plate. Bolts with a shear strength sufficient to develop the yield strength of the plate should be used to anchor the plate at the ends of the beam where a fracture is less likely to occur. Additional bolts should be located along the length of the plate as required sealing against the penetration of moisture (AASHTO LRFD Section 6.13.2.6.2).

7.2.2: Stringer Details:

In new construction or when stringers are replaced as part of a retrofit, flexural continuity can be provided by detailing staggered, two-span stringers. It was shown in Chapter 6 that this provides adequate redundancy to the floor beam so that the floor beams spaced up to 16'-0' can be considered to be not fracture critical. It is recommended that continuity be neglected during the design of the stringers when it reduces the demand on the stringers (i.e. despite the continuity, design the stringers as if they are simply supported).

A robust connection must be provided between the stringer and floor beams, however, in order for the stringer continuity to be beneficial to the floor beams. With respect to flexural continuity, this means providing for the transfer of vertical forces. A conservative approach would be to detail the connection to transfer a force equal to the lesser of the plastic shear capacity of the stringer or the force required to develop the plastic moment of the section over the panel length of the bridge. For a W12x30 member with $F_y = 50^{\text{ksi}}$, the plastic shear strength would be approximately 96^{kip} and for a panel length of 13'-0", the force required to develop the plastic moment would be approximately 28^{kip}. This force is easily accommodated by a pair of ¾" diameter A325 bolts or a pair of ¼" fillet welds.

To provide a secondary load path to the bottom truss chords, longitudinal continuity can be provided in underslung stringers with a simple splice plate detailed between the webs of adjacent in-line stringers. In lieu of making the stringers axially continuous, post-tensioned bars could be placed in parallel with the stringers. In an underslung floor system, the PT bars could be placed between the deck and floor beams, either outside of the first stringer line or between the first and second stringer line.

In framed floor systems, cover plates and stiffened seat angles can be detailed to splice the top flange of one stringer with the adjacent in-line stringer on the opposite side of the floor beam. If a temporary seat angle is present, it can be reinforced to the web of the floor beam as needed and then bolted to the bottom flange of the stringers using fill material as needed. Alternatively, holes can be drilled in the webs of the floor beams to provide access for PT bars to be placed parallel to the stringers. It is noted, though, that the cost of this retrofit will not likely be justified by the increase in redundancy realized by implementing it.

7.2.3: Decks and Decking Details:

Bridge decks and decking can provide flexural and longitudinal redundancy to the floor system and superstructure. Metal decking was shown to provide significant strength to the floor system, even in the absence of stringer continuity. A robust decking-to-stringer

connection is required, however, for this to be effective. Further, a robust connection between the stringers and the floor beam is critical if the deck is to provide redundancy to the floor beams. A robust decking-to-stringer connection is provided when the decking is attached to every stringer via bolted clips at every other deck rib or when the decking is attached to every stringer via plug welds at every deck rib.

Reinforced concrete decks with adequate reinforcing that are attached to the stringers via shear studs (along with stringers that are robustly attached to the floor beams) are also considered to provide significant flexural and longitudinal redundancy. Although timber decks have the potential to provide significant flexural redundancy, the typical metal clip connections of timber decks to the stringers was not deemed to be robust enough to transfer that flexural redundancy to the stringers or floor beams. Further, the strip nature of timber decks does not lend them to providing any appreciable longitudinal strength.

A steel plate deck welded to the stringers could also be an option. It could be waterproofed (spray applied) with a thin pavement layer atop it to provide cross slope and driving surface. The stringer spacing would need to be tight (flange tip to flange tip not to exceed approximately 3'-6") but this would provide a lot of continuity and be a de facto splice for stringer top flanges. A steel plate deck (1/2"-3/4" plate) is common in the railroad industry, though it is generally not used for primary strength calculations.

7.3: Fracture Critical Inspection Strategies for Floor Beams:

Figure 7-2 shows a flow chart that is recommended for determining when fracture critical inspections may be required for floor beams in pony truss bridges. The first criterion is whether or not a 1978 type fracture control plan (FCP) exists for the structure. A 1978 FCP includes information such Charpy V-notch (CVN) toughness requirements for the bridge material, welding and fabrication procedures that were followed, and AWS/AASHTO/AISC certification for the shop where the structure was fabricated. The FCP is created when the bridge is constructed and its purpose is to ensure that material-level toughness exists and that proper fabrication procedures are followed to avoid fractures. The purpose of a FCP is not to identify members requiring fracture critical inspections.

Based on the second criterion, if the floor beam is internally redundant, it can be regarded as not fracture critical with respect to inspections. “Robust” in this case is intended to mean that, in the event of a fracture, the remaining unfractured elements will be able to keep the floor system from collapsing. This robustness can be demonstrated through a fracture critical analysis like that described in Chapters 5 and 6, wherein it is assumed that a fracture in the floor beam would initiate in the tension flange and propagate, at most, through the depth of the web to the underside of the compression flange. In that case, the remaining effective cross section at the location of the fracture would consist of the top flange of the section providing shear transfer but not moment continuity. Alternatively, the presence of an adequately designed, bolted cover plate as described earlier in this chapter would be sufficient to declare that the floor beam is robust and can be treated as not fracture critical. It is noted that the FHWA currently does not consider the demonstration of internal member redundancy alone as sufficient to classify a member as non-fracture critical, but research on-going at the time of this report is being conducted to further evaluate internal member redundancy, thus the second criterion is included in Figure 7-2.

The third, fourth, and fifth criteria all depend on the connection between the stringers and the floor beam. A robust stringer-to-floor beam connection in this case is one that will remain effective in transferring shear in the event of a tension flange and web fracture in the floor beam. Two bolts between the stringer flange and floor beam flange in an underslung floor system or a double web-angle connection with two or three bolts in shear in a framed floor system can be considered robust.

The third criterion recognizes that the metal decking provides supplemental strength to the floor beams provided that the decking is properly attached to the stringers and that the stringers are properly attached to the floor beams. Connection of the metal decking to the stringers using a single bolt and clip at every other deck valley as is shown previously in Figure 3-16 or a plug weld at every deck valley is considered to be robust. Similarly, criterion four recognizes that a reinforced concrete deck that is composite with stringers, which are properly connected to the floor beams, would provide a redundant system.

Finally, the fifth criterion requires that at least half the stringers be flexurally continuous. If every other stringer is continuous, then the floor beam can be regarded as not fracture critical with respect to inspections. It was shown in Section 6.3 that when every other

stringer is continuous at any given floor beam that the floor beam will remain stable so long as a robust connection exists between the stringers and floor beam.

It is noted that the Bridge Inspectors Reference Manual (BIRM) (FHWA, 2012) includes criteria that may be used to determine when floor beams may be considered as fracture critical for the purposes of inspection. One of the criteria suggests that when the spacing of the floor beams in the bridge is greater 14'-0" that the floor beams may be regarded as fracture critical with respect to inspections. The UC research team was not able to identify a rational basis for this criterion aside from the correlation of 14'-0" to the axle spacing of the "H" and "HS" series design trucks. Further, conversations between the UC research team and several FHWA representatives have resulted in the understanding that the BIRM criteria are considered by FHWA to be "rules of thumb" and not "provisions" that are to be strictly adhered to. Thus a criteria regarding the floor-beam spacing in the bridge is not included in Figure 7-2.

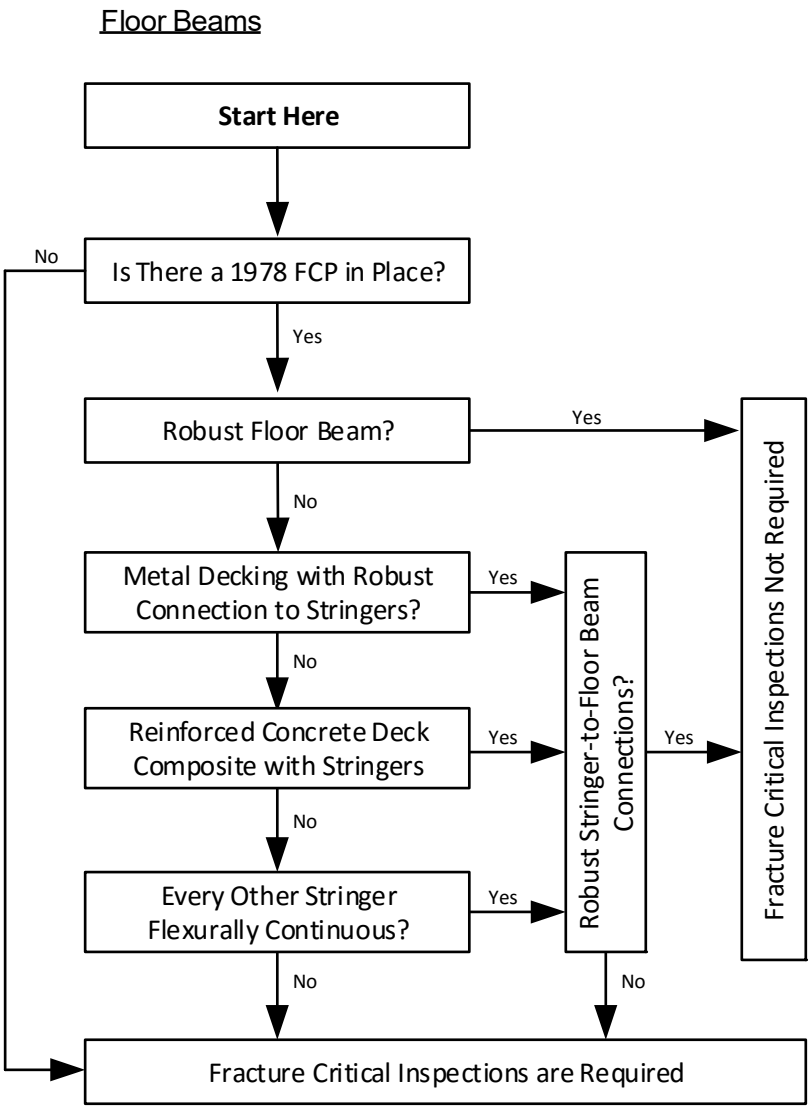

Figure 7-2: Suggested Flow Chart for Fracture Critical Inspections of Floor Beams

References

AASHTO-LRFD, 2015, LRFD Bridge Design Specifications 7th Ed with 2015 Interim Revisions, American Association of State Highway and Transportation Officials

AASHTO, 1978, Guide Specifications for Fracture Critical Non-Redundant Steel Bridge Members, American Association of State Highway and Transportation Officials

AASHTO-MBE, 2016, Manual for Bridge Evaluation, 2nd Edition, with 2011, 2013, 2014, 2015, and 2016 Interim Revisions, American Association of State Highway and Transportation Officials

Adkins, K. A., 2012, A Model for Prediction of Fracture Initiation in Finite Element Analysis of Welded Steel Connections, MS Thesis, University of Cincinnati, 2012

Applebury, C. R., 2011, Reliability-Based Methodology for Bridge Inspection Planning, MS Thesis, University of Missouri – Columbia

AREMA, 2015, American Railway Engineering and Maintenance-of-Way Association, Manual for Railway Engineering, Lanham, MD, Volume 2, Chapter 15, 2015

ASCE/SEI 7-10, 2010, Minimum Design Loads for Buildings and Other Structures, American Society of Civil Engineers, 2010

ASCE 41-13, Seismic Evaluation and Retrofit of Existing Buildings, Structural Engineering Association of California Convention Proceedings, 2012

AWD D1.5, 2010, Bridge Welding Code, American Welding Society

Barth, K. E. and Michaelson, G. K., 2014, Reliability-Based Assessment of the Redundancy of Short-Span Steel Truss Bridges, Report submitted to U.S. Bridge Corporation, 2014

Barth, K. E., Michaelson, G. K., Stains, J. M. (2012). Towards the Development of Redundancy Assessment Protocols for Steel Truss Bridges. Cambridge, OH: U.S. Bridge, Inc.

CFR23, 2011, Code of Federal Regulations, Title 23: Highways, National Bridge Inspections Standards, US Government printing Office, Washington DC, Apr 2011

Connor, R.J., Dexter, R., and Mahmoud, H. (2005). “NCHRP Synthesis 354 - Inspection and Management of Bridges with Fracture-Critical Details.” Transportation Research Board, Washington, DC.

Csagoly, P. F., and Jaeger, L. G., 1979 "Multi-Load-Path Structures for Highway Bridges," Transportation Research Record 711, National Academy of Sciences, Washington, D.C., 1979, pp. 34-39.

Daniels, J.H., Wilson, J.L., and Kim, W., 1987, Guidelines for Determining Redundancy in Two-Girder Steel Bridges, Interim Report Submitted to NCHRP, Fritz Laboratory Report No. 510.1, February 1987

Diggelmann, L.M., Connor, R.J., and Sherman, R.J., 2013, Evaluation of Member and Load-Path Redundancy on the US 421 Bridge Over the Ohio River, Report No. FHWA-HRT-13-104, Oct 2013

FHWA, 2012a, Clarification of Requirements for Fracture Critical Members, Memorandum from Federal Highway Administration HIBT-10, June 20, 2012

FHWA, 2012b, Steel Bridge Design Handbook: Redundancy, US Department of Transportation, Federal Highway Administration, Publication No. FHWA-IF-12-052 - Vol. 9, Nov 9, 2012

FHWA, 2009, Load Rating Guidance and Examples for Bolted and Riveted Gusset Plates in Truss Bridges, US Department of Transportation, Federal Highway Administration, Publication No FHWA-IF-09-014, 2009

FHWA, 2012, Bridge Inspector's Reference Manual (BIRM), Federal Highway Administration and National Highway Institute (HNHI-10), Arlington, Virginia, Publication No. FHWA-NHI 12-049

Frangopol, D.M. and Curley, J.P., 1987, "Effects of Damage and Redundancy on Structural Reliability," ASCE-Journal of Structural Engineering, 1987, pgs 1533-1549

Furuta, H., Shinozuka, M., and Yao, J. T. P., "Probabilistic and Fuzzy Representation of Redundancy in Structural Systems," presented at the July 1985 First International Fuzzy Systems Associated Congress held at Palma de Mailorca, Spain.

Ghosn, M., Moses, F., and Frangopol, D.M., 2010, "Redundancy and Robustness of Highway Bridge Superstructures and Substructures," Structure and Infrastructure Engineering, Taylor and Francis, Vol. 6, Feb - Apr 2010

Jankowiak, T., and Lodygowski T. 2005, "Identification of Parameters of Concrete Damage Plasticity Constitutive Model," Publishing House of Poznan University of Technology, Poznan, 2005

ISSN 1642-9303

Ludlow, R., 2012, "Bridges Must Be Watched Closely," The Columbus Dispatch, Feb 12, 2012

McConnell, J., Wurst, D., McCarthy, G., Sparacino, M., 2013, Investigation of Load-Path Redundancy in Aging Steel Bridges, A report submitted to the University of Delaware University Transportation Center (UD-UTC), Dec 2013

NBIS, 2004, Nation Bridge Inspection Standards, Federal Register Vol. 69, No. 239, Tuesday, December 14, 2004

NCHRP 354, Inspection and Management of Bridges with Fracture-Critical Details, National Cooperative Highway Research Program, Report 354, National Academy Press, Washington DC, 2005

NCHRP 406, Ghosn, M., and Moses, F., Redundancy in Highway Bridge Superstructures, National Cooperative Highway Research Program, Report 406, National Academy Press, Washington DC, 1998

Nowak and Collins, 2013, Reliability of Structures, 2nd Ed., CRC Press

Nowak and Collins, 2000, Reliability of Structures, 1st Ed., CRC Press

Nowak, A., 1992, Calibration Report for NCHRP Project 12-33, Department of Civil Engineering, University of Michigan, Ann Arbor, MI (May 1992).

NYSDOT, 1999, Steel Vulnerability Manual, New York State Department of Transportation, 1999

ORC 5501.47, 2010, "Ohio Revised Code Section 5501.47: Bridge Inspections," http://codes.ohio.gov/orc/5501.47, referenced March, 2014

PennDOT DM-4, 2012, Design Manual Part 4 - Structures, Pennsylvania Department of Transportation Publication 15M, May 2012

RFP Solicitation Number: 2015-ORIL6, "Protocols for Alternate Load Paths within Non-Redundant Steel Structures," Request for Proposal Issued by the Ohio Department of Transportation, Mar 3, 2014

Schenck, T.S., Laman, J.A., and Boothby, T.E., 1999, "Comparison of Experimental and Analytical Load-Rating Methodologies for a Pony-Truss Bridge," Transportation Research Record 1688, Paper No 99-0822

Schippers, J. D., 2012, A Design Procedure for Bolted Top-and-Seat Angle Connections for Use in Seismic Applications, MS Thesis, University of Cincinnati, 2012

Wolf, C, 2012, "U.S. Bridge Inspections Vital but Pricey," The Columbus Dispatch, Feb 5, 2012

Wurzelbacher, K. P., 2012, A Model for Prediction of Fracture Initiation in Finite Element Analysis of Bolted Steel Connections, MS Thesis, University of Cincinnati, 2012

Ziemian R.D., 2010, Guide to Stability Design Criteria for Metal Structures, 6th Ed., Wiley

Appendix A - Bridge Example #1 Using SAP2000

Table of Contents

Appendix A

Figure A-1: A Photo of Bridge #1

Bridge Description and Details:

Bridge #1 is a well-known historical structure in western Ohio. Informally, it is known as the Bloody Bridge because of a murder that allegedly occurred on the bridge in 1854. Formally, it is designated with the structure file number 634484 and carries Bloody Bridge Rd over the Miami-Erie Canal in Auglaize County.

The bridge spans 66'-0" center to center of the bearings and carries a 24'-0" wide roadway. The deck is asphalt-filled corrugated metal decking supported by 7 W12x30 stringers which are in turn supported by W24x94 floor beams. The trusses consist of 5 panels each 13'-2$^3/_8$" = 13.20' long. At its deepest, the height of the truss from top to bottom chord is 7'-6" = 7.50'. Transversely, the trusses are spaced at 25'-6$^3/_8$" = 25.53' cc. The length of the floor beams, which is equal to the out-to-out spacing of the trusses, is 26'-6$^3/_4$" = 26.56'. All steel in the bridge is grade A588 with F_u = 50^{ksi} and F_u = 70^{ksi}.

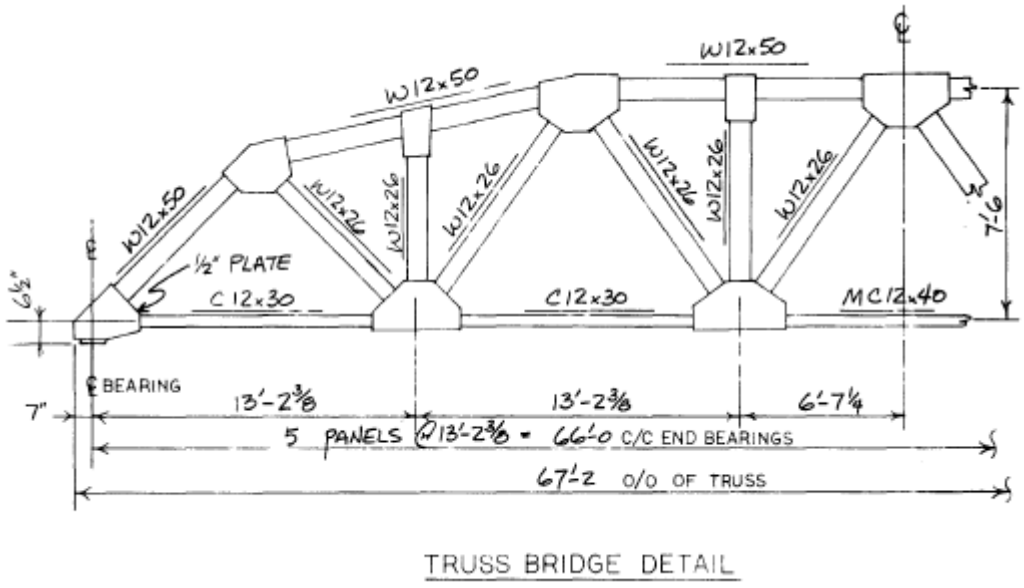

Figure A-2: Bridge #1 Truss Elevation Showing Topological and Member Data

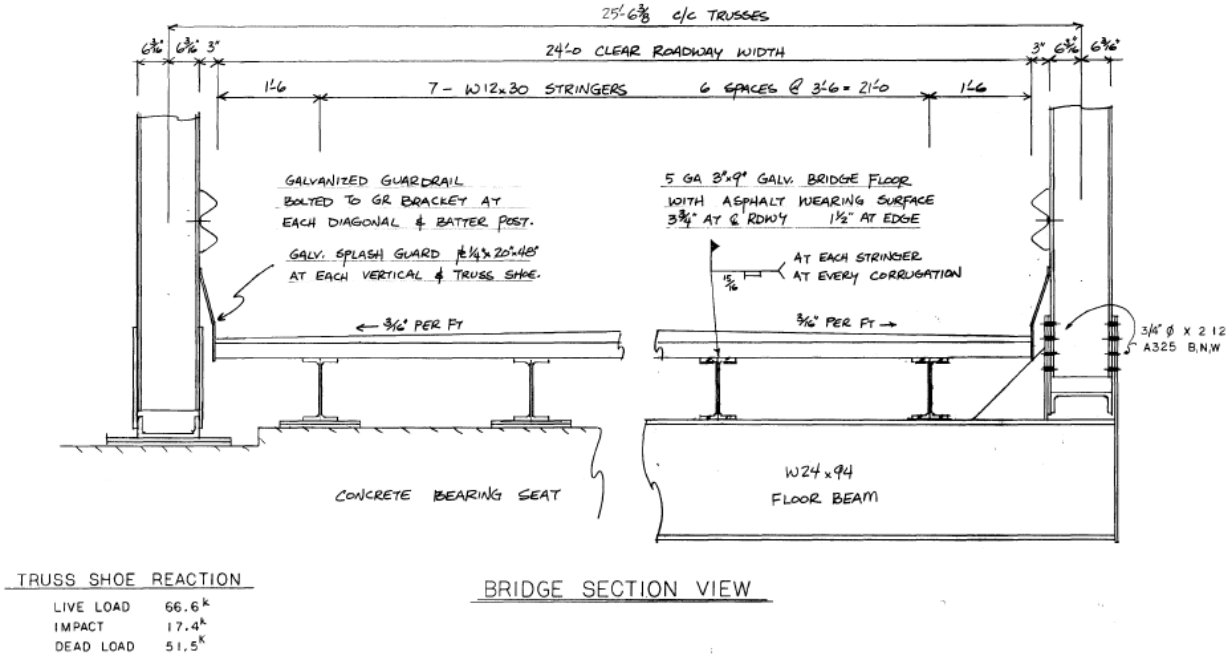

Figure A-3: Bridge Example #1 Cross Section

2D Finite Element Model:

A 2D model of the truss was created in the SAP2000 finite element software using the node and member numbers shown in Figure A-4. Members in the FE model were created with member end releases for in-plane bending moments, which would correspond to the

weak-axis moments for all members. The wide flange sections and channels were stipulated using sections that were included in the SAP2000 library. The model was created with a pinned support at the left end and a roller support at the right end. A perspective view of the model is shown in Figure A-5.

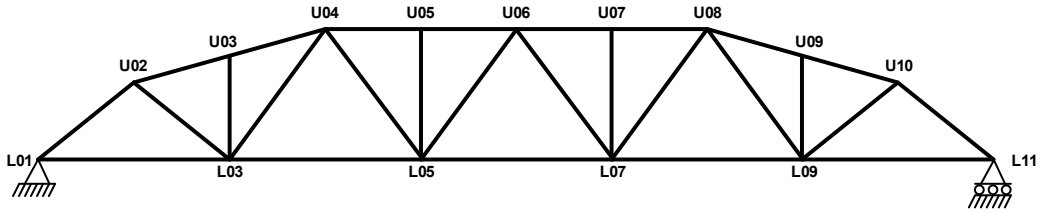

(a) Node Labels

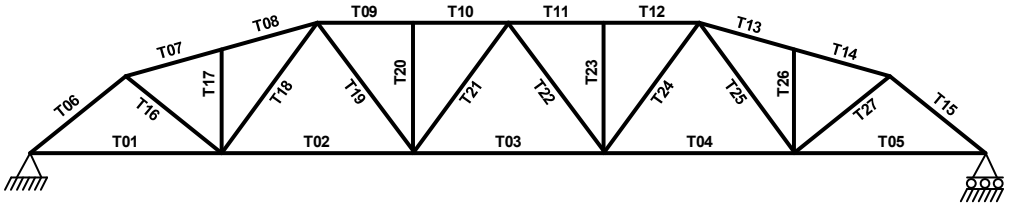

(b) Member Labels

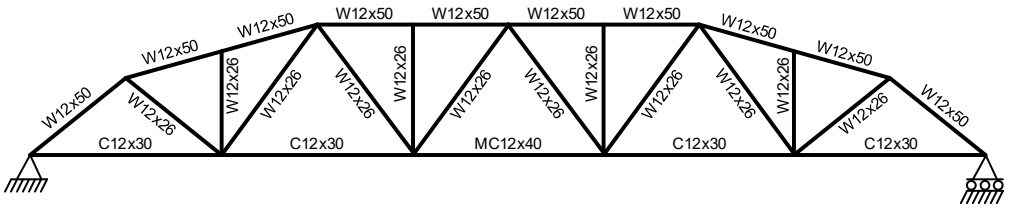

(c) Member Sections

Figure A-4: 2D SAP2000 Model of Bridge #1

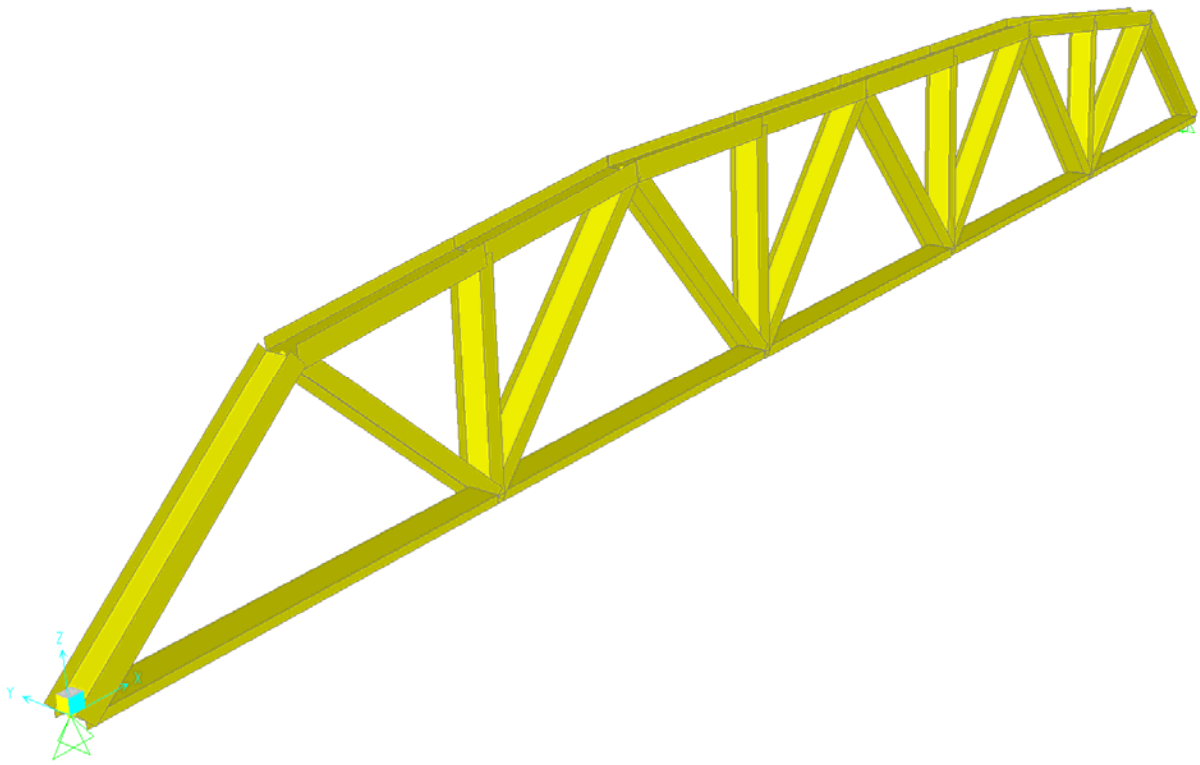

Figure A-5: Perspective View of 2D SAP2000 Model of Bridge #1

2D Dead Load Determination:

2D Dead Load Definitions:

The bridge has an asphalt-filled metal deck and is designed for a uniform asphalt dead load of 50^{psf} and a decking self-weight of 15^{psf}, which are included in the *DC* load pattern. The self-weight of the stringers and floor beams is multiplied by a factor of 1.15 to account for miscellaneous steel such as connection elements, bolts, etc., and is included in the *DC* load pattern, too. A uniform pressure of 35^{psf} is included to represent possible future wearing surface and is included as a *DW* load pattern. These dead loads are assumed to be equally shared by the two trusses and are resolved into point loads that are applied at the panel points along the lower chord of the 2D truss model.

Decking and Asphalt Fill: $\left(65^{psf}\right)\left(\frac{24.00'}{2\ \text{Trusses}}\right)(13.20') = 10.30\,\frac{kip}{pp}$

Stringers: $\left(30^{plf}\right)(13.20')\left(\frac{7\ \text{Stringers}}{2\ \text{Trusses}}\right)(1.15) = 1.59\,\frac{kip}{pp}$

Floor Beams: $\left(94^{plf}\right)\left(\frac{26.56'}{2\ \text{Trusses}}\right)(1.15) = 1.44\,\frac{kip}{pp}$

Total Floor System Steel: $\left(10.30\frac{\text{kip}}{\text{pp}}+1.59\frac{\text{kip}}{\text{pp}}+1.44\frac{\text{kip}}{\text{pp}}\right)=13.33\frac{\text{kip}}{\text{pp}}$ (DC)

Future Wearing: $\left(35^{\text{psf}}\right)\left(\frac{24.00'}{2\text{ Trusses}}\right)(13.20')=5.54\frac{\text{kip}}{\text{pp}}$ (DW)

These dead loads (divided by 2) are applied to supported truss nodes at L1 and L11 even though in the actually bridge the stringers would bear directly on the abutments. This approach was chosen so that the reactions of the truss could be used as a measure of the full self-weight of the bridge to make comparisons between the 2D model and 3D model easier.

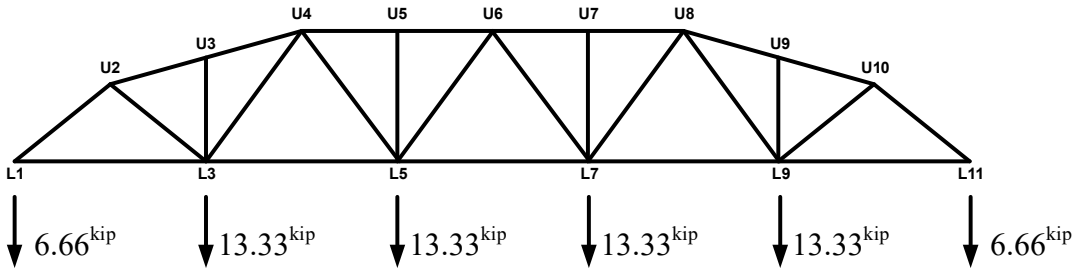

Figure A-6: Unfactored *DC* Load Definition for 2D Modeling of Bridge #1

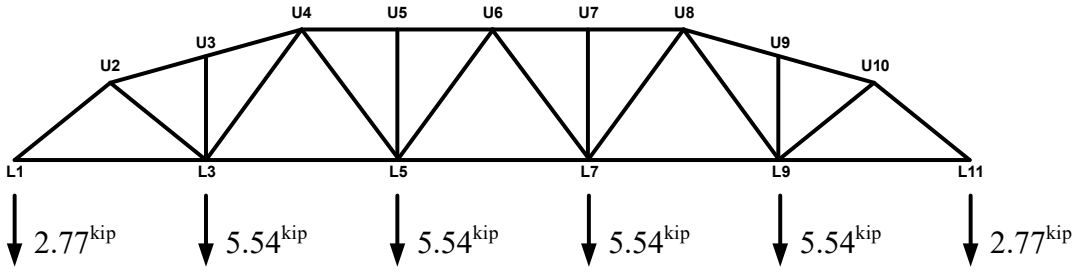

Figure A-7: Unfactored *DW* Load Definition for 2D Modeling of Bridge #1

The self-weight of the steel within the truss is accounted for by SAP2000, is also multiplied by 1.15 to account for miscellaneous steel, and is included in the *SW* load pattern. This is implemented by stipulating a self-weight multiplier of 1.15 when defining load patterns in SAP2000 as is shown in Figure A-8. The *SW* load pattern is treated the same as the *DC* load pattern for purposes of AAASHTO load combinations and load factors.

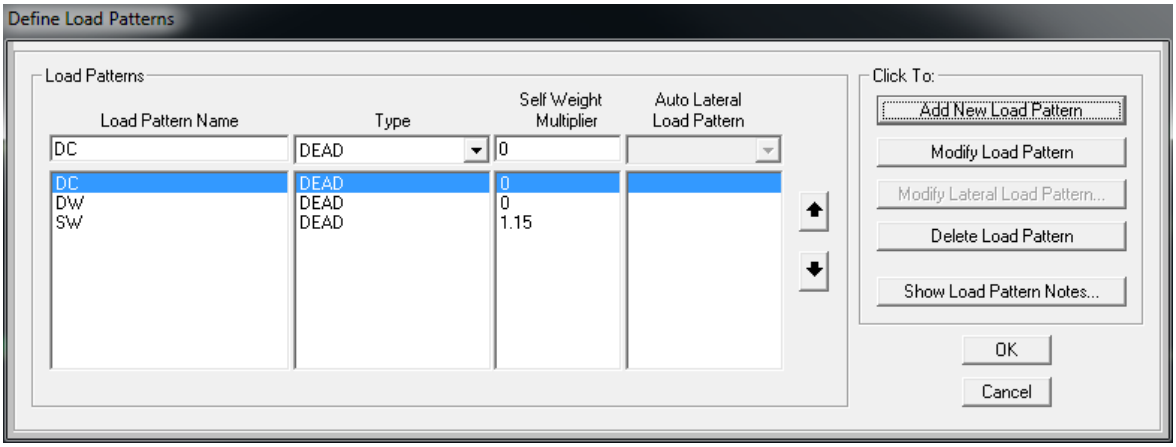

Figure A-8: Definition of Dead Load Patterns in SAP2000

2D Dead Load Truss Reactions:

Reactions for the truss were calculated as shown here. Since the trusses are symmetrical,

$$DC: \quad R = \frac{(4\text{ pp})\left(13.33\,\frac{\text{kip}}{\text{pp}}\right)+(2\text{ pp})\left(6.66\,\frac{\text{kip}}{\text{pp}}\right)}{2\text{ Seats}} = 33.32\,\frac{\text{kip}}{\text{seat}}$$

$$DW: \quad R = \frac{(4\text{ pp})\left(5.54\,\frac{\text{kip}}{\text{pp}}\right)+(2\text{ pp})\left(2.77\,\frac{\text{kip}}{\text{pp}}\right)}{2\text{ Seats}} = 13.85\,\frac{\text{kip}}{\text{seat}}$$

Reactions for the truss as computed using the SAP2000 software are:

DC:	$R = 33.32^{\text{kip}}$	(per seat)
DW:	$R = 13.86^{\text{kip}}$	(per seat)
SW:	$R = 4.83^{\text{kip}}$	(per seat)
Total DL:	$R = 52.01^{\text{kip}}$	(per seat)
Total DL:	$R = 104.0^{\text{kip}}$	(per truss)
Total DL:	$R = 208.0^{\text{kip}}$	(per bridge)

2D Truss Member Forces Due to Dead Load

A static analysis was performed with the *DC*, *DW*, and *SW* loads as defined above and the member forces shown in Table A-1 were determined.

Table A-1: Unfactored Truss Member Forces for Dead Load in Bridge #1 from 2D SAP2000 Model

Member	DC	SW	DW	Total DL
	(kip)	(kip)	(kip)	(kip)
T01R	29.32	4.78	12.20	46.30
T02R	58.64	9.29	24.39	92.33
T03R	70.37	11.15	29.27	110.79
T04R	58.64	9.29	24.39	92.33
T05R	29.32	4.78	12.20	46.30
T06R	-39.63	-6.63	-16.48	-62.74
T07R	-52.33	-8.03	-21.77	-82.12
T08R	-52.30	-8.03	-21.75	-82.08
T09R	-70.22	-10.87	-29.21	-110.29
T10R	-70.22	-10.87	-29.21	-110.29
T11R	-70.22	-10.87	-29.21	-110.29
T12R	-70.22	-10.87	-29.21	-110.29
T13R	-52.30	-7.99	-21.75	-82.04
T14R	-52.33	-7.98	-21.77	-82.08
T15R	-39.63	-6.29	-16.48	-62.40
T16R	30.63	4.20	12.74	47.57
T17R	0.30	-0.63	0.12	-0.21
T18R	-10.08	-2.14	-4.19	-16.41
T19R	17.53	2.27	7.29	27.09
T20R	0.35	-0.64	0.14	-0.15
T21R	-0.23	-0.54	-0.10	-0.86
T22R	-0.23	-0.54	-0.10	-0.86
T23R	0.35	-0.64	0.14	-0.15
T24R	17.53	2.27	7.29	27.09
T25R	-10.08	-2.14	-4.19	-16.41
T26R	0.30	-0.63	0.12	-0.21
T27R	30.63	4.20	12.74	47.57

2D Live Load Calculations:

The bridge will be analyzed for an H20 loading, and HS-20 loading, and an HL-93 loading, which include the HS-20 truck, tandem, and lane load. An impact factor of 1.33 will be used with truck and axel components of these loads. A moving load analysis was performed in SAP2000 and verified with hand calculations. The partial results of the moving load analysis in SAP2000 are shown in Table A-2. These are axial forces that would result from a single lane of loading on the structure and need to be multiplied by appropriate distribution factors to obtain the design member forces in the truss.

Table A-2: Unfactored Lane Member Forces Due to Live Load in Bridge #1 2D SAP2000 Model

Lane Forces

	Tandem*		H-20*		HS-20*		HL-93	
Member	**(pos)**	**(neg)**	**(pos)**	**(neg)**	**(pos)**	**(neg)**	**(pos)**	**(neg)**
	(kip)	(kip)	(kip)	(kip)	(kip)	(kip)	(kip)	(kip)
T01R	42.32	0.00	33.32	0.00	52.14	0.00	87.93	0.00
T02R	76.52	0.00	59.93	0.00	97.00	0.00	166.17	0.00
T03R	87.99	0.00	69.96	0.00	117.52	0.00	200.89	0.00
T04R	76.52	0.00	59.93	0.00	97.00	0.00	166.17	0.00
T05R	42.32	0.00	33.32	0.00	52.14	0.00	87.93	0.00
T06R	0.00	-57.20	0.00	-45.04	0.00	-70.47	0.00	-118.84
T07R	0.00	-75.43	0.00	-59.40	0.00	-93.02	0.00	-156.88
T08R	0.00	-75.35	0.00	-59.34	0.00	-92.95	0.00	-156.77
T09R	0.00	-99.93	0.00	-78.24	0.00	-118.88	0.00	-202.60
T10R	0.00	-99.93	0.00	-78.24	0.00	-118.88	0.00	-202.60
T11R	0.00	-99.93	0.00	-78.24	0.00	-118.88	0.00	-202.60
T12R	0.00	-99.93	0.00	-78.24	0.00	-118.88	0.00	-202.60
T13R	0.00	-75.35	0.00	-59.34	0.00	-92.95	0.00	-156.77
T14R	0.00	-75.43	0.00	-59.40	0.00	-93.02	0.00	-156.88
T15R	0.00	-57.20	0.00	-45.04	0.00	-70.47	0.00	-118.84
T16R	44.05	0.00	34.69	0.00	54.40	0.00	91.76	0.00
T17R	0.67	0.00	0.51	0.00	0.61	0.00	1.07	0.00
T18R	20.87	-29.63	15.74	-23.20	15.74	-34.34	30.74	-55.06
T19R	37.46	-11.39	29.34	-8.59	43.52	-8.59	70.41	-16.57
T20R	0.71	0.00	0.54	0.00	0.67	0.00	1.16	0.00
T21R	24.15	-24.75	18.69	-19.15	24.64	-25.18	38.30	-39.17
T22R	24.15	-24.75	18.69	-19.15	24.64	-25.18	38.30	-39.17
T23R	0.71	0.00	0.54	0.00	0.67	0.00	1.16	0.00
T24R	37.46	-11.39	29.34	-8.59	43.52	-8.59	70.41	-16.57
T25R	20.87	-29.63	15.74	-23.20	15.74	-34.34	30.74	-55.06
T26R	0.67	0.00	0.51	0.00	0.61	0.00	1.07	0.00
T27R	44.05	0.00	34.69	0.00	54.40	0.00	91.76	0.00

* Tandem, H-20, and HS-20 loads do not include impact

Truss Distribution Factor Calculations:

Distribution factors were calculated to be used in determining how much of each lane's loading is supported by each of the two trusses. The distribution factors were computed for the cases of only the near lane loaded and the case of both lanes loaded. The distribution factors were computed using the lever rule assuming that the lanes and the truck loads within the lanes were positioned laterally as close to the right truss as is shown in Figure A-9.

The nearest wheel of the nearest lane was positioned 2'-0" from the edge of the deck. The second wheel of the near lane is positioned 6'-0" to the left of the first wheel. Strictly following AASHTO-LRFD lane definitions would necessitate 6'-0" of space between the two trucks. 4'-0" was used in these calculations as an extra level of conservatism.

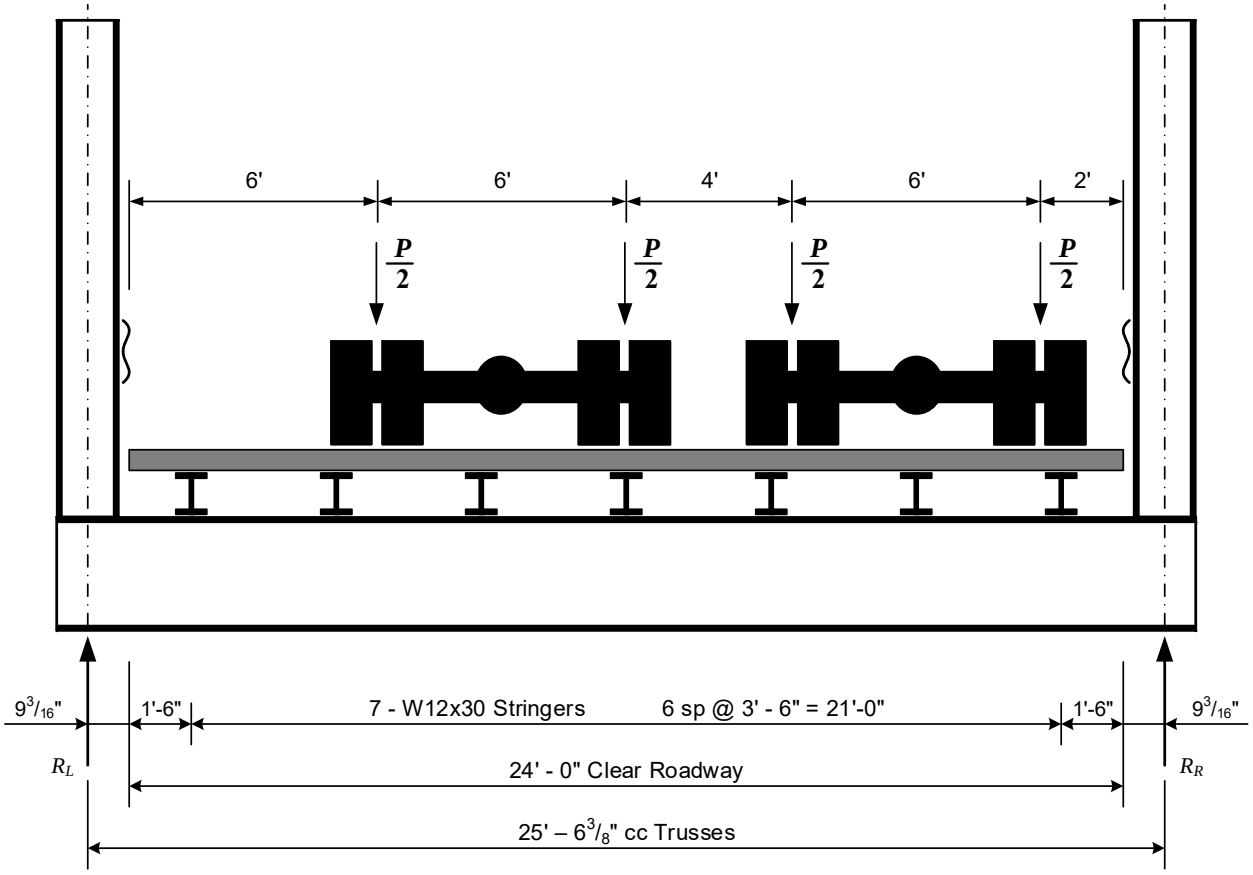

Figure A-9: Position of Truck Loads for Distribution Factor Calculations for Bridge #1

A.1.1.1: Right Lane Loaded:

Taking the sum of the moments about the right truss considering only the right lane loaded as shown in Figure A-9:

$$\circlearrowleft \sum M_L \rightarrow \left(\frac{P}{2}\right)(16.77' + 22.77') = 25.53' R_R$$

$$R_R = \left(\frac{39.54'}{25.53'}\right)\left(\frac{P}{2}\right) = 0.7744P$$

Considering the multiple presence factor for one lane loaded, which is 1.20:

$$R_R = (1.20)(0.7744 P_{Truck}) = 0.9293 P_{Truck}$$

A.1.1.2: Both Lanes Loaded:

Taking the sum of the moments about the right truss considering only the right lane loaded as shown in Figure A-9:

$$\circlearrowleft \sum M_L \rightarrow \left(\frac{P}{2}\right)(6.77' + 12.77' + 16.77' + 22.77') = 25.53 R_R$$

$$R_R = \left(\frac{59.08'}{25.53'}\right)\left(\frac{P}{2}\right) = 1.157P$$

The multiple presence factor for two lanes loaded is 1.00.

A.1.1.3: Summary of Distribution Factors:

A summary of the distribution factors calculated above is shown in Table A-3.

Table A-3: Summary of Truss Distribution Factors for 2D Live Load Analysis of Bridge #1

	Right Truss
Right Lane Loaded:	0.9293 Lanes
Both Lanes Loaded:	1.157 Lanes

The member forces due to one lane's loading, shown in Table A-2, are multiplied by the governing distribution factor of 1.157 to determine the maximum service member forces that can be expected in the truss due to all live load on the bridge. Those member forces are shown in Table A-4.

Table A-4: Unfactored Truss Member Forces Due to Live Load in Bridge #1 2D SAP2000 Model

	Tandem*		H-20*		HS-20*		HL-93	
Member	**(pos)**	**(neg)**	**(pos)**	**(neg)**	**(pos)**	**(neg)**	**(pos)**	**(neg)**
	(kip)	(kip)	(kip)	(kip)	(kip)	(kip)	(kip)	(kip)
T01R	48.96	0.00	38.55	0.00	60.33	0.00	101.73	0.00
T02R	88.53	0.00	69.34	0.00	112.23	0.00	192.26	0.00
T03R	101.80	0.00	80.94	0.00	135.97	0.00	232.43	0.00
T04R	88.53	0.00	69.34	0.00	112.23	0.00	192.26	0.00
T05R	48.96	0.00	38.55	0.00	60.33	0.00	101.73	0.00
T06R	0.00	-66.18	0.00	-52.11	0.00	-81.53	0.00	-137.50
T07R	0.00	-87.27	0.00	-68.72	0.00	-107.63	0.00	-181.51
T08R	0.00	-87.19	0.00	-68.66	0.00	-107.55	0.00	-181.38
T09R	0.00	-115.62	0.00	-90.52	0.00	-137.54	0.00	-234.41
T10R	0.00	-115.62	0.00	-90.52	0.00	-137.54	0.00	-234.41
T11R	0.00	-115.62	0.00	-90.52	0.00	-137.54	0.00	-234.41
T12R	0.00	-115.62	0.00	-90.52	0.00	-137.54	0.00	-234.41
T13R	0.00	-87.19	0.00	-68.66	0.00	-107.55	0.00	-181.38
T14R	0.00	-87.27	0.00	-68.72	0.00	-107.63	0.00	-181.51
T15R	0.00	-66.18	0.00	-52.11	0.00	-81.53	0.00	-137.50
T16R	50.96	0.00	40.14	0.00	62.95	0.00	106.17	0.00
T17R	0.77	0.00	0.59	0.00	0.71	0.00	1.24	0.00
T18R	24.14	-34.28	18.21	-26.84	18.21	-39.74	35.57	-63.71
T19R	43.34	-13.18	33.94	-9.94	50.36	-9.94	81.47	-19.17
T20R	0.82	0.00	0.63	0.00	0.78	0.00	1.34	0.00
T21R	27.94	-28.64	21.62	-22.16	28.51	-29.14	44.31	-45.32
T22R	27.94	-28.64	21.62	-22.16	28.51	-29.14	44.31	-45.32
T23R	0.82	0.00	0.63	0.00	0.78	0.00	1.34	0.00
T24R	43.34	-13.18	33.94	-9.94	50.36	-9.94	81.47	-19.17
T25R	24.14	-34.28	18.21	-26.84	18.21	-39.74	35.57	-63.71
T26R	0.77	0.00	0.59	0.00	0.71	0.00	1.24	0.00
T27R	50.96	0.00	40.14	0.00	62.95	0.00	106.17	0.00

* Tandem, H-20, and HS-20 loads do not include impact

2D Factored Member Forces

AASHTO LRFD Load Combination Strength I is assumed to govern.

Member 3: (Tension Only)

HS-20: $F_{3,Max} = (1.25)(70.37^{kip} + 11.15^{kip}) + (1.50)(29.27^{kip}) + (1.75)(1.33)(136.0^{kip}) = 462.3^{kip}$

HL-93: $F_{3,Max} = (1.25)(70.37^{kip} + 11.15^{kip}) + (1.50)(29.27^{kip}) + (1.75)(232.4^{kip}) = 552.5^{kip}$

Member 1: (Tension Only)

HS-20: $F_{1,Max} = (1.25)(29.32^{kip} + 4.78^{kip}) + (1.50)(12.20^{kip}) + (1.75)(1.33)(60.33^{kip}) = 201.3^{kip}$

HL-93: $F_{1,Max} = (1.25)(29.32^{kip} + 4.78^{kip}) + (1.50)(12.20^{kip}) + (1.75)(101.7^{kip}) = 239.0^{kip}$

Member 10: (Compression Only)

HS-20: $F_{10,Min} = (1.25)(-70.22^{kip} - 10.87^{kip}) + (1.50)(-29.21^{kip}) +...$

$...+ (1.75)(1.33)(-137.5^{kip}) = -465.3^{kip}$

HL-93: $F_{10,Min} = (1.25)(-70.22^{kip} - 10.87^{kip}) + (1.50)(-29.21^{kip}) + (1.75)(-234.4^{kip}) = -555.4^{kip}$

Member 21: (Subject to Load Reversals)

HS-20: $F_{21,Max} = (0.90)(-0.23^{kip} - 0.54^{kip}) + (0.65)(-0.10^{kip}) + (1.75)(1.33)(28.51^{kip}) = 65.60^{kip}$

HS-20: $F_{21,Min} = (1.25)(-0.23^{kip} - 0.54^{kip}) + (1.50)(-0.10^{kip}) +...$

$... + (1.75)\ (1.33)\ (-29.14^{kip}) = -68.92^{kip}$

HL-93: $F_{21,Max} = (0.90)(-0.23^{kip} - 0.54^{kip}) + (0.65)(-0.10^{kip}) + (1.75)(44.31^{kip}) = 76.79^{kip}$

HL-93: $F_{21,Min} = (1.25)(-0.23^{kip} - 0.54^{kip}) + (1.50)(-0.10^{kip}) + (1.75)(-45.32^{kip}) = -80.40^{kip}$

Note that the minimum load factors are used for γ_p in computing the tensile force in Member 21 since the permanent loads create compression but the transient loads create a maximum effect that is tensile. If an inspection showed that there was no wearing surface on the bridge deck, then an argument could be made to use a γ_p = 0.00 for DW since bridge was in operation without the wearing surface.

Table A-5: Factored Truss Member Forces in Bridge #1

Member	Strength I - HS-20 Max	Strength I - HS-20 Min	Strength I - HL-93 Max	Strength I - HL-93 Min
	(kip)	(kip)	(kip)	(kip)
T01R	201.33	38.62	238.95	38.62
T02R	382.71	77.00	457.95	77.00
T03R	462.27	92.39	552.55	92.39
T04R	382.71	77.00	457.95	77.00
T05R	201.33	38.62	238.95	38.62
T06R	-52.35	-272.32	-52.35	-323.17
T07R	-68.47	-358.60	-68.47	-425.74
T08R	-68.44	-358.36	-68.44	-425.46
T09R	-91.96	-465.30	-91.96	-555.39
T10R	-91.96	-465.30	-91.96	-555.39
T11R	-91.96	-465.30	-91.96	-555.39
T12R	-91.96	-465.30	-91.96	-555.39
T13R	-68.40	-358.30	-68.40	-425.40
T14R	-68.43	-358.55	-68.43	-425.69
T15R	-52.04	-271.89	-52.04	-322.74
T16R	209.15	39.63	248.44	39.63
T17R	1.43	-0.22	1.96	-0.22
T18R	28.65	-114.05	48.53	-133.05
T19R	152.89	-0.58	178.25	-10.99
T20R	1.63	-0.17	2.17	-0.17
T21R	65.60	-68.92	76.79	-80.40
T22R	65.60	-68.92	76.79	-80.40
T23R	1.63	-0.17	2.17	-0.17
T24R	152.89	-0.58	178.25	-10.99
T25R	28.65	-114.05	48.53	-133.05
T26R	1.43	-0.22	1.96	-0.22
T27R	209.15	39.63	248.44	39.63

Member Capacities:

Member capacities and capacity to demand rations are shown below in Table A-6.

Table A-6: Member Capacities and Capacity to Demand Ratios for Truss Members

	Design Member Capacity		Capacity to Demand Ratios HS-20		Capacity to Demand Ratios HL-93	
Member	Ten	Comp	Ten	Comp	Ten	Comp
	(kip)	(kip)	(kip)	(kip)	(kip)	(kip)
T01R	418.0	406.3	2.08		1.75	
T02R	418.0	406.3	1.09		0.91	
T03R	557.7	542.0	1.21		1.01	
T04R	418.0	406.3	1.09		0.91	
T05R	418.0	406.3	2.08		1.75	
T06R	693.5	613.4		2.25		1.90
T07R	693.5	647.9		1.81		1.52
T08R	693.5	647.9		1.81		1.52
T09R	693.5	648.5		1.39		1.17
T10R	693.5	648.5		1.39		1.17
T11R	679.7	648.5		1.39		1.17
T12R	679.7	648.5		1.39		1.17
T13R	679.7	647.9		1.81		1.52
T14R	679.7	647.9		1.81		1.52
T15R	679.7	613.4		2.26		1.90
T16R	355.1	295.5	1.70		1.43	
T17R	355.1	322.8				
T18R	355.1	280.4	12.39	2.46	7.32	2.11
T19R	355.1	280.4	2.32		1.99	25.51
T20R	355.1	314.0				
T21R	355.1	280.4	5.41	4.07	4.62	3.49
T22R	355.1	280.4	5.41	4.07	4.62	3.49
T23R	355.1	314.0				
T24R	355.1	280.4	2.32		1.99	25.51
T25R	355.1	280.4	12.39	2.46	7.32	2.11
T26R	355.1	322.8				
T27R	355.1	295.5	1.70		1.43	

Load Factors for Member Failure Limit State:

Member Failure Load Factors, LF_1, computed based on the 2D analysis are shown in Table A-7. The governing value is 5.01 for Member T02 / T04 for the H-20 loading and 3.10 for Member T02 / T04 for the HS-20 loading.

Table A-7: Member Capacities and Capacity to Demand Ratios for Truss Members

Member	Total DL	Nominal Member Capacity Ten	Nominal Member Capacity Comp	LF_1 for H-20 Ten	LF_1 for H-20 Comp	LF_1 for HS-20 Ten	LF_1 for HS-20 Comp
	(kip)	(kip)	(kip)				
T01R	46.30	440.0	427.7	10.21		6.53	
T02R	92.33	440.0	427.7	5.01		3.10	
T03R	110.79	587.0	570.6	5.88		3.50	
T04R	92.33	440.0	427.7	5.01		3.10	
T05R	46.30	440.0	427.7	10.21		6.53	
T06R	-62.74	730.0	645.7		11.19		7.15
T07R	-82.12	730.0	682.0		8.73		5.57
T08R	-82.08	730.0	682.0		8.74		5.58
T09R	-110.29	730.0	682.6		6.32		4.16
T10R	-110.29	730.0	682.6		6.32		4.16
T11R	-110.29	730.0	682.6		6.32		4.16
T12R	-110.29	730.0	682.6		6.32		4.16
T13R	-82.04	730.0	682.0		8.74		5.58
T14R	-82.08	730.0	682.0		8.73		5.57
T15R	-62.40	730.0	645.7		11.19		7.15
T16R	47.57	382.5	311.1	8.34		5.32	
T17R	-0.21	382.5	339.8				
T18R	-16.41	382.5	295.1	21.91	10.38	21.91	7.01
T19R	27.09	382.5	295.1	10.47	32.42	7.06	32.42
T20R	-0.15	382.5	330.5				
T21R	-0.86	382.5	295.1	17.73	13.28	13.45	10.10
T22R	-0.86	382.5	295.1	17.73	13.28	13.45	10.10
T23R	-0.15	382.5	330.5				
T24R	27.09	382.5	295.1	10.47	32.42	7.06	32.42
T25R	-16.41	382.5	295.1	21.91	10.38	21.91	7.01
T26R	-0.21	382.5	339.8				
T27R	47.57	382.5	311.1	8.34		5.32	
				Min = 5.01		Min = 3.10	

2D Fracture Critical Analysis for Bridge #1

This section will illustrate the fracture critical assessment process for Member T03 of Bridge Example #1 to determine whether the member should be classified as a fracture critical member or non-fracture critical member. While using a two dimensional refined analysis to reclassify members as not-fracture critical will likely not be effective, using a 2D example is a good way to illustrate the process while keeping the problem size small. After the assessment is conducted using a 2D analysis, the same approach will be applied using a 3D analysis.

Member T03, a bottom chord member at midspan of the bridge, will be the focus of this analysis. Member T03 is made up a single MC12x40 channel. The damage state associated with a fracture of Member T03 / MC12x40 is the removal of that member from the model. The 2D truss, however, would be completely unstable if any of the members are removed, making the Member T03 by definition fracture critical. To make a more interesting problem, and one appropriate for demonstrating the fracture critical assessment procedure, the single channels that make up the five members of the bottom chord will be replaced with pairs of channels. Members T01, T02, T04, and T05 will be replaced with 2C9x15s and Member T03 will be replaced with a 2C10x20. These replacement members offer the same cross sectional area as the original members, but the damaged state associated with a fracture in these members is the loss of one of the two channels instead of the loss of the entire member. The bridge in this modified condition will hereafter be referred to as Bridge #1M.

Step 1 - Creation of the Finite Element Model:

Creation of the FE Model:

The same 2D model that was used earlier in this appendix will be used here as a starting point. As was stated above, though, Members T01, T02, T04, and T05 will be replaced with 2C9x15s and Member T03 will be replaced with a 2C10x20 in such a way that the members are internally redundant. Simultaneous fracture of both channels is statistically unlikely, but the fracture of only one channel could still lead to collapse of the structure if the remaining channel does not have sufficient strength alone. Given that, the damaged state associated with a fracture of member T03 will be the loss of one of the two channels. That damaged state will be considered in Step 5 of this example by removing one of the two channels making up member 5 from the SAP2000 model. The modified model is shown in Figure A-10.

By default, gravity acts in the negative Z direction in SAP2000. This can be changed in the model settings, but was left as-is for this study. As a result, the trusses are constructed in the XZ plane. Thus, for a 2D model, displacements in the Y direction and rotations about the X and Z axes are deactivated. If the analysis options haven't already

been defined as shown in Figure A-11, then do so to start off. This inactivates degrees of freedom associated with out-of-plane behavior of the truss. SAP2000 will typically converge to a correct solution for a linear 2D problem without deactivating degrees of freedom, but it may encounter convergence problems in the solution of nonlinear 2D problems unless the structure is adequately restrained, or if the out-of-plane degrees of freedom are deactivated.

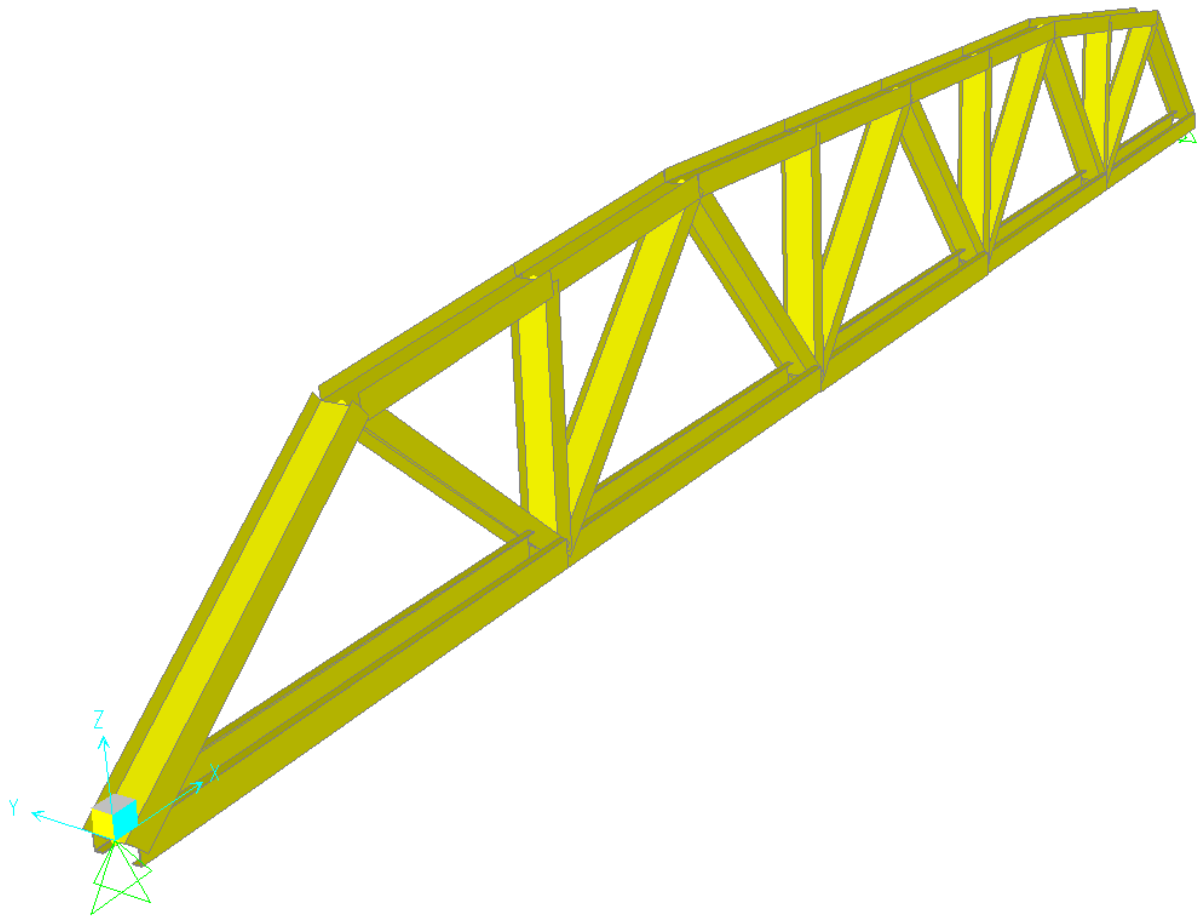

Figure A-10: Perspective View of 2D SAP2000 Model of Bridge #1M with Modified Bottom Chord

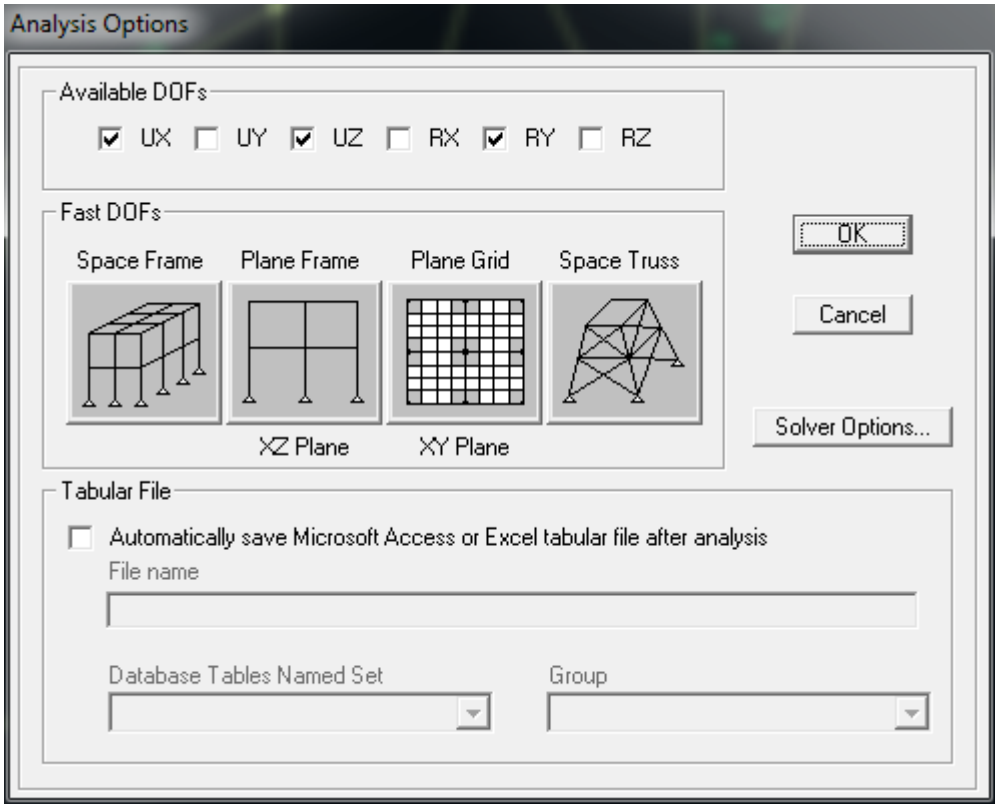

Figure A-11: Active Degrees of Freedom for 2D Analysis of Bridge #1M

Step 2 - 2D Dead and Live Loads:

Definition of Load Patterns and Load Cases:

A modified version of the dead loads shown in Figure A-6 and Figure A-7 will be used in this analysis. As such, load patterns for DC, DW, and SW are defined as was previously discussed. Additionally, live loads consisting of HS-20 and H-20 trucks will be considered. It can be shown that an HS-20 truck positioned with its middle axle at node L07 and an H-20 truck positioned with its rear axle at node L05 will create the critical response in Member T03 for each truck, respectively. Thus load patterns for those two trucks in their critical position are also defined, as shown in Figure A-12. Five linear static load cases thus include three dead load patterns and two live load patterns.

Next, three nonlinear static cases are created for total dead load (nDL), the total dead with the HS-20 truck (nDL+HS-20xT03), and the total dead with the H-20 truck (nDL+H-20xT03). The load cases defined are shown in Figure A-13.

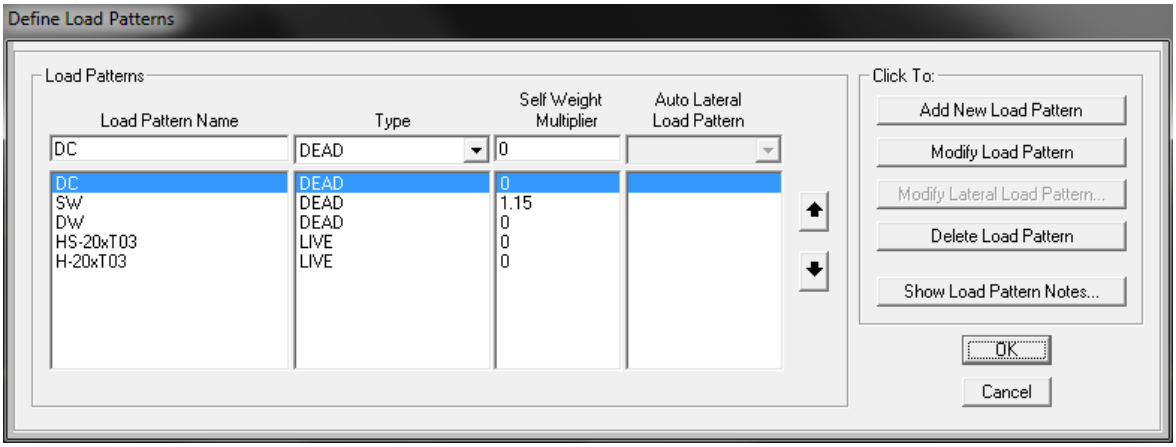

Figure A-12: Load Pattern Definitions in SAP2000 for Bridge Example #1

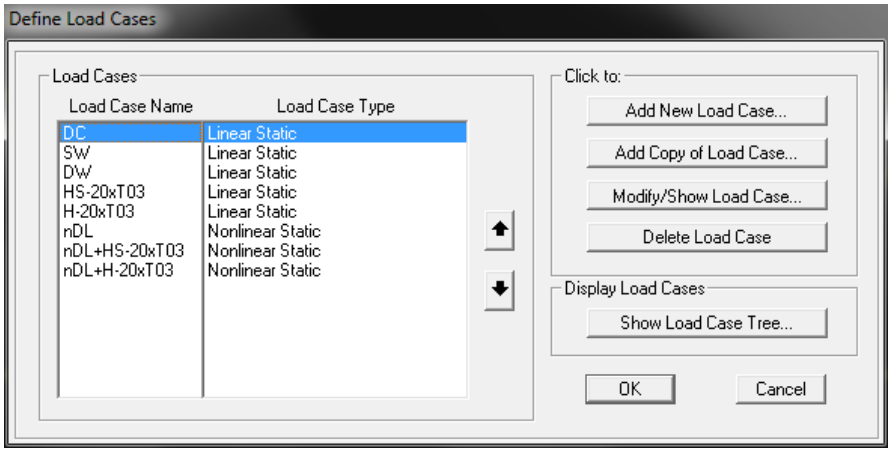

Figure A-13: Load Case Definitions

The total dead loads are defined as load case “nDL” as is shown in Figure A-14. It is assumed that the FCA is performed after an inspection of the structure such that precise data is available regarding the state of the bridge justifying the use of $\gamma_p = 1.00$ for DC and SW dead loads. Further, reduced dead loads such as future wearing surface, DW, could be justified in practice if actual conditions on the bridge can be verified and proper management can be implemented to ensure that those conditions are maintained. To be used as the first step in a multi-step nonlinear analysis in SAP2000, dead loads are defined as a nonlinear static load combination. The “P-Delta plus Large Displacements” option is selected since analysis of the damaged structure might involve large displacements.

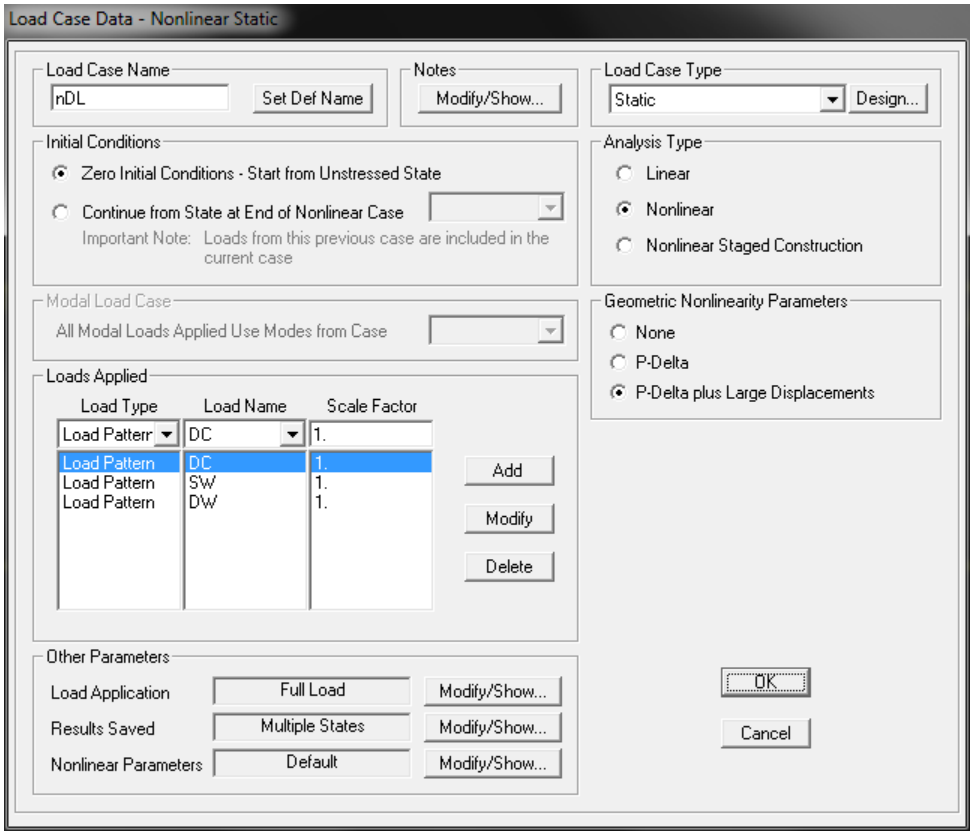

Figure A-14: Load Case Data for “nDL”

The “nDL” Load Case in SAP2000 is defined to be run in load control while monitoring an appropriate degree of freedom in the structure. The degree of freedom chosen to be monitored is generally the vertical displacement, defined as U3 in SAP2000, of the node that is expected to have the highest displacement. In the case of Bridge #1, considering the damage state associated with Member T03, the vertical displacement of node L05 is chosen. Figure A-15 shows the load application control data for the load case “nDL."

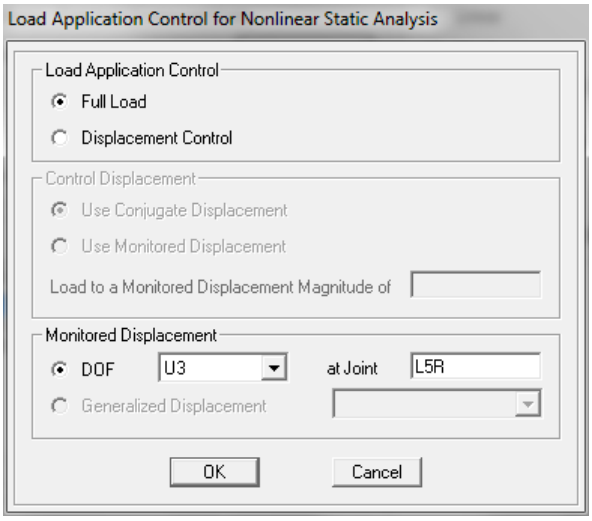

Figure A-15: Load Application Control Data for "nDL"

The next step is to define the results that are saved during the nonlinear solution of "nDL." The response of the undamaged bridge during this load step will almost definitely be linear and elastic, thus saving the "Final State Only" would be satisfactory, but the damaged bridge may respond nonlinearly during the application of dead loads. Thus, it is recommended that results be saved from "Multiple States" so that a full load response can be plotted. In this example a minimum of 20 and a maximum of 20 states will be saved. If the response of the bridge under dead load is expected to be nonlinear, then using a larger number of saved states might be appropriate.

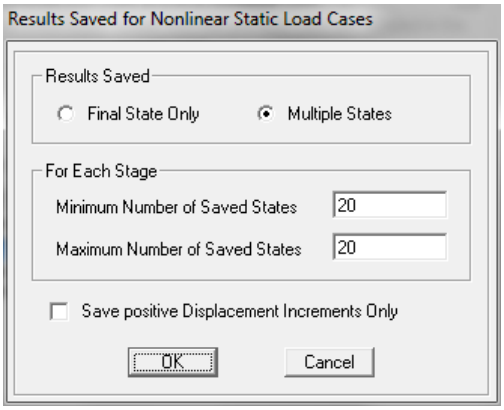

Figure A-16: Results Data for "nDL"

Live Load Patterns:

The Load Case Data form for "nDL+HS-20xT03" is shown in Figure A-17. The initial conditions are set such that the live load pattern is applied incrementally starting from the factored dead load state. The scale factor of 1.157 that is entered into the form is the product of the distribution factor for the truss for two lanes loaded. Since the reserve ratio is in fact a "ratio" and not an absolute measure of strength, and since the live loads in a

nonlinear static analysis are really just a “load pattern” that is applied incrementally, the scale factor shown in Figure A-17 does not affect the reserve ratio for the member. Thus it makes no difference conceptually in this analysis whether an impact factor is included or not, and in a 2D analysis, it makes no difference whether the left lane is loaded, the right lane is loaded, or if both lanes are loaded.

The live load is applied in displacement control monitoring the same degree of freedom defined for the “nDL” load case as is shown in Figure A-18. A target displacement or $L / 50 = 66\text{'-}0\text{''} / 50 = 15.84\text{''}$ is used in this example, though the magnitude may need to be increased for other structures to obtain the desired failure mechanism. This target displacement is imposed in addition to the displacement resulting from the application of the factored dead loads. Use care to ensure that the magnitude of the target displacement is entered in consistent units in SAP2000.

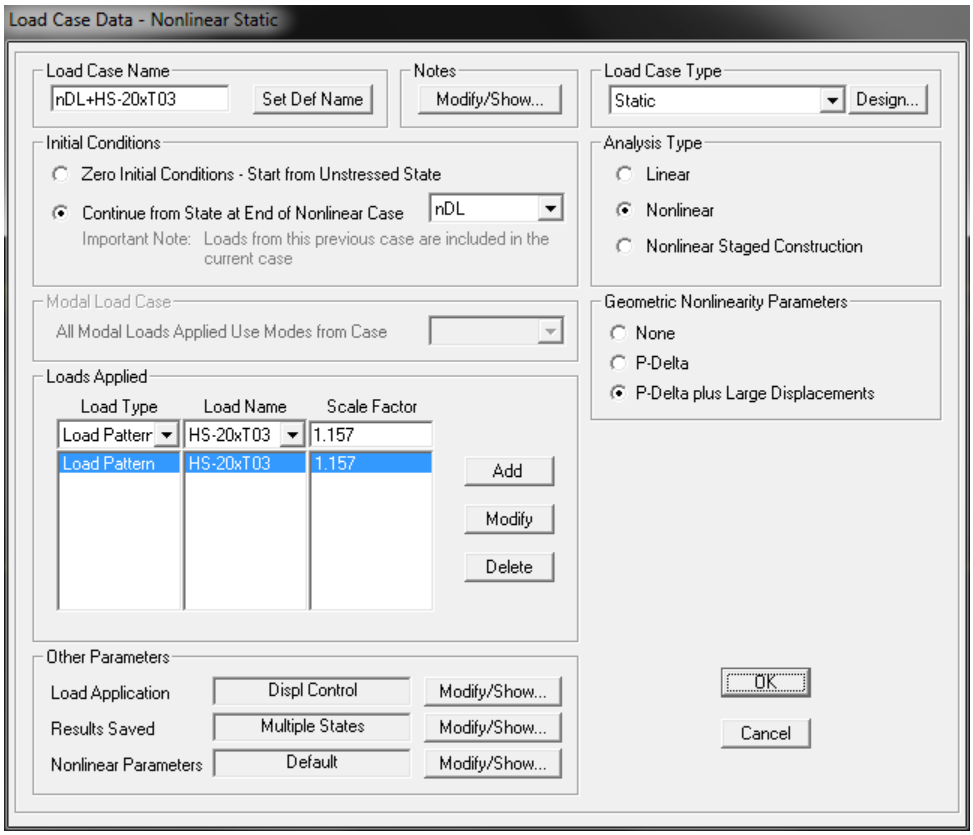

Figure A-17: Load Case Data for “nDL+HS-20xT03”

Results for the application of live load patterns are stipulated for 100 saved states, as is shown in Figure A-19, so that the resulting load-deformation response will have sufficient resolution such that a plot of load vs displacement is sufficiently smooth.

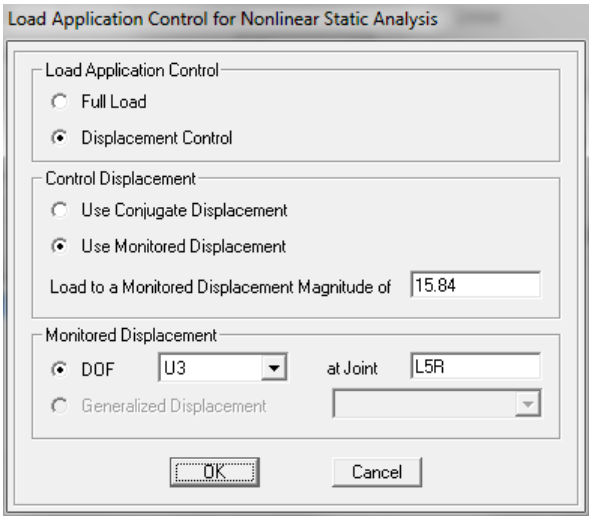

Figure A-18: Load Control Data for "nDL+HS-20xT03" and "nDL+H-20xT03" Load Cases (inch units)

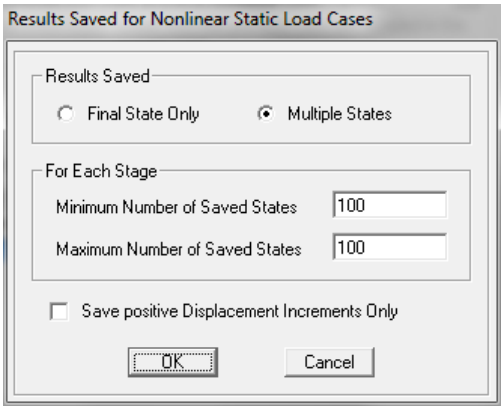

Figure A-19: Results Data for "nDL+HS-20xT03" and "nDL+H-20xT03" Load Cases

Step 3 - Define the Nonlinear Member Behavior:

One axial hinge is defined at the mid-length of each of the truss members. Load-deformation responses for the hinges in the truss members are defined as discussed in Chapter 5. An EPF model is defined in tension and an EPB model is defined in compression as is shown in Figure A-20. SAP2000 defines the limits in the hinge properties dialog as functions of the expected yield and expected ultimate strengths, F_{ye} and F_{ue}. By default, these values are set to the corresponding values from the AISC Seismic Provisions (AISC 341-10) and should be set to desired values. For this example, the expected yield and expected ultimate strengths, F_{ye} and F_{ue} , are set to the nominal values, F_y and F_u, as shown in Figure A-21.

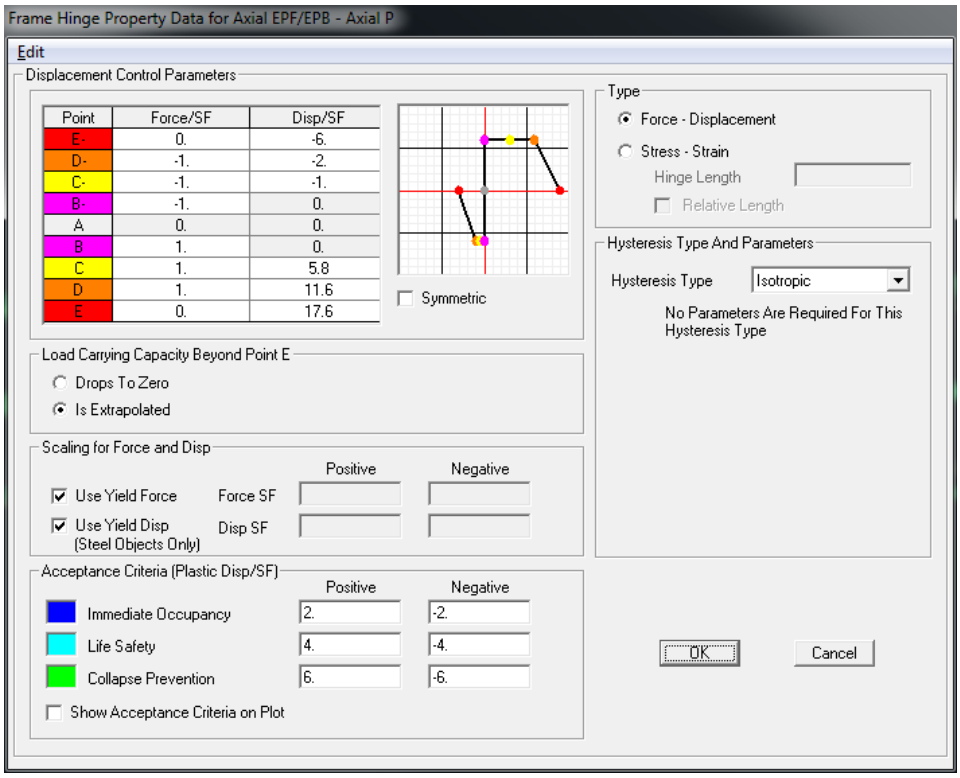

Figure A-20: EPF/EPB Axial Hinge Data for Truss Members

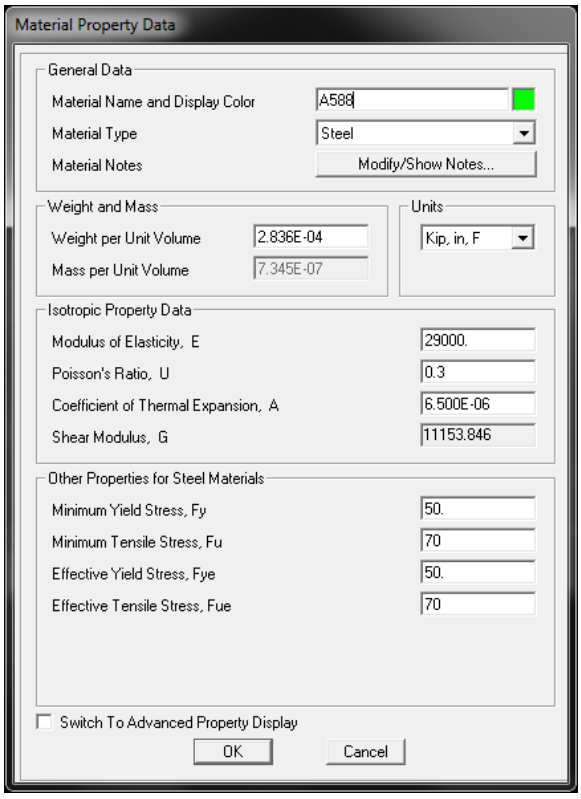

Figure A-21: Material Property Data for All Truss Members

Hinge properties are also a function of the flexural buckling strength of the member, which is a function of the effective length factor, K, that can be defined using the steel design overwrites dialog as shown in Figure A-22. A value of $K = 0.75$ is used for all members in the truss for this example. In the case that one wishes to use the yield force in both tension and compression, the effective length factor used to compute the buckling force can be set to a small value, say 0.001. Both tensile and compressive loads are by default computed without resistance factors.

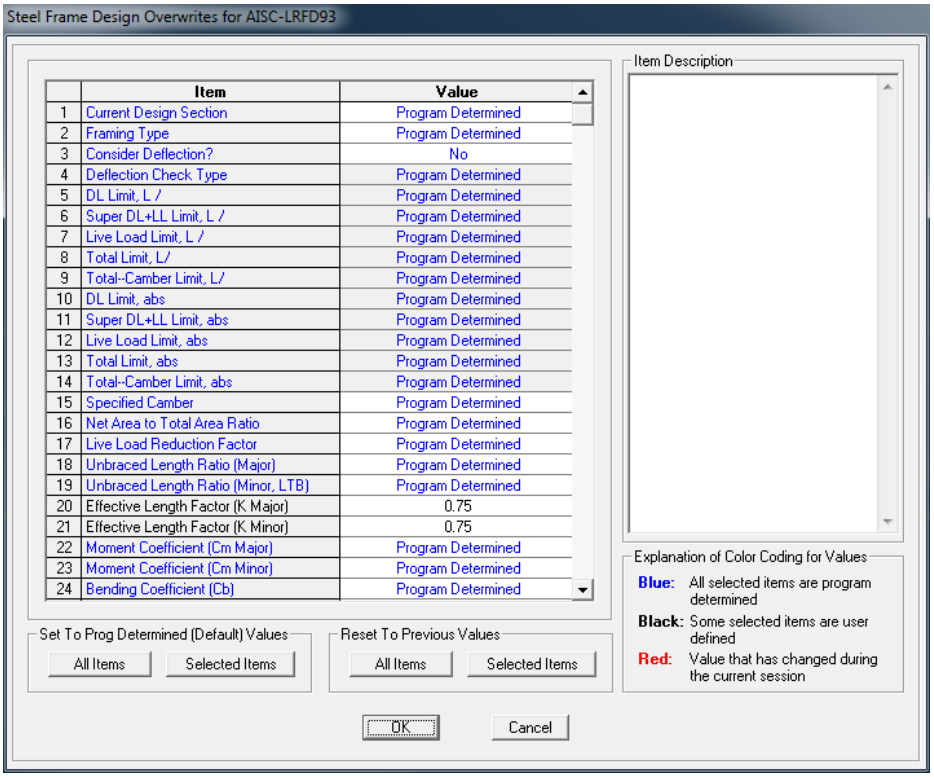

Figure A-22: Steel Design Overwrites Showing Defined Effective Length Factor for Compression

Step 4 - Conduct an Analysis of the Undamaged Bridge:

Next, the load cases are analyzed in SAP2000 for the undamaged structure. For a model of this size on a modern PC, the run time of the analyses should take less than a minute.

After the analyses are complete, results can be examined graphically to ensure that the analysis results are admissible. Examining displaced shapes, distribution of member forces and stresses, and hinge states can help to identify errors in the modeling process. Figure A-23 shows the hinge state at load Step 14 of the nDL+HS-20xT03 analysis of the undamaged structure. This represents the collapse mechanism of the structure in that state under the HS-20 loading, which is a tensile failure of Member T04. Note that despite the fact that the truck load was defined in a location critical for Member T03, first failure

is in a different member, Member T04. Under the H-20 loading in its critical position for Member T03, failure was observed first in Member T02.

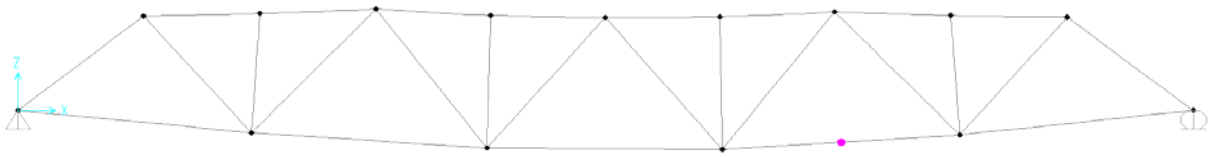

Figure A-23: Hinge Formation at Step 14 for Undamaged Truss under HS-20 Loading

A load deformation response for each nonlinear static load case can be examined in SAP2000 as further validation of the admissibility of the results. Since this type of analysis in SAP2000 was considered as part of a FEMA 356 / ASCE 41 seismic evaluation, this is referred to in SAP2000 as a static pushover curve, as is shown in Figure A-24. The values that are plotted by default are the total base shear and monitored displacement. In the case of a bridge structure, the base shear is really the sum of the vertical reactions for the structure. The curve shown in Figure A-24 is plotted from right to left since the monitored displacement has negative values under the stipulated load patterns.

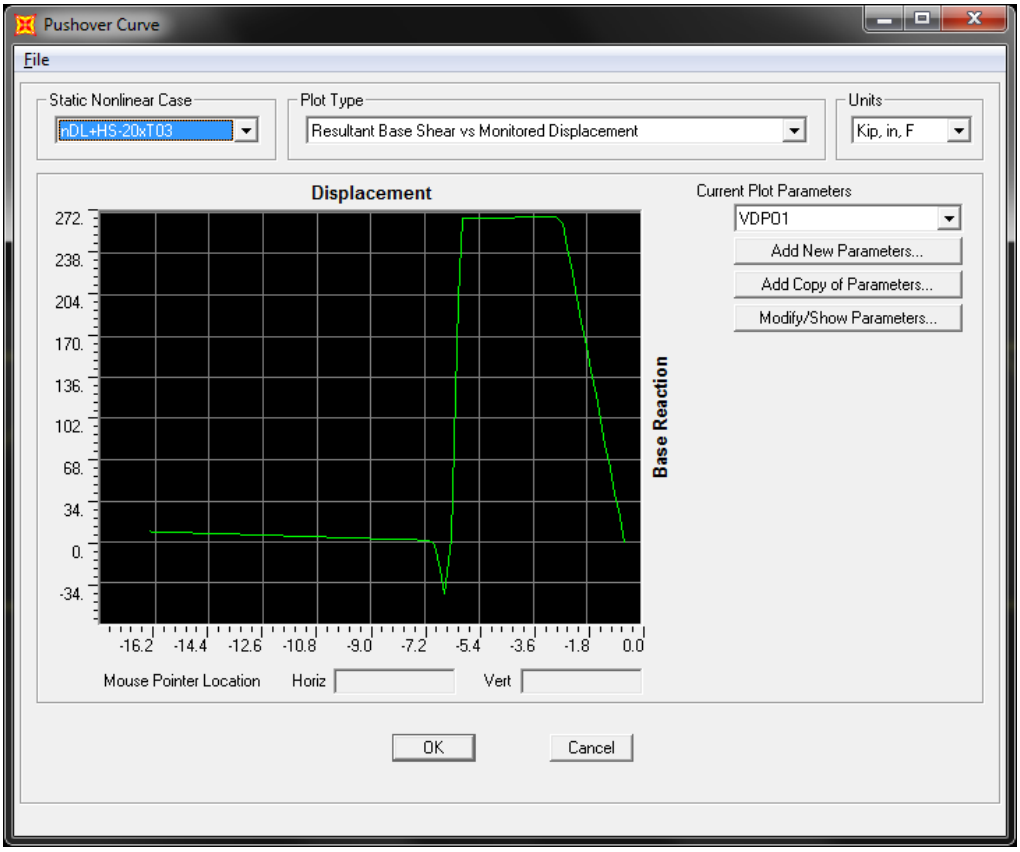

Figure A-24: Static Pushover Curve from SAP2000 for Load Case “nDL+HS-20xT03” in SAP2000

After the model and its results have been validated as admissible, the results can be exported for more refined post-processing. This is accomplished by exporting data to a spreadsheet using the "Display Tables" function in SAP2000 as shown in Figure A-25 and Figure A-26.

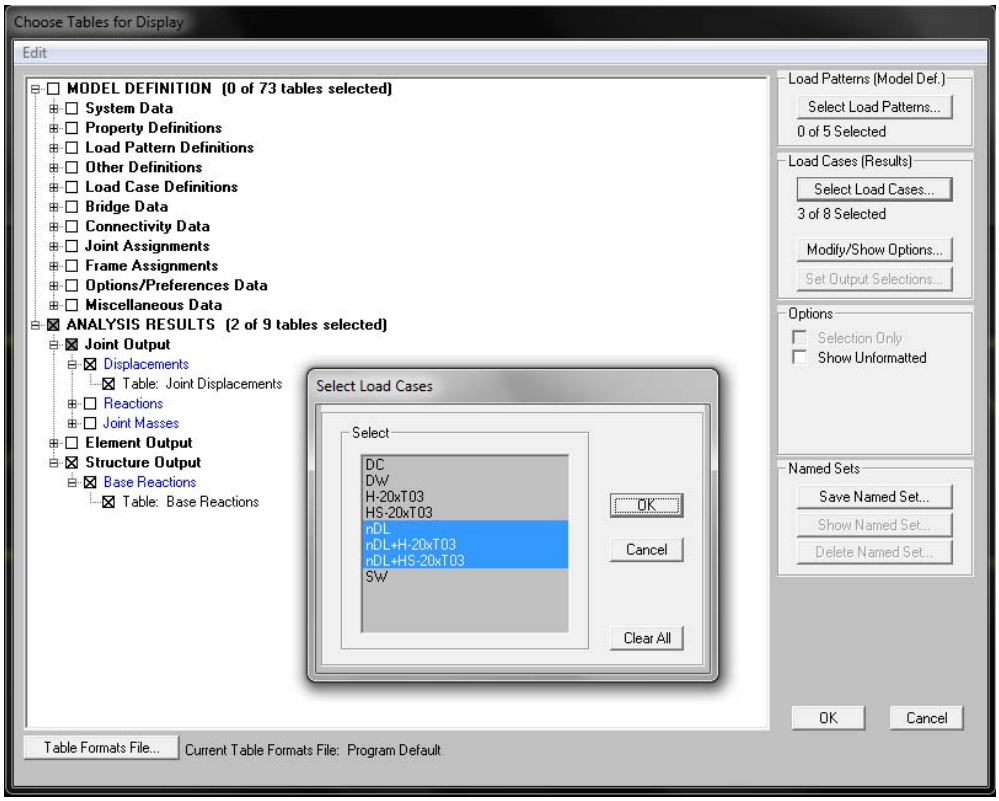

Figure A-25: Output Options for Displaying Tables in SAP2000

Figure A-27 shows load deformation results for the undamaged bridge subjected to the nDL+HS-20xT03 and nDL+HS-20xT03 analysis cases. The full dead load $P_{DL} = 104.0^{\text{kip}}$ is reached at a displacement of 0.5582". A change in stiffness of the load-deformation response can be noticed at this point. Next, the HS-20 and H-20 truck load patterns are applied and are incrementally increased in magnitude until the total applied load reaches $P_1 = 372.8^{\text{kip}}$ in the case of the HS-20 or $P_1 = 339.3^{\text{kip}}$ and the case of the H-20 load. At these points, Member T04 yields under the HS-20 and Member T02 yields under the H-20 loading, and the load-deformation responses of the bridge go approximately flat. At a displacement of $\delta_u = 5.945$" for the HS-20 load or $\delta_u = 7.663$" for the H-20 load, a sudden loss of strength is experienced as a result of Member T04 or Member T02, respectively, reaching its ultimate limit state. Data beyond these points has little physical meaning.

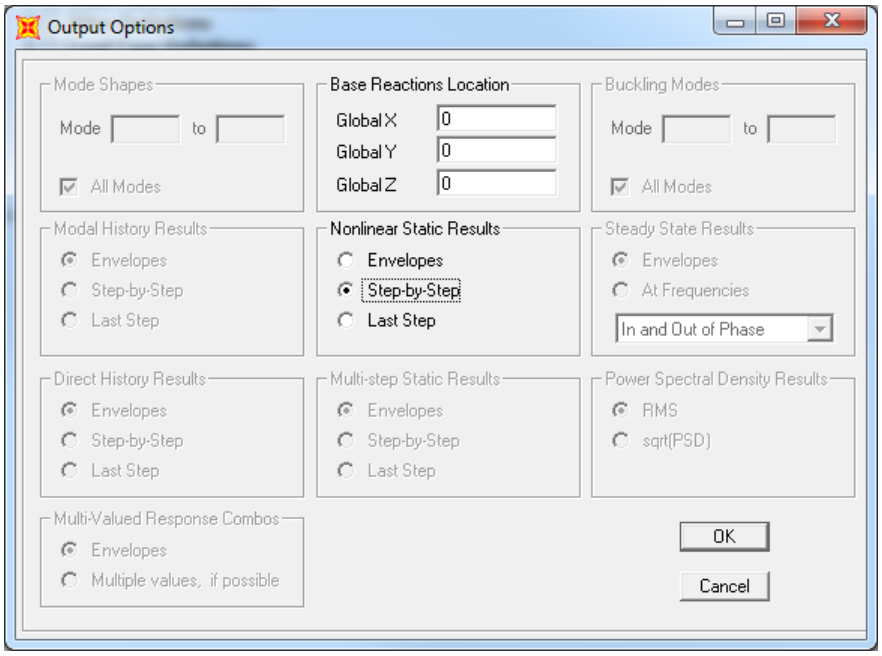

Figure A-26: Data Output Options for Displaying Tables in SAP2000

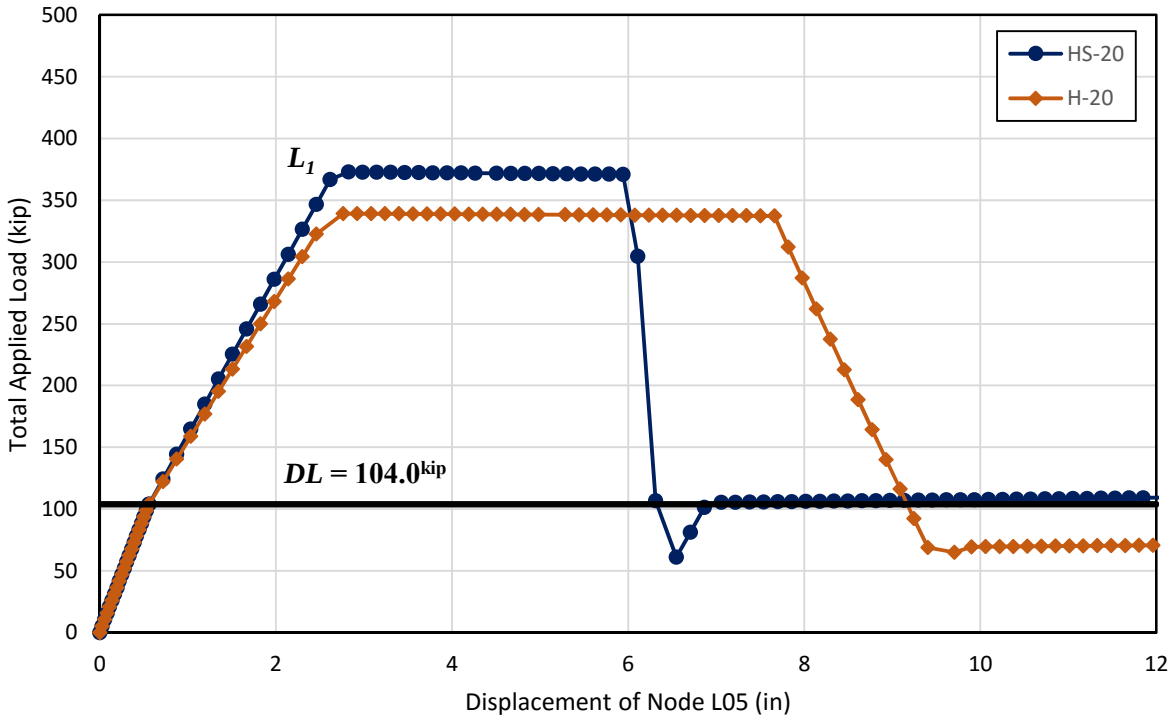

Figure A-27: Response of the Bridge #1M with EPF/EPB Hinges

Step 5 - Conduct an Analysis of the Damaged Bridge:

Next, a damage scenario is simulated by removing one of the two channel sections that collectively make up Member T03. This is intended to simulate the fracture of one of the two channels. This is implemented in the model by redefining Member 03 as a C10x20 instead of the user defined 2C10x20.

Figure A-28 shows the load-deformation response of the truss with one of the two channels making up Member T03 removed, superimposed on the load-deformation response of the undamaged truss. The full Factored $DL = 104.0^{kip}$ is reached at a displacement of 0.6456". A change in stiffness of the load-deformation response can be noticed at this point. At a load of approximately $L_d = 216.2^{kip}$ in the case of the HS-20 or $L_d = 208.7^{kip}$ in the case of the H-20, the load-deformation response goes flat indicating yielding in the damaged Member T03. At a displacement of approximately $\delta_u = 7.2$", a sudden loss of strength is experienced as a result of Member T03 reaching its ultimate limit state. Data beyond these points has little meaning. Data from the four nonlinear SAP2000 analyses is presented in Table A-8.

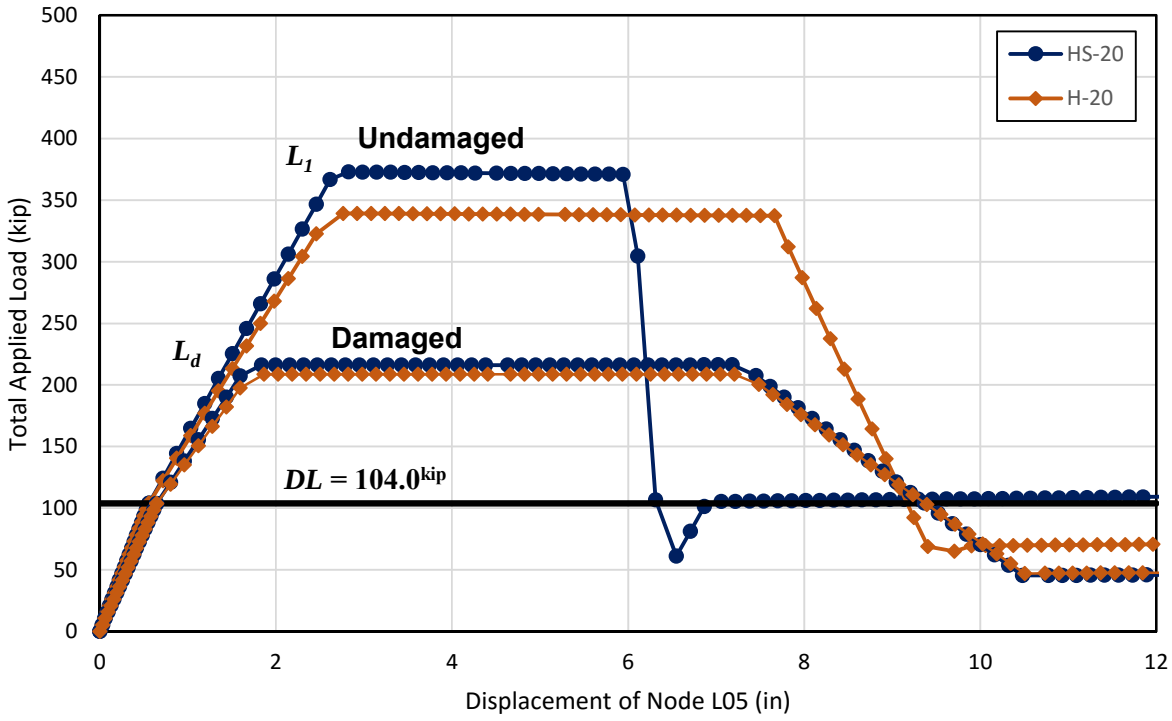

Figure A-28: Response of the Bridge #1M with EPF/EPB Hinges with Member T03 Damaged

Table A-8: Partial Data from the FCA of Member T03 in Bridge #1M with EPF/EPB Hinges

Undamaged H-20			Undamaged HS-20			Damaged H-20			Damaged HS-20		
Step	δ	P	Step	δ	P	Step	δ	P	Step	δ	P
	(in)	(kip)		(in)	(kip)		(in)	(kip)		(in)	(kip)
0	0.0000	0.0	0	0.0000	0.0	0	0.0000	0.0	0	0.0000	0.0
1	0.0279	5.2	1	0.0279	5.2	1	0.0323	5.2	1	0.0323	5.2
2	0.0558	10.4	2	0.0558	10.4	2	0.0645	10.4	2	0.0645	10.4
3	0.0837	15.6	3	0.0837	15.6	3	0.0968	15.6	3	0.0968	15.6
4	0.1116	20.8	4	0.1116	20.8	4	0.1290	20.7	4	0.1290	20.7
5	0.1395	26.0	5	0.1395	26.0	5	0.1613	25.9	5	0.1613	25.9
6	0.1674	31.2	6	0.1674	31.2	6	0.1936	31.1	6	0.1936	31.1
7	0.1953	36.4	7	0.1953	36.4	7	0.2259	36.3	7	0.2259	36.3
8	0.2232	41.6	8	0.2232	41.6	8	0.2581	41.5	8	0.2581	41.5
9	0.2511	46.8	9	0.2511	46.8	9	0.2904	46.7	9	0.2904	46.7
10	0.2790	52.0	10	0.2790	52.0	10	0.3227	51.8	10	0.3227	51.8
11	0.3069	57.2	11	0.3069	57.2	11	0.3550	57.0	11	0.3550	57.0
12	0.3348	62.4	12	0.3348	62.4	12	0.3873	62.2	12	0.3873	62.2
13	0.3627	67.6	13	0.3627	67.6	13	0.4195	67.4	13	0.4195	67.4
14	0.3907	72.8	14	0.3907	72.8	14	0.4518	72.6	14	0.4518	72.6
15	0.4186	78.0	15	0.4186	78.0	15	0.4841	77.8	15	0.4841	77.8
16	0.4465	83.2	16	0.4465	83.2	16	0.5164	83.0	16	0.5164	83.0
17	0.4744	88.4	17	0.4744	88.4	17	0.5487	88.1	17	0.5487	88.1
18	0.5023	93.6	18	0.5023	93.6	18	0.5810	93.3	18	0.5810	93.3
19	0.5303	98.8	19	0.5303	98.8	19	0.6133	98.5	19	0.6133	98.5
20	0.5582	104.0	20	0.5582	104.0	20	0.6456	103.7	20	0.6456	103.7
0	0.5582	104.0	0	0.5582	104.0	0	0.6456	103.7	0	0.6456	103.7
1	0.7166	122.2	1	0.7166	124.3	1	0.8040	119.4	1	0.8040	121.0
2	0.8750	140.5	2	0.8750	144.5	2	0.9624	135.0	2	0.9624	138.3
3	1.0334	158.7	3	1.0334	164.7	3	1.1208	150.7	3	1.1208	155.6
4	1.1918	176.9	4	1.1918	185.0	4	1.2792	166.3	4	1.2792	172.9
5	1.3502	195.1	5	1.3502	205.2	5	1.4376	181.9	5	1.4376	190.1
6	1.5086	213.3	6	1.5086	225.4	6	1.5960	197.6	6	1.5960	207.4
7	1.6670	231.6	7	1.6670	245.6	7	1.8675	208.7	7	1.8357	216.2
8	1.8254	249.8	8	1.8254	265.8	8	2.0264	208.7	8	1.9950	216.2
9	1.9838	268.0	9	1.9838	286.0	9	2.1853	208.7	9	2.1542	216.2
10	2.1422	286.1	10	2.1422	306.2	10	2.3442	208.7	10	2.3135	216.2
11	2.3006	304.3	11	2.3006	326.4	11	2.5031	208.7	11	2.4727	216.2
12	2.4590	322.5	12	2.4590	346.6	12	2.6620	208.7	12	2.6319	216.2
13	2.7641	339.3	13	2.6174	366.8	13	2.8209	208.7	13	2.7912	216.2
14	2.9226	339.2	14	2.8254	372.8	14	2.9798	208.7	14	2.9504	216.2
15	3.0812	339.1	15	2.9851	372.7	15	3.1387	208.7	15	3.1097	216.2
16	3.2397	339.1	16	3.1448	372.6	16	3.2976	208.7	16	3.2689	216.2
17	3.3982	339.0	17	3.3045	372.5	17	3.4565	208.7	17	3.4281	216.2
18	3.5568	338.9	18	3.4641	372.5	18	3.6153	208.7	18	3.5874	216.2
19	3.7153	338.9	19	3.6238	372.4	19	3.7742	208.7	19	3.7466	216.2
20	3.8739	338.8	20	3.7835	372.3	20	3.9331	208.7	20	3.9058	216.2
21	4.0324	338.8	21	3.9432	372.2	21	4.0920	208.7	21	4.0651	216.2
22	4.1909	338.7	22	4.1029	372.1	22	4.2509	208.7	22	4.2243	216.2
23	4.3495	338.6	23	4.2625	372.0	23	4.4098	208.7	23	4.3836	216.2
24	4.5080	338.6	24	4.5078	371.8	24	4.6665	208.7	24	4.6345	216.2
25	4.6665	338.5	25	4.6675	371.7	25	4.8254	208.7	25	4.7937	216.2
26	4.8251	338.4	26	4.8271	371.6	26	4.9843	208.7	26	4.9530	216.2
27	4.9836	338.4	27	4.9868	371.5	27	5.1432	208.7	27	5.1122	216.2
28	5.2844	338.3	28	5.1465	371.4	28	5.3021	208.7	28	5.2714	216.2
29	5.4430	338.2	29	5.3062	371.3	29	5.4610	208.7	29	5.4307	216.2
30	5.6015	338.1	30	5.4659	371.2	30	5.6199	208.7	30	5.5899	216.2

Step 6 - Calculate the Research Ratio for the Member:

The reserve ratio of the bridge corresponding to the member being evaluated is computed next.

$$R_d = \frac{LF_d}{LF_1} \qquad \text{where:} \quad LF_1 = \frac{R_n - P_{DL}}{P_{LL}} \quad \text{and} \quad LF_d = \frac{L_d - DL}{LL}$$

<u>For the H-20 Truck Loading</u>

For Member T02 or T04:

$R_n = 440.0^{\text{kip}}$
$P_{DL} = 92.33^{\text{kip}}$
$P_{LL} = 69.34^{\text{kip}}$

$$LF_1 = \frac{440.0^{\text{kip}} - 92.33^{\text{kip}}}{69.34^{\text{kip}}} = 5.014$$

From the NL Damaged Analysis:

$L_d = 208.7^{\text{kip}}$
$DL = 104.0^{\text{kip}}$
$LL = (1.157)(40^{\text{kip}}) = 46.28^{\text{kip}}$

$$LF_d = \frac{208.7^{\text{kip}} - 104.0^{\text{kip}}}{46.28^{\text{kip}}} = 2.262$$

$$R_d = \frac{LF_d}{LF_1} = \frac{2.262}{5.014} = 0.4512$$

<u>For the HS-20 Truck Loading</u>

For Member T02 or T04:

$R_n = 440.0^{\text{kip}}$
$P_{DL} = 92.33^{\text{kip}}$
$P_{LL} = 112.2^{\text{kip}}$

$$LF_1 = \frac{440.0^{\text{kip}} - 92.33^{\text{kip}}}{112.2^{\text{kip}}} = 3.099$$

From the NL Damaged Analysis:

$L_d = 216.2^{\text{kip}}$
$DL = 104.0^{\text{kip}}$
$LL = (1.157)(72^{\text{kip}}) = 83.30^{\text{kip}}$

$$LF_d = \frac{216.2^{\text{kip}} - 104.0^{\text{kip}}}{83.30^{\text{kip}}} = 1.347$$

$$R_d = \frac{LF_d}{LF_1} = \frac{1.347}{3.099} = 0.4346$$

Since the reserve ratios for Member T03 in the damaged state are less than 0.50, the member should be considered fracture critical.

Consideration of Future Wearing Surface:

If an inspection of the structure shows that wearing surface is not present on the deck and proper maintenance can assure that it won't be added, then the future wearing surface loading, DW, can be neglected in the fracture critical assessment. The calculations below summarize that procedure, and shows that for Bridge #1, the reserve ratios increase by a marginal amount - approximately 8.6%.

For the H-20 Truck Loading

For Member T02 or T04:

$$R_n = 440.0^{\text{kip}}$$
$$P_{DL} = 67.94^{\text{kip}}$$
$$P_{LL} = 69.34^{\text{kip}}$$

$$LF_1 = \frac{440.0^{\text{kip}} - 67.94^{\text{kip}}}{69.34^{\text{kip}}} = 5.366$$

From the NL Damaged Analysis:

$$L_d = 197.7^{\text{kip}}$$
$$DL = 75.98^{\text{kip}}$$
$$LL = (1.157)(40^{\text{kip}}) = 46.28^{\text{kip}}$$

$$LF_d = \frac{197.7^{\text{kip}} - 75.98^{\text{kip}}}{46.28^{\text{kip}}} = 2.637$$

$$R_d = \frac{LF_d}{LF_1} = \frac{2.637}{5.366} = 0.4913$$

For the HS-20 Truck Loading

For Member T02 or T04:

$$R_n = 440.0^{\text{kip}}$$
$$P_{DL} = 67.94^{\text{kip}}$$
$$P_{LL} = 112.2^{\text{kip}}$$

$$LF_1 = \frac{440.0^{\text{kip}} - 67.94^{\text{kip}}}{112.2^{\text{kip}}} = 3.316$$

From the NL Damaged Analysis:

$$L_d = 206.4^{\text{kip}}$$
$$DL = 75.98^{\text{kip}}$$
$$LL = (1.157)(72^{\text{kip}}) = 83.30^{\text{kip}}$$

$$LF_d = \frac{206.4^{\text{kip}} - 75.98^{\text{kip}}}{83.30^{\text{kip}}} = 1.566$$

$$R_d = \frac{LF_d}{LF_1} = \frac{1.566}{3.316} = 0.4722$$

Consideration of Strain Hardening in Tension:

If the analysis is run using a hinge model that includes strain hardening in tension, i.e. an EPHF/EPB hinge model as is shown in Figure A-29, then the load deformation responses that are shown in Figure A-30 result. The reserve ratios of Member T03 in the analysis with EPHF/EPB hinges were approximately 35% larger than reserve ratios computed based on analyses incorporating EPF/EPB hinges.

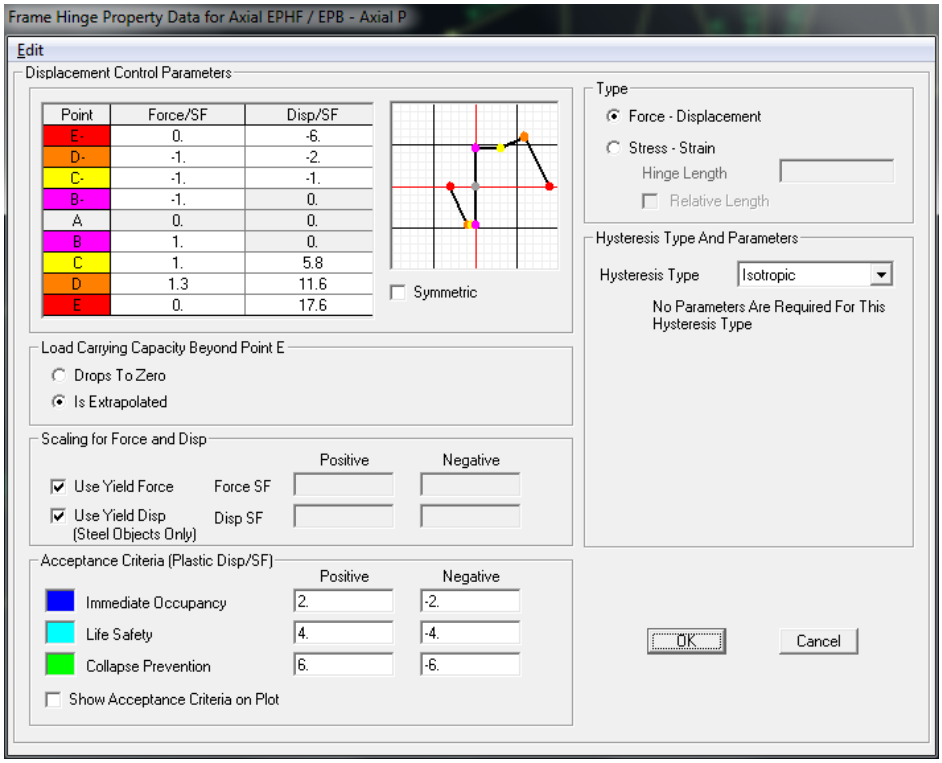

Figure A-29: EPHF/EPB Hinge Definition

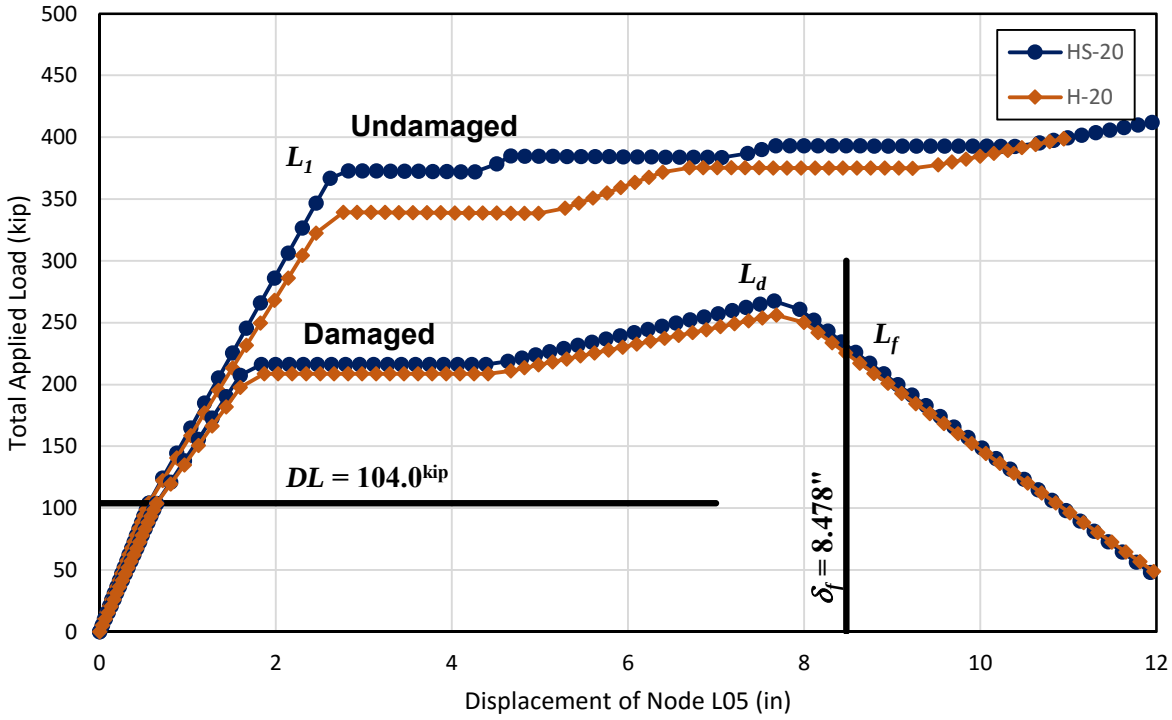

Figure A-30: Bridge #1M Load-Deformation with EPHF/EPB Axial Hinges

Reserve ratios can be computed based on the EPHF/EPB analysis results:

For the H-20 Truck Loading

For Member T02 or T04:

$R_n = 440.0^{\text{kip}}$
$P_{DL} = 92.33^{\text{kip}}$
$P_{LL} = 69.34^{\text{kip}}$

$$LF_1 = \frac{440.0^{\text{kip}} - 92.33^{\text{kip}}}{69.34^{\text{kip}}} = 5.014$$

From the NL Damaged Analysis:

$L_d = 256.1^{\text{kip}}$
$DL = 104.0^{\text{kip}}$
$LL = (1.157)(40^{\text{kip}}) = 46.28^{\text{kip}}$

$$LF_d = \frac{256.1^{\text{kip}} - 104.0^{\text{kip}}}{46.28^{\text{kip}}} = 3.287$$

$$R_d = \frac{LF_d}{LF_1} = \frac{3.287}{5.014} = 0.6556$$

For the HS-20 Truck Loading

For Member T02 or T04:

$R_n = 440.0^{\text{kip}}$
$P_{DL} = 92.33^{\text{kip}}$
$P_{LL} = 112.2^{\text{kip}}$

$$LF_1 = \frac{440.0^{\text{kip}} - 92.33^{\text{kip}}}{112.2^{\text{kip}}} = 3.099$$

From the NL Damaged Analysis:

$L_d = 267.4^{\text{kip}}$
$DL = 104.0^{\text{kip}}$
$LL = (1.157)(72^{\text{kip}}) = 83.30^{\text{kip}}$

$$LF_d = \frac{267.4^{\text{kip}} - 104.0^{\text{kip}}}{83.30^{\text{kip}}} = 1.962$$

$$R_d = \frac{LF_d}{LF_1} = \frac{1.962}{3.099} = 0.6331$$

Table A-9: Partial Data from the Nonlinear FCA of Member T03 in Bridge #1M with EPHF/EPB Hinges

Undamaged H-20			Undamaged HS-20			Damaged H-20			Damaged HS-20		
Step	δ	P	Step	δ	P	Step	δ	P	Step	δ	P
	(in)	(kip)		(in)	(kip)		(in)	(kip)		(in)	(kip)
0	0.0000	0.0	0	0.0000	0.0	0	0.0000	0.0	0	0.0000	0.0
1	0.0279	5.2	1	0.0279	5.2	1	0.0323	5.2	1	0.0323	5.2
2	0.0558	10.4	2	0.0558	10.4	2	0.0645	10.4	2	0.0645	10.4
3	0.0837	15.6	3	0.0837	15.6	3	0.0968	15.6	3	0.0968	15.6
4	0.1116	20.8	4	0.1116	20.8	4	0.1290	20.7	4	0.1290	20.7
5	0.1395	26.0	5	0.1395	26.0	5	0.1613	25.9	5	0.1613	25.9
6	0.1674	31.2	6	0.1674	31.2	6	0.1936	31.1	6	0.1936	31.1
7	0.1953	36.4	7	0.1953	36.4	7	0.2259	36.3	7	0.2259	36.3
8	0.2232	41.6	8	0.2232	41.6	8	0.2581	41.5	8	0.2581	41.5
9	0.2511	46.8	9	0.2511	46.8	9	0.2904	46.7	9	0.2904	46.7
10	0.2790	52.0	10	0.2790	52.0	10	0.3227	51.8	10	0.3227	51.8
11	0.3069	57.2	11	0.3069	57.2	11	0.3550	57.0	11	0.3550	57.0
12	0.3348	62.4	12	0.3348	62.4	12	0.3873	62.2	12	0.3873	62.2
13	0.3627	67.6	13	0.3627	67.6	13	0.4195	67.4	13	0.4195	67.4
14	0.3907	72.8	14	0.3907	72.8	14	0.4518	72.6	14	0.4518	72.6
15	0.4186	78.0	15	0.4186	78.0	15	0.4841	77.8	15	0.4841	77.8
16	0.4465	83.2	16	0.4465	83.2	16	0.5164	83.0	16	0.5164	83.0
17	0.4744	88.4	17	0.4744	88.4	17	0.5487	88.1	17	0.5487	88.1
18	0.5023	93.6	18	0.5023	93.6	18	0.5810	93.3	18	0.5810	93.3
19	0.5303	98.8	19	0.5303	98.8	19	0.6133	98.5	19	0.6133	98.5
20	0.5582	104.0	20	0.5582	104.0	20	0.6456	103.7	20	0.6456	103.7
0	0.5582	104.0	0	0.5582	104.0	0	0.6456	103.7	0	0.6456	103.7
1	0.7166	122.2	1	0.7166	124.3	1	0.8040	119.4	1	0.8040	121.0
2	0.8750	140.5	2	0.8750	144.5	2	0.9624	135.0	2	0.9624	138.3
3	1.0334	158.7	3	1.0334	164.7	3	1.1208	150.7	3	1.1208	155.6
4	1.1918	176.9	4	1.1918	185.0	4	1.2792	166.3	4	1.2792	172.9
5	1.3502	195.1	5	1.3502	205.2	5	1.4376	181.9	5	1.4376	190.1
6	1.5086	213.3	6	1.5086	225.4	6	1.5960	197.6	6	1.5960	207.4
7	1.6670	231.6	7	1.6670	245.6	7	1.8675	208.7	7	1.8357	216.2
8	1.8254	249.8	8	1.8254	265.8	8	2.0264	208.7	8	1.9950	216.2
9	1.9838	268.0	9	1.9838	286.0	9	2.1853	208.7	9	2.1542	216.2
10	2.1422	286.1	10	2.1422	306.2	10	2.3442	208.7	10	2.3135	216.2
11	2.3006	304.3	11	2.3006	326.4	11	2.5031	208.7	11	2.4727	216.2
12	2.4590	322.5	12	2.4590	346.6	12	2.6620	208.7	12	2.6319	216.2
13	2.7641	339.3	13	2.6174	366.8	13	2.8209	208.7	13	2.7912	216.2
14	2.9226	339.2	14	2.8254	372.8	14	2.9798	208.7	14	2.9504	216.2
15	3.0812	339.1	15	2.9851	372.7	15	3.1387	208.7	15	3.1097	216.2
16	3.2397	339.1	16	3.1448	372.6	16	3.2976	208.7	16	3.2689	216.2
17	3.3982	339.0	17	3.3045	372.5	17	3.4565	208.7	17	3.4281	216.2
18	3.5568	338.9	18	3.4641	372.5	18	3.6153	208.7	18	3.5874	216.2
19	3.7153	338.9	19	3.6238	372.4	19	3.7742	208.7	19	3.7466	216.2
20	3.8739	338.8	20	3.7835	372.3	20	3.9331	208.7	20	3.9058	216.2
21	4.0324	338.8	21	3.9432	372.2	21	4.0920	208.7	21	4.0651	216.2
22	4.1909	338.7	22	4.1029	372.1	22	4.2509	208.7	22	4.2243	216.2
23	4.3495	338.6	23	4.2625	372.0	23	4.4098	208.7	23	4.3836	216.2
24	4.5080	338.6	24	4.5078	378.3	24	4.6665	211.1	24	4.6345	218.8
25	4.6665	338.5	25	4.6675	384.7	25	4.8254	213.5	25	4.7937	221.4
26	4.8251	338.4	26	4.8271	384.7	26	4.9843	215.9	26	4.9530	223.9
27	4.9836	338.4	27	4.9868	384.6	27	5.1432	218.3	27	5.1122	226.5
28	5.2844	342.5	28	5.1465	384.5	28	5.3021	220.6	28	5.2714	229.1
29	5.4430	346.7	29	5.3062	384.4	29	5.4610	223.0	29	5.4307	231.7
30	5.6015	350.9	30	5.4659	384.4	30	5.6199	225.4	30	5.5899	234.2

Computation of LF1 Using System Behavior:

It is possible to compute member failure load factor based on system performance. This would be accomplished using the following relationship.

$$LF_{1S} = \frac{L_1 - DL}{LL} \simeq LF_1 = \frac{R_n - P_{DL}}{P_{LL}}$$

Referring to Figure A-30, The load corresponding to the limit of the linear response to an HS-20 truck is $L_{1S} = 372.8^{\text{kip}}$. Similarly, the load corresponding to the limit of the linear response to an HS-20 truck is $L_{1S} = 339.3^{\text{kip}}$.

For the H-20 Truck Loading

From the Nonlinear Analysis:

$L_1 = 339.3^{\text{kip}}$
$L_d = 256.1^{\text{kip}}$
$DL = 104.0^{\text{kip}}$
$LL = (1.157)(40^{\text{kip}}) = 46.28^{\text{kip}}$

$$LF_{1S} \simeq \frac{339.3^{\text{kip}} - 104.0^{\text{kip}}}{46.28^{\text{kip}}} = 5.084$$

$$LF_d = \frac{256.1^{\text{kip}} - 104.0^{\text{kip}}}{46.28^{\text{kip}}} = 3.287$$

$$R_d = \frac{LF_d}{LF_{1S}} = \frac{3.287}{5.084} = 0.6465$$

For the HS-20 Truck Loading

From the Nonlinear Analysis:

$L_1 = 372.8^{\text{kip}}$
$L_d = 267.4^{\text{kip}}$
$DL = 104.0^{\text{kip}}$
$LL = (1.157)(72^{\text{kip}}) = 83.30^{\text{kip}}$

$$LF_{1S} \simeq \frac{372.8^{\text{kip}} - 104.0^{\text{kip}}}{83.30^{\text{kip}}} = 3.227$$

$$LF_d = \frac{267.4^{\text{kip}} - 104.0^{\text{kip}}}{83.30^{\text{kip}}} = 1.962$$

$$R_d = \frac{LF_d}{LF_{1S}} = \frac{1.135}{1.867} = 0.6079$$

2D Fracture Critical Analysis Summary and Comments:

While it isn't likely that a 2D analysis will be used to reevaluate a member for redundancy, this problem serves a good and compact example to illustrate the process that is applied to 3D analyses.

	Loading	
	H-20	HS-20
EPF/EPB Hinge:	0.4512	0.4346
EPF/EPB Hinge without DW:	0.4913	0.4722
EPHF/EPB Hinge:	0.6556	0.6331
EPHF/EPB Hinge using LF_{1S}:	0.6465	0.6079

3D Analysis of Bridge #1M

A three-dimensional model of Bridge #1M including the modified bottom chord as described previously was constructed and is shown in Figure A-31. Two truss were modeled identical to the one created for the 2D model, and W24x94 floor beam members were used to connect the trusses at their panel points. Next, W12x30 stringers were constructed spanning parallel to the trusses between adjacent floor beams. Finally, the deck was modeled by creating beam elements perpendicular to the stringers at one foot intervals.

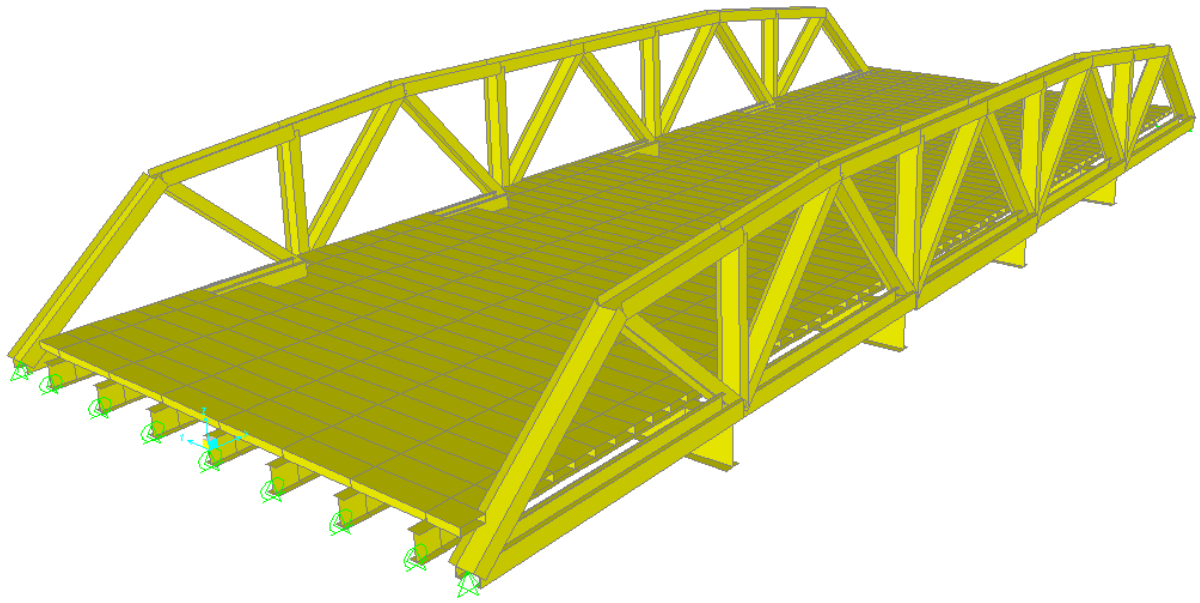

Figure A-31: Perspective View of the 3D Model of Bridge #1M

Floor beams were each connected to the trusses with moment connections. As a baseline, the stringers were attached to the floor beams with moment releases and, for all floor beams except the first and last, were connected with axial force releases. The stringers were supported at the abutments with roller supports permitting end rotation and end translation parallel to the axes of the stringers. Section properties were assigned to the decking members consistent with 5 gage 3”x9” decking without asphalt fill. As a baseline, decking members were assigned with moment releases over all stringers except for the first and last stringers (consistent with application of the lever rule). Decking members were also defined with shear releases in the plane of the deck. Finally, the floor beams, stringers, and decking members were all defined with end offsets in the vertical direction to reflect the underslung configuration of the floor system. These offsets are

reflected in the member forces that are developed in these members; axial compression in the decking members is an example of that behavior.

Analysis options were modified as is shown in Figure A-32 to include all translational and rotational degrees of freedom.

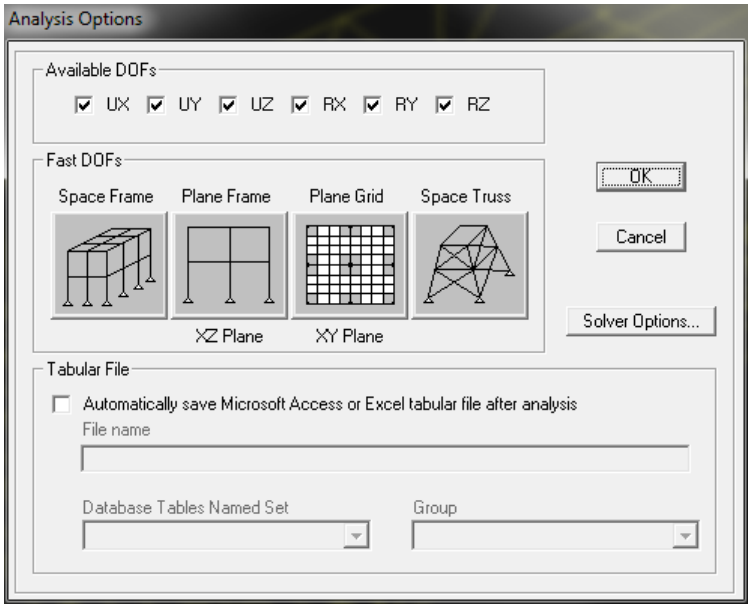

Figure A-32: Active Degrees of Freedom for 3D Analysis of Bridge #1M

Self-weight of the truss members, floor beams, and stringers was included in a *SW* load pattern including an additional 15% for miscellaneous steel. Self-weight of the decking members is not included in the *SW* load pattern by means of a mass / self-weight property modifier for those elements. A dead load of 65^{psf} associated with the decking and asphalt fill was included as a uniform load on the decking members as a *DC* load pattern. A dead load of 35^{psf} representing future wearing surface was included as a *DW* load pattern. *DC*, *DW*, and *SW* load patterns were defined as is shown in Figure A-8. Truss member forces resulting from the dead loads and self-weight are shown in Table A-10. Dead load and self-weight member forces from the three-dimensional analysis compare favorably to those determined in the two-dimensional analysis. *DC* forces in the 3D analysis are smaller than the 2D analysis and *SW* forces are larger in the 3D analysis than the 2D analysis but this is to be expected. *DW* forces are nearly identical in the two analyses.

Live loads were applied in static positions for the tandem, H-20, and HS-20 truck loads. Critical positions were determined for each truck for each member for both tension and compression based on an influence line analysis of the two-dimension truss. All truck positions included two lanes positioned as shown in Figure A-9 making the right truss the critical truss. Trucks in both lanes were defined as being exactly parallel and facing in the same direction, either facing forward or backward. Truck loads were implemented by assigning point loads to the appropriate deck members. Since the deck members were

defined a one foot increments along the length of the bridge, the axles critical positions were rounded to the nearest foot relative the rear abutment of the bridge. Axles that were positioned off the bridge due the location of the truck were ignored. Member forces due to live loads are shown in Table A-11 and compared favorably to those determined using the two-dimensional analysis with distribution factors. The maximum deviation noted was 6% in members T16R and T27R.

Table A-10: Dead Load Member Forces from 3D Model of Bridge #1M

Member	*DC*	*SW*	*DW*	Total *DL*
	(kip)	(kip)	(kip)	(kip)
T01R	22.48	12.411	12.11	47.00
T02R	44.97	24.54	24.21	93.72
T03R	53.96	29.433	29.06	112.45
T04R	44.97	24.54	24.21	93.72
T05R	22.48	12.411	12.11	47.00
T06R	-30.38	-16.944	-16.36	-63.69
T07R	-40.22	-21.658	-21.66	-83.54
T08R	-40.22	-21.658	-21.66	-83.54
T09R	-53.96	-29.136	-29.06	-112.16
T10R	-53.96	-29.136	-29.06	-112.16
T11R	-53.96	-29.136	-29.06	-112.16
T12R	-53.96	-29.136	-29.06	-112.16
T13R	-40.22	-21.615	-21.66	-83.50
T14R	-40.22	-21.615	-21.66	-83.50
T15R	-30.38	-16.601	-16.36	-63.34
T16R	23.63	12.192	12.72	48.55
T17R	0.00	-0.582	0.00	-0.58
T18R	-7.57	-4.717	-4.08	-16.36
T19R	13.62	6.844	7.33	27.80
T20R	0.00	-0.602	0.00	-0.60
T21R	0.00	-0.563	0.00	-0.56
T22R	0.00	-0.563	0.00	-0.56
T23R	0.00	-0.602	0.00	-0.60
T24R	13.62	6.844	7.33	27.80
T25R	-7.57	-4.717	-4.08	-16.36
T26R	0.00	-0.582	0.00	-0.58
T27R	23.63	12.19	12.72	48.55

Table A-11: Truck Load Member Forces from 3D Model of Bridge #1M

Tandem*		**H-20***		**HS-20***	
(pos)	**(neg)**	**(pos)**	**(neg)**	**(pos)**	**(neg)**
(kip)	(kip)	(kip)	(kip)	(kip)	(kip)
51.04	0.00	39.96	0.00	63.12	0.00
92.73	0.00	72.36	0.00	118.07	0.00
106.57	0.00	84.61	0.00	143.23	0.00
92.87	0.00	72.47	0.00	118.25	0.00
51.26	0.00	40.14	0.00	63.46	0.00
0.00	-69.28	0.00	-54.25	0.00	-85.77
0.00	-91.71	0.00	-71.82	0.00	-113.55
0.00	-91.71	0.00	-71.82	0.00	-113.55
0.00	-121.90	0.00	-94.70	0.00	-145.04
0.00	-121.90	0.00	-94.70	0.00	-145.04
0.00	-121.89	0.00	-94.70	0.00	-145.03
0.00	-121.89	0.00	-94.70	0.00	-145.03
0.00	-91.71	0.00	-71.82	0.00	-113.55
0.00	-91.71	0.00	-71.82	0.00	-113.55
0.00	-69.27	0.00	-54.25	0.00	-85.77
53.88	0.00	42.19	0.00	66.71	0.00
0.00	0.00	0.00	0.00	0.00	0.00
25.02	-34.51	18.92	-26.46	18.92	-40.35
45.01	-13.02	34.68	-9.85	52.53	-9.85
0.00	0.00	0.00	0.00	0.00	0.00
29.10	-29.09	22.52	-22.52	29.76	-29.76
29.09	-29.10	22.52	-22.52	29.76	-29.76
0.00	0.00	0.00	0.00	0.00	0.00
45.01	-13.02	34.68	-9.85	52.53	-9.85
25.02	-34.51	18.92	-26.46	18.92	-40.34
0.00	0.00	0.00	0.00	0.00	0.00
53.88	0.00	42.19	0.00	66.71	0.00

* Tandem, H-20, and HS-20 loads do not include impact

3D Fracture Critical Analysis of Bridge #1M

Following the linear elastic three-dimensional analysis of Bridge #1, a fracture critical analysis was conducted for the truss members in the bridge. Based on member forces from the 2D analysis that are shown in Table A-5 along with consideration of bridge symmetry, it was determined that members T01, T02, T03, T16, T18, T19, and T21 would be assessed to determine fracture criticality.

A nonlinear load case was defined for the nonlinear application of dead lead. As was done with the 2D FCA, this load case was named “nDL” and was defined as is shown in Figure A-14 through Figure A-16 using the vertical displacement of node L05R as the monitored degree of freedom. Two additional load cases were defined for each member being assessed, one for the H-20 load pattern and a second for the HS-20 load pattern, each corresponding to the critical truck position for the member being considered. These load cases were defined as is shown in Figure A-17 through Figure A-19 with the exception that that the scale factor of 1.157 was changed to 1.000. The factor of 1.157 in the 2D analysis represented the truss distribution factor and was not needed in the 3D analysis since load distribution was inherently included in the model. Additionally, the monitored degree of freedom was different for some of the members being considered, selected based on which node was expected to experience the maximum displacement.

After an analysis of the bridge in its undamaged state was completed, the bridge model was systematically modified to reflect the damaged state for each member. In the cases of the bottom chord members, this meant changing the member definitions from a pair of channels to a single channel. In the cases of the diagonal members, this meant deleting the member entirely. The analyses were rerun for each damaged model and the load displacement data was recorded. Figure A-33 shows the load deformation data for Member T03R.

The total dead load on the bridge was $DL = 202.9^{\text{kip}}$ and the corresponding dead load displacement of the undamaged bridge at node L05R, Δ_{DL}, was approximately 0.5513”. With a span length of 66’-0”, $L / 100$ for the bridge was 7.920” meaning that the functionality displacement limit was $\Delta_f = 0.5513\text{”} + 7.920\text{”} = 8.471\text{”}$. The response of the undamaged bridge becomes nonlinear at a load L_1 of approximately 500^{kip} to 550^{kip} and the response of the damaged bridge peaks at a load L_d of approximately 480^{kip} to 505^{kip}. The displacement corresponding to the peak at L_d is less than the displacement Δ_f, thus the performance of the bridge in its damaged state is defined by strength, not displacement / functionality.

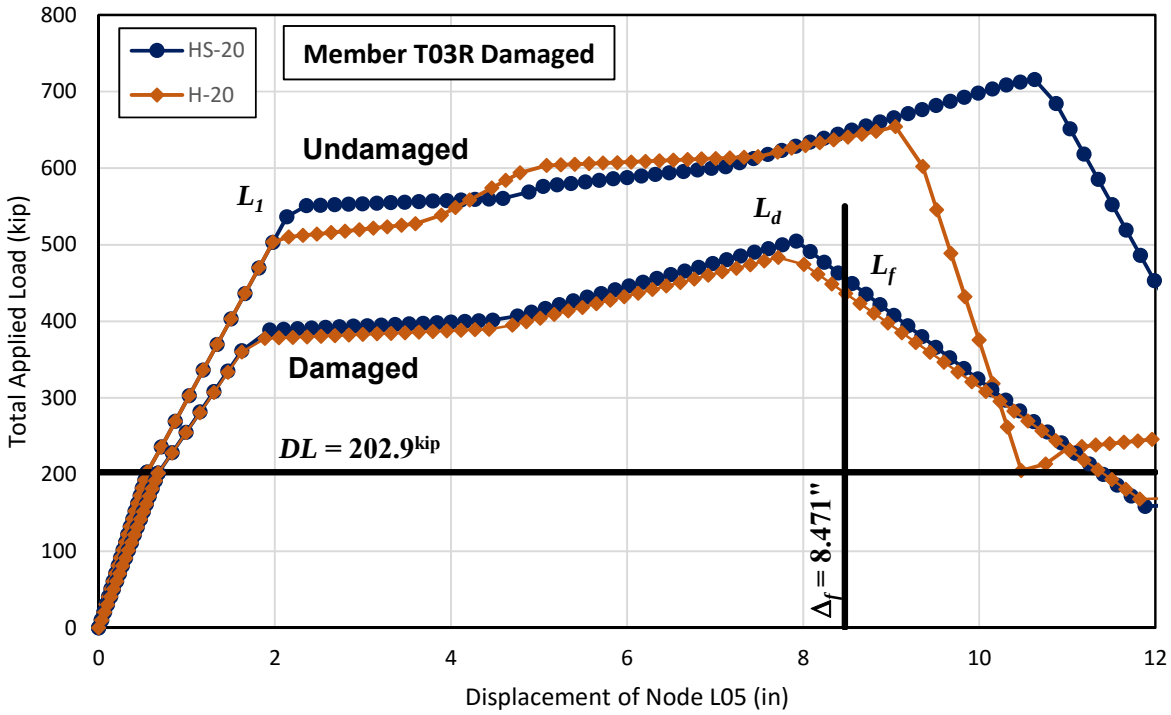

Figure A-33: 3D FCA Response of Bridge #1M with Member T03R Damaged

Calculations showing the development of R_d for Member T03R are shown here:

<u>For the H-20 Truck Loading</u>

From the Nonlinear Analyses:

$L_1 = 478.0^{kip}$
$L_d = 482.7^{kip}$
$DL = 202.9^{kip}$
$LL = (2)(40^{kip}) = 80^{kip}$

$$LF_{1S} = \frac{478.0^{kip} - 202.9^{kip}}{80^{kip}} = 3.439$$

$$LF_d = \frac{482.7^{kip} - 202.9^{kip}}{80^{kip}} = 3.498$$

$$R_d = \frac{LF_d}{LF_{1S}} = \frac{3.498}{3.439} = 1.017$$

<u>For the HS-20 Truck Loading</u>

From the Nonlinear Analyses:

$L_1 = 540.8^{kip}$
$L_d = 505.2^{kip}$
$DL = 202.9^{kip}$
$LL = (2)(72^{kip}) = 144^{kip}$

$$LF_{1S} = \frac{540.8^{kip} - 202.9^{kip}}{144^{kip}} = 2.347$$

$$LF_d = \frac{505.2^{kip} - 202.9^{kip}}{144^{kip}} = 2.100$$

$$R_d = \frac{LF_d}{LF_{1S}} = \frac{2.100}{2.347} = 0.8946$$

Fracture Critical Assessment parameters for the seven members in Bridge #1M are showing in Table A-12 and Table A-13 for the H-20 and HS-20 loadings, respectively. FCA responses for the members are shown in Figure A-33 through Figure A-39. Notes about the assessments are provided following Figure A-39. Based on the assessment, Member T01, T02, T03, T18, and T21 can be reclassified as not fracture critical.

Table A-12: 3D FCA Analysis Parameters for H-20 on Bridge #1M

	Member						
Parameter	**T01R**	**T02R**	**T03R**	**T16R**	**T18R**	**T19R**	**T21R**
Mon Node:	L03R	L05R	L05R	L03R	L03R	L05R	L05R
Damage State:	C9x15	C9x15	C10x20	Mem Loss	Mem Loss	Mem Loss	Mem Loss
DL**:**	202.9kip	202.9kip	202.9kip	202.9kip	202.9kip	202.9kip	202.9kip
Δ_{DL}**:**	0.3635”	0.5513”	0.5513”	0.3635”	0.3635”	0.5513”	0.5513”
Truck Pos:	27 Fwd	26 Bwd	40 Fwd	27 Fwd	13 Bwd	40 Fwd	26 Bwd
LL**:**	80kip	80kip	80kip	80kip	64kip	80kip	80kip
L_1**:**	519.0kip	495.8kip	478.0kip	519.0kip	537.5kip	478.0kip	495.8kip
L_d**:**	743.2kip	454.1kip	482.7kip	---	---	---	---
Δ_d**:**	8.151”	6.798”	7.815”	---	---	---	---
L_f**:**	743.2kip	358.8kip	447.1kip	60.78kip	569.7kip	295.9kip	526.8kip
Δ_f**:**	8.284”	8.471”	8.471”	8.284”	8.284”	8.471”	8.471”
LF_{1s}**:**	3.952	3.661	3.439	3.952	5.228	3.439	3.661
LF_d**:**	6.755	3.140	3.498	-1.776	5.731	1.163	4.050
R_d**:**	1.709	0.8577	1.017	-0.4494	1.096	0.3382	1.106
Classification:	NFC	NFC	NFC	FC	NFC	FC	NFC

Table A-13: 3D FCA Analysis Parameters for HS-20 on Bridge #1M

	Member						
Parameter	**T01R**	**T02R**	**T03R**	**T16R**	**T18R**	**T19R**	**T21R**
Mon Node:	L03R	L05R	L05R	L03R	L03R	L05R	L05R
Damage State:	C9x15	C9x15	C10x20	Mem Loss	Mem Loss	Mem Loss	Mem Loss
DL**:**	202.9kip	202.9kip	202.9kip	202.9kip	202.9kip	202.9kip	202.9kip
Δ_{DL}**:**	0.3635”	0.5513”	0.5513”	0.3635”	0.3635”	0.5513”	0.5513”
Truck Pos:	41 Fwd	41 Fwd	54 Fwd	41 Fwd	13 Bwd	54 Fwd	26 Bwd
LL**:**	144kip	144kip	144kip	144kip	64kip	144kip	128kip
L_1**:**	513.3kip	532.1kip	540.8kip	513.3kip	537.5kip	540.8kip	506.4kip
L_d**:**	711.5kip	480.9kip	505.2kip	---	---	---	---
Δ_d**:**	7.313”	6.791”	7.909”	---	---	---	---
L_f**:**	550.3kip	376.3kip	463.7kip	60.78kip	569.7kip	313.1kip	574.6kip
Δ_f**:**	8.284”	8.471”	8.471”	8.284”	8.284”	8.471”	8.471”
LF_{1s}**:**	2.156	2.286	2.347	2.156	5.228	2.347	2.371
LF_d**:**	3.532	1.931	2.100	-0.9867	5.761	0.7654	2.904
R_d**:**	1.639	0.8446	0.8946	-0.4577	1.096	0.3261	1.225
Classification:	NFC	NFC	NFC	FC	NFC	FC	NFC

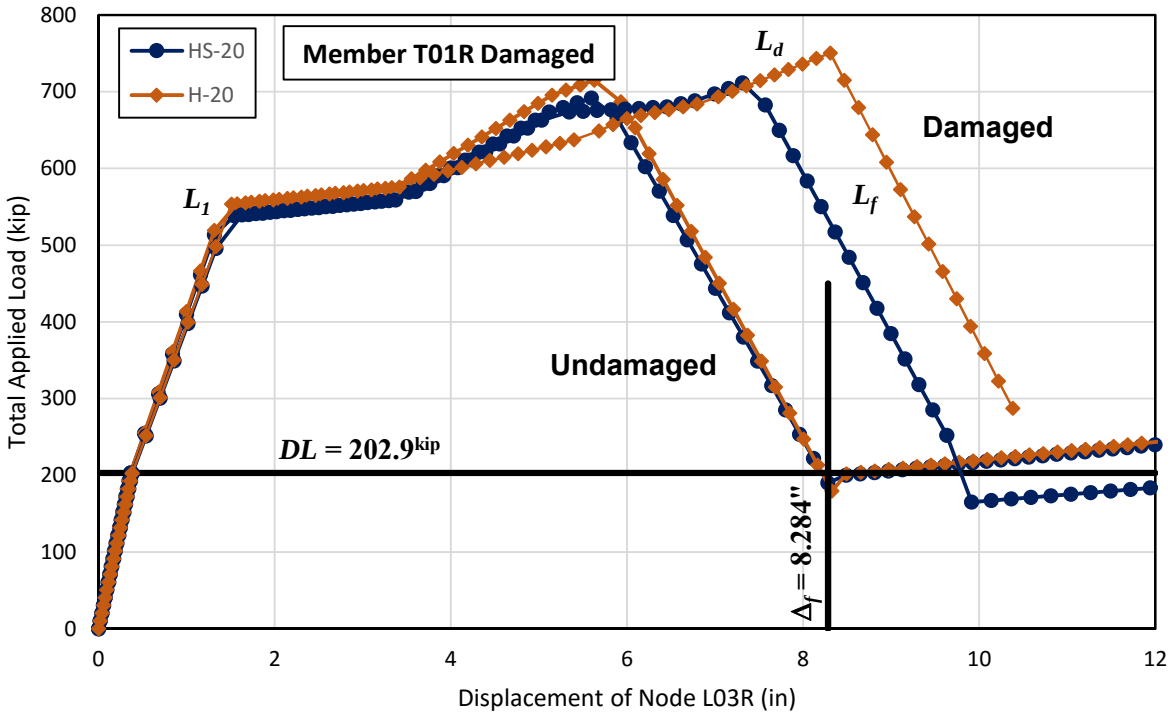

Figure A-34: 3D FCA Response of Bridge #1M with Member T01R Damaged

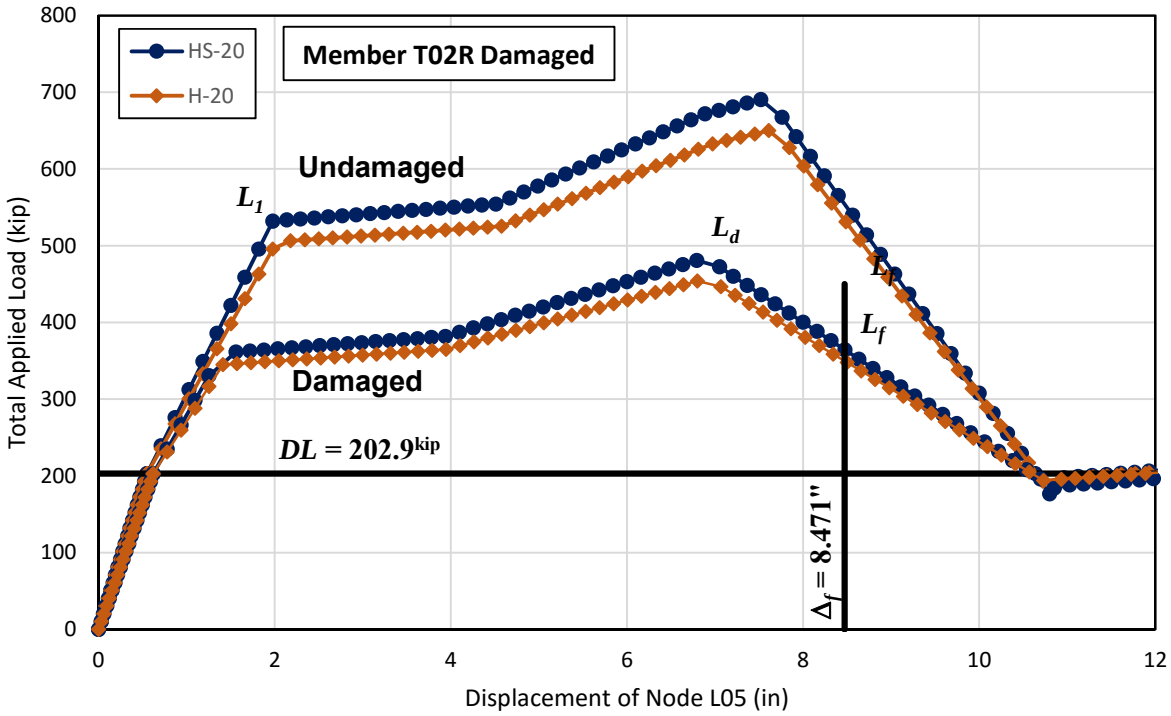

Figure A-35: 3D FCA Response of Bridge #1M with Member T02R Damaged

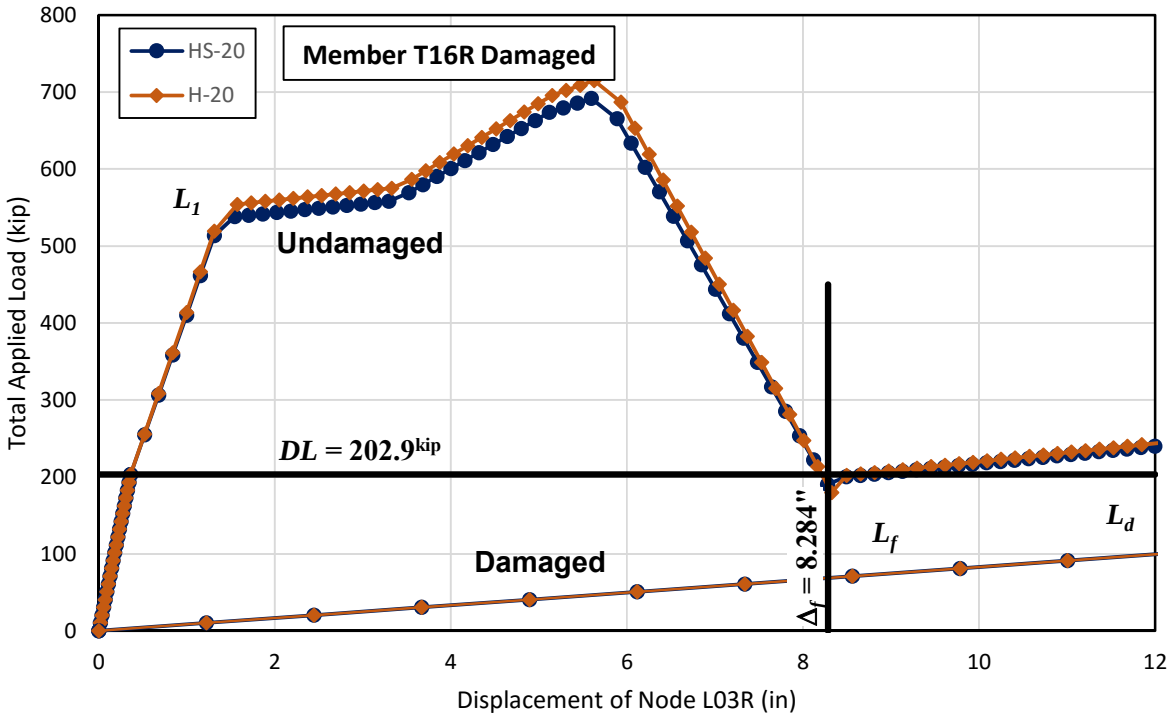

Figure A-36: 3D FCA Response of Bridge #1M with Member T16R Damaged

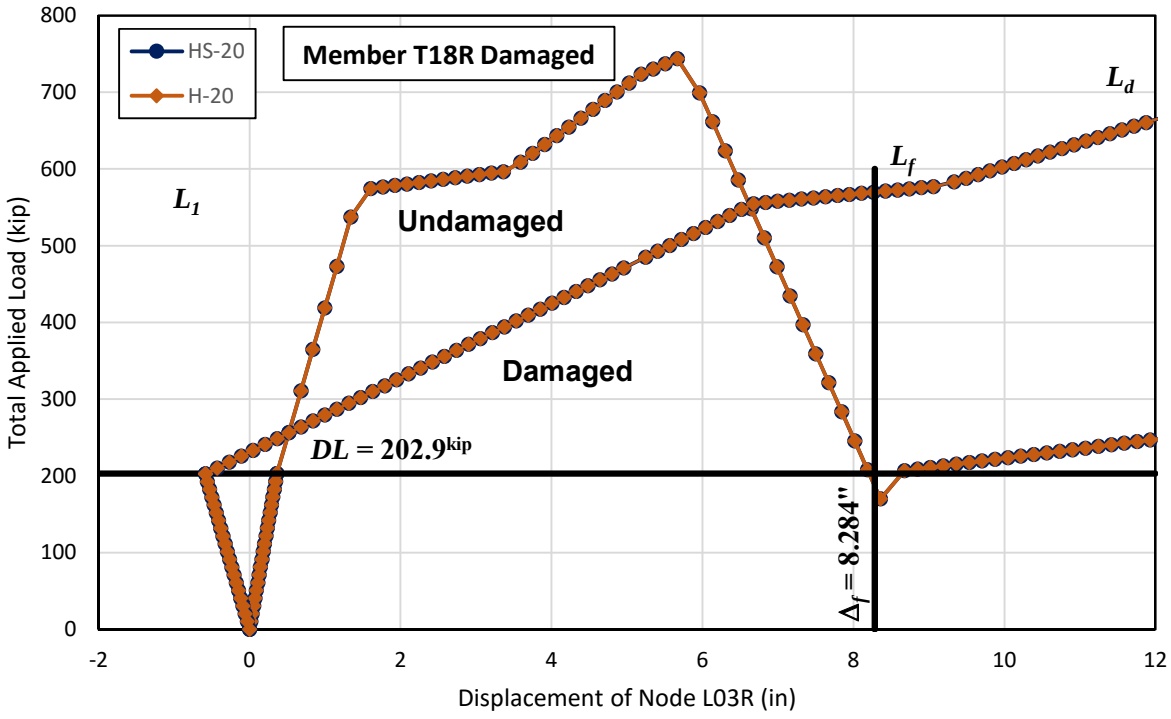

Figure A-37: 3D FCA Response of Bridge #1M with Member T18R Damaged

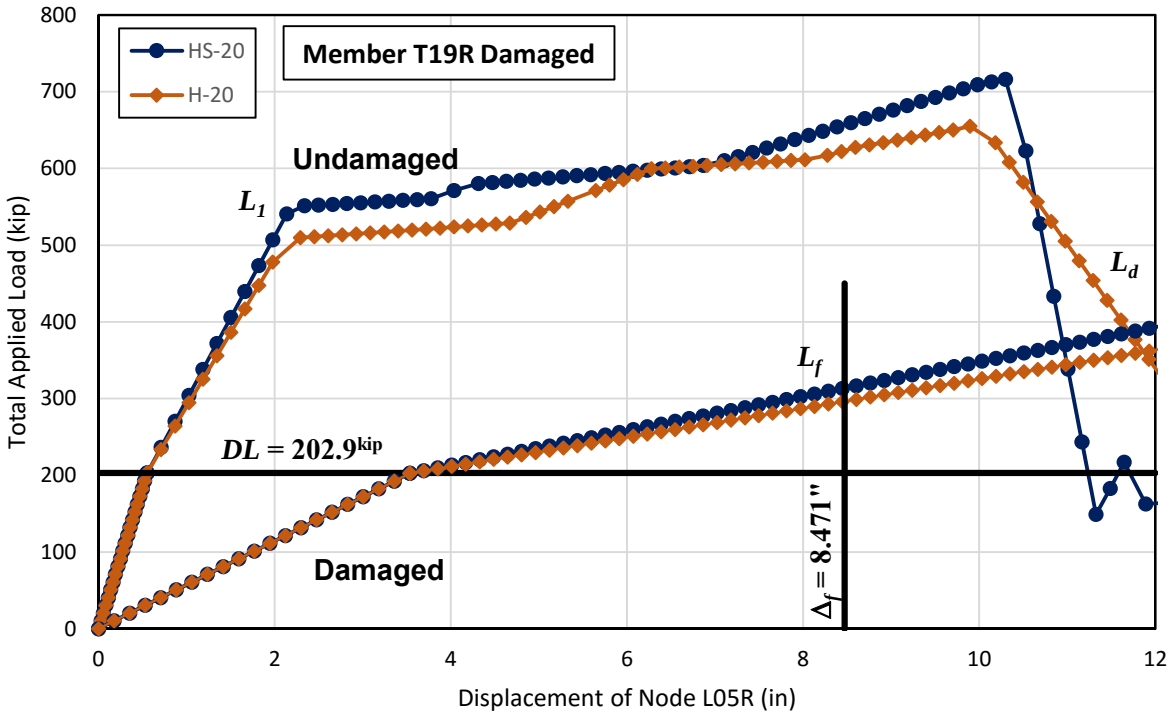

Figure A-38: 3D FCA Response of Bridge #1M with Member T19R Damaged

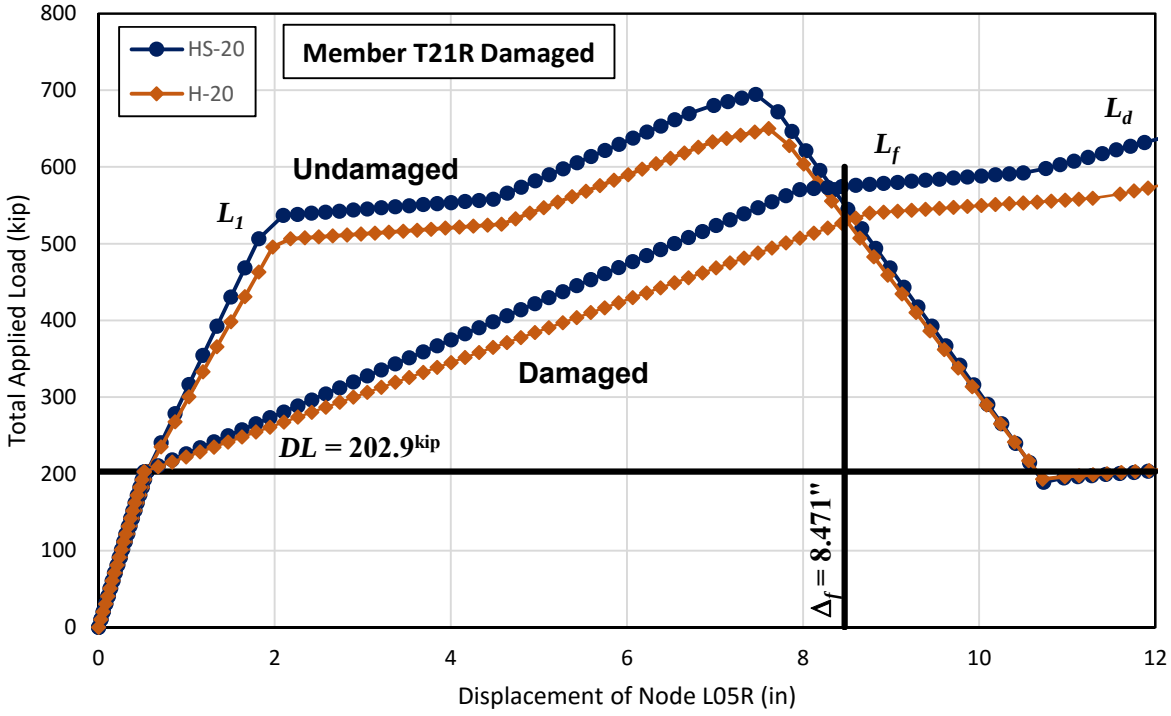

Figure A-39: 3D FCA Response of Bridge #1M with Member T21R Damaged

Notes and Observations about FCA Assessment of Bridge #1M:

1. The notation used for truck position is the location of the lead axle of truck in feet followed by the direction of the truck. For example, “40 Fwd” for an H-20 truck means that the 8^{kip} axles is located at station 40 of the bridge and the 32^{kip} axle is located at station 26. As another example, “26 Bwd” for an H-20 truck indicates that the 32^{kip} axle is located at station 26 and the 8^{kip} axle is located at station 12.
2. The live load used in the FCAs varies occasionally because some axles fall outside the limits of the bridge. Considering the FCA of Member T21R under an HS-20 truck for example, the 8^{kip} axle of the truck would be positioned 2 feet off the rear abutment.
3. The response of the bridge for FCA of Member T01R shows the damaged bridge sustaining a larger displacement than the undamaged bridge before failure. This may seem odd but is the result of the progression of failure of the members. In the undamaged bridge, Member T02R reaches its yield load and ultimate load before Member T01R reaches its yield load, thus all of the inelastic deformation in the undamaged bridge is isolated in Member T02R. In the damaged bridge, Members T01R and T02R yield their yield loads at the same load step, then both members deform inelastically until an ultimate limit is reached in a process that distributes the inelastic deformation over both members. Thus the deformation capacity of the bridge is essentially doubled.
4. The response of the bridge for FCA of Member T18R shows a negative displacement for the damaged bridge under dead load. This is a peculiarity of the node selected for monitoring. Node L03R deflects upwards under dead load in the damaged bridge, then Node L03R deflects downwards under the application of the truck loads.
5. The HS-20 truck loading governed five of the seven members that were evaluated. In the sixth case, Member T18R, the H-20 and HS-20 yielded the same reserve ratio since, because of the position of the trucks close to the rear abutment, both trucks result in the same loading on the bridge. In the seventh case, where the H-20 governed by approximately 10%, Member T21R, the front axles of the HS-20 were located off the bridge.
6. The reserve ratio, R_d, of Member T16R is negative indicating that in its damaged state the bridge is not able to support its own dead load.
7. The reserve ratio, R_d, of Member T19R is less than 0.50 indicating that it should be classified as fracture critical. If the owner elects to employ the member strength reserve ratio, r_1, then R_d can be multiplied by r_1, which will increase R_d, possibly enough to justify reclassification of the member as not fracture critical. For Member T19R, the reserve ratio, R_d, is governed by the HS-20 loading and net section fracture governs the strength of the member in tension. Thus, the required member strength can be determined as,

$$0.80R_{req} = 1.25DC + 1.50DW + 1.75(LL + IM)$$
$$= 152.9^{kip}$$
$$R_{req} = 191.1^{kip}$$

Next, the required member load factor can be calculated as,

$$LF_{1,req} = \frac{191.1^{kip} - 27.09^{kip}}{(1.33)(33.94^{kip})} = 3.633 \qquad (1.33 = IM)$$

Then, the member reserve ratio can be calculated as,

$$r_1 = \frac{LF_1}{LF_{1,req}} = \frac{7.058}{3.633} = 1.943$$

Finally, the refined reserve ratio for the damaged bridge can be calculated as,

$$R_d' = (r_1)(R_d) = (1.943)(0.3261) = 0.6335$$

Thus Member T19R can be reclassified as not fracture critical if the bridge owner elects to employ the member reserve ratio as part of the fracture critical assessment process.